



UNIVERSITAT
POLITÈCNICA
DE VALÈNCIA

Engineering of CRISPR-Cas9-based systems for diagnostics and biocomputing

Author:

Rosa Márquez Costa

Thesis Advisor:

Dr. Guillermo Rodrigo Tárrega

UPV Advisor:

Prof. Carmelo López del Rincón

València, July 2024

Dr. Guillermo J. Rodrigo Tárrega, doctor en Biotecnología por la Universitat Politècnica de Valencia (UPV) y Científico Titular del Consejo Superior de Investigaciones Científicas (CSIC) en el Instituto de Biología Integrativa y de Sistemas (I2SysBio) centro mixto del CSIC y de la Universitat de València Estudio General (UVEG),

CERTIFICA:

Que Dña. Rosa Márquez Costa, graduada en Biotecnología por la Universitat Politècnica de Valencia, ha realizado bajo su supervisión el trabajo titulado “Engineering of CRISPR-Cas9-based systems for diagnostics and biocomputing”, que presenta para optar al grado internacional de Doctora en Biotecnología por la Universitat Politècnica de Valencia.

Y para que así conste a los efectos oportunos, firman el presente certificado

Dr. Guillermo Rodrigo Tárrega



En València, Julio 2024

To the one who taught me resilience
and made me bloom.

一期一会

Japanese cultural concept,
treasuring the unrepeatable nature of a moment

TABLE OF CONTENTS

ABBREVIATIONS	11
SUMMARY	15
RESUMEN	17
RESUM	21
CHAPTER 1	25
GENERAL INTRODUCTION	25
CRISPR-Cas systems	25
Point-of-care diagnostics	29
CRISPR-based diagnostics.....	31
Signal integration by CRISPR-Cas systems.....	39
Motivation for Expanding the CRISPR Toolkit	46
REFERENCES	47
CHAPTER 2	61
OBJECTIVES	61
CHAPTER 3	63
Multiplexable Virus Detection by CRISPR-Cas9-Mediated Strand Displacement	63
1. INTRODUCTION.....	65
2. RESULTS	67
2.1 Rational Design of COLUMBO	67
2.2 SARS-CoV-2 Detection with COLUMBO	69
2.3 Evaluation of Modifications of COLUMBO	75
2.4 Multiplexed SARS-CoV-2 Detection with COLUMBO	77
2.5 Differential Virus Detection with COLUMBO.....	82
3. DISCUSSION	87

4. MATERIALS AND METHODS.....	89
4.1 Test Samples	89
4.2 Clinical Samples	90
4.3 Primers.....	90
4.4 CRISPR Elements.....	90
4.5 Molecular Beacons	91
4.6 Nucleic Acid Amplification by PCR.....	91
4.7 Nucleic Acid Amplification by RPA.....	92
4.8 CRISPR-Cas9-Based Detection.....	93
4.9 Activity assessment of different Cas9 versions	94
4.10 CRISPR-Cas9-based detection with no prior purification.....	94
4.11 Combined CRISPR-Cas9- and CRISPR-Cas12a-Based Detection	95
4.12 Single-point mutation detection with CRISPR-Cas9	95
4.13 RT-qPCR.....	96
4.14 Gel Electrophoresis.....	96
4.15 Fluorometry	97
4.16 Data set	99
5. REFERENCES.....	103
CHAPTER 4.....	107
Pathogen detection by CRISPR-Cas9-mediated strand displacement in a lateral flow assay	107
1. INTRODUCTION.....	109
2. RESULTS.....	112
2.1 Working principle and design of the Cas9-mediated detection LFA	112
2.2 Validation of the platform with test SARS-CoV-2 samples.....	114

2.3 Validation of the platform with SARS-CoV-2 clinical samples ...	119
2.4 Validation of the platform with plant infected samples	122
3. DISCUSSION	127
4. MATERIALS AND METHODS.....	129
4.1 Test Samples	129
4.2 Clinical Samples	129
4.3 Plant Infection with Viruses.....	130
4.4 Plant tissue preparation.....	130
4.5 CRISPR Elements.....	131
4.6 Probes	131
4.7 Nucleic Acid Amplification by RT-PCR.....	131
4.8 Nucleic Acid Amplification by RT-RPA	132
4.9 RT-qPCR.....	132
4.10 CRISPR-Cas9-Based detection coupled to Lateral Flow Assay.	133
4.11 CRISPR-Cas12a-Based detection.....	133
4.12 Data set	135
5. REFERENCES.....	139
CHAPTER 5.....	143
Integration of multiple signals into a CRISPR-Cas9-based detection mechanism	143
1. INTRODUCTION.....	145
2. RESULTS.....	147
2.1 Biocomputational Virus Detection with CRISPR-Cas9	147
2.2 Development and Optimization of a Spike Protein Aptamer-Regulated CRISPR-Cas9 System	150
3. DISCUSSION	161
4. MATERIALS AND METHODS.....	163

4.1 Nucleic acid sequences	163
4.2 CRISPR Elements.....	163
4.3 Spike Protein.....	164
4.4 Nucleic Acid Amplification by PCR.....	164
4.5 Biocomputing Coupled to CRISPR-Cas9-Based Detection	165
4.6 Conditional CRISPR-Cas9-Based Detection.....	166
4.7 Data Set.....	168
5. REFERENCES.....	171
CHAPTER 6	175
GENERAL DISCUSSION.....	175
REFERENCES.....	184
CHAPTER 7	191
CONCLUSIONS	191
FUNDING AND SUPPORT	193
SCIENTIFIC CONTRIBUTION	195
ACKNOWLEDGEMENTS.....	197

ABBREVIATIONS

ASSURED: affordable, sensitive, specific, user friendly, rapid and robust, equipment-free and deliverable to end users

AU: arbitrary unit

BHQ1: black hole quencher 1

bp: base pairs

CARMEN: combinatorial arrayed reactions for multiplexed evaluation of nucleic acids

Cas: CRISPR-associated

Cas9n: Cas9 H840A nickase

CDC: centers for disease control and prevention

COLUMBO: CRISPR-Cas9 R-loop usage for the molecular beacon opening

CONAN: Cas3-Operated nucleic acid detection

COVID-19: coronavirus disease 2019

CRISPR: clustered regularly interspaced short palindromic repeats

crRNA: CRISPR RNA

C_T: cycle threshold

Cy5: cyanine 5

dCas9: catalytically dead Cas9 protein

del: deletion

DETECTR: DNA endonuclease-targeted CRISPR *trans* reporter

DNA: deoxyribonucleic acid

dNTPs: deoxynucleotide triphosphates

dsDNA: double-stranded DNA

EDTA: ethylenediaminetetraacetic acid

EXPAR: exponential amplification reaction

FAM: carboxyfluorescein

FDA: food and drug administration

GFP: green fluorescent protein

HEPES: 4-(2-hydroxyethyl)-1-piperazineethanesulfonic acid

HiFi: high-fidelity

HIV: human immunodeficiency virus

HOLMES: one-hour low-cost multipurpose highly efficient system

IB_{FQ}: Iowa Black FQ

IB_{RQ}: Iowa Black RQ

IDT: integrated DNA technologies

K_d: dissociation constant

LAMP: loop-mediated isothermal amplification

LEOPARD: leveraging engineered tracrRNAs and on-target DNAs for parallel RNA detection

LFA: lateral flow assay

LNA: locked nucleic acids

MERS-CoV: middle east respiratory syndrome coronavirus

MST: microscale thermophoresis

NASBA: nucleic acid sequence-based amplification

ncrRNA: noncanonical crRNA

nt: nucleotide

PAM: protospacer adjacent motif

PCR: polymerase chain reaction

PFS: protospacer flanking site

PNA: peptide nucleic acid

POC: point-of-care

qPCR: quantitative polymerase chain reaction

RNA: ribonucleic acid

RPA: recombinase polymerase amplification

rpm: revolutions per minute

RT: reverse transcription

RT-PCR: reverse transcription polymerase chain reaction

RT-qPCR: reverse transcription quantitative polymerase chain reaction

RT-RPA: reverse transcription recombinase polymerase amplification

SARS-CoV-1: severe acute respiratory syndrome coronavirus 1

SARS-CoV-2: severe acute respiratory syndrome coronavirus 2

SBH: spacer blocking hairpin

SELEX: selected through systematic evolution of ligands by exponential enrichment

sgRNA: single guide RNA

SHERLOCK: specific high-sensitivity enzymatic reporter unlocking

SNP: single nucleotide polymorphism

SPR: Surface plasmon resonance

SpyCas9: *Streptococcus pyogenes* Cas9 nuclease

ssDNA: single-stranded DNA

TAE: tris acetate EDTA

TAMRA: carboxytetramethylrhodamine

TBE: tris borate EDTA

tracrRNA: *trans*-activating CRISPR RNA

U: units

UTR: untranslated region

UV: ultraviolet

WT: wild-type

ZIKV: Zika virus

SUMMARY

CRISPR-Cas systems are based on an adaptive immune system mechanism found in bacteria and archaea. They function using RNA-guided endonucleases (Cas proteins), to target and recognize specific nucleic acid sequences. This recognition is done in combination with a guide RNA, which enables precision and programmability in an easy and rapid way. These features have made CRISPR-Cas systems revolutionary in the field of genetic engineering, enabling specific genome editing, gene regulation assays and, developed in recent years, diagnostic applications.

Nucleic acid detection methods, such as qPCR, are the gold-standard diagnostic technique in the clinic due to their high sensitivity and specificity. However, these techniques often require sophisticated equipment, time-consuming procedures, and highly trained personnel, which makes them ill-suited to be used in resource-limited or large-scale contexts, such as pandemics. Recurrent disease outbreaks caused by different viruses, including the novel respiratory virus SARS-CoV-2, are challenging our society at a global scale. Going forward, we must develop versatile virus detection methods that enable fast and reliable diagnostics and that can overcome the limitations of the current techniques and can be easily used outside the laboratory for point-of-care (POC) applications.

CRISPR-Cas systems have been repurposed as nucleic acid diagnostic tools made possible by the ability of some Cas proteins to perform non-specific collateral cleavage upon target recognition. These platforms are mainly based on Cas12 and Cas13 effectors. We aim to expand the CRISPR-Cas diagnostic toolkit by developing a novel nucleic acid detection strategy based on CRISPR-Cas9, whose mode of action relies on strand displacement rather than on collateral catalysis, using the *Streptococcus pyogenes* Cas9 nuclease. For a given preamplification process, we introduce a suitable molecular beacon to produce a fluorescent signal upon interaction with the ternary CRISPR complex. We show that SARS-CoV-2 DNA amplicons generated from patient samples can be detected with CRISPR-Cas9. We also demonstrate the ability to perform simultaneous detection of different DNA

amplicons with the same nuclease, either to identify different SARS-CoV-2 regions or different respiratory viruses.

To advance toward POC applications, we coupled the isothermal preamplification step with biotinylated oligos to produce labelled amplicons. When combined with CRISPR-Cas9 targeting and FAM-labelled probes, this allows for colorimetric visualization of detection using lateral flow assays (LFA) on commercially available strips. The colorimetric readout enables interpretation of the results with the naked eye, surpassing the need for a fluorimeter. We successfully detected SARS-CoV-2 from patient samples in the LFA setup, and when combined with multiplexed RT-RPA, the detection of two distinct regions of the virus was achieved in a single test.

Furthermore, the absence of collateral activity in our methodology allows for the processing of additional downstream sequences. This is not feasible with Cas12 or Cas13 proteins, as their collateral activity, while useful for diagnostics, would degrade any additional sequences in the reaction. Therefore, we also aim to explore the signal integration capability of our CRISPR-Cas9-based detection method. We demonstrate that engineered DNA logic circuits can process different SARS-CoV-2 signals detected by the CRISPR complexes. We also aimed to enhance our CRISPR-Cas9 system to sense both proteins and nucleic acids. We aimed to engineer a conditional guide RNA that responds to the presence of the SARS-CoV-2 spike protein. To achieve this, we inserted an aptamer sequence within the guide RNA to block Cas9 activity in the absence of the protein. Upon the presence of the spike protein, aptamer-protein interaction makes the blocking motif undergo a conformational change, releasing the guide RNA and activating Cas9. While we successfully achieved the blocking scenario using the regulatory sequences, further work is needed to identify a sequence that can induce the specific conformational change required to restore Cas9 activity upon spike protein presence.

Collectively, this CRISPR-Cas9 diagnostic platform allows a multiplexed detection in a single tube, complementing the existing CRISPR-based methods, and offering an extensible system for applications in point-of-care diagnostics and biocomputing.

RESUMEN

Los sistemas CRISPR-Cas se basan en un mecanismo del sistema inmune adaptativo que se encuentra en bacterias y arqueas. Funcionan utilizando endonucleasas guiadas por ARN (proteínas Cas) para localizar y reconocer secuencias específicas de ácidos nucleicos. Este reconocimiento se realiza en conjunto con un ARN guía, lo que permite precisión y programabilidad de forma fácil y rápida. Estas características han hecho que los sistemas CRISPR-Cas sean revolucionarios en el campo de la ingeniería genética, permitiendo la edición específica del genoma, ensayos de regulación genética y, desarrolladas en los últimos años, aplicaciones de diagnóstico.

Los métodos de detección de ácidos nucleicos, como la qPCR, son la técnica de diagnóstico de referencia en la clínica debido a su alta sensibilidad y especificidad. Sin embargo, estas técnicas suelen requerir equipos sofisticados, procedimientos que requieren mucho tiempo y personal altamente cualificado, lo que las hace poco adecuadas para su uso en contextos de gran escala o con recursos limitados, como las pandemias. Los brotes recurrentes de enfermedades causados por diferentes virus, incluido el nuevo virus respiratorio SARS-CoV-2, suponen un reto a nuestra sociedad a escala global. De cara al futuro, debemos desarrollar métodos versátiles de detección de virus que permitan diagnósticos rápidos y fiables, que superen las limitaciones de las técnicas actuales y puedan usarse fácilmente fuera del laboratorio para aplicaciones en puntos de atención (POC).

Los sistemas CRISPR-Cas se han reconvertido en herramientas de diagnóstico de ácidos nucleicos gracias a la capacidad de algunas proteínas Cas de realizar cortes colaterales no específicos al reconocer su diana. Estas plataformas se basan principalmente en las proteínas Cas12 y Cas13. Nuestro objetivo es ampliar el conjunto de herramientas de diagnóstico CRISPR-Cas mediante el desarrollo de una nueva estrategia de detección de ácidos nucleicos basada en CRISPR-Cas9, cuyo modo de acción se basa en el desplazamiento de hebra en lugar de en la catálisis colateral, utilizando la nucleasa Cas9 de *Streptococcus pyogenes*. A partir de una preamplificación, introducimos una baliza molecular adecuada para producir una señal

fluorescente al interactuar con el complejo ternario CRISPR. Demostramos que los amplicones de ADN del SARS-CoV-2 generados a partir de muestras de pacientes pueden detectarse con CRISPR-Cas9. También demostramos la capacidad de realizar la detección simultánea de diferentes amplicones de ADN con la misma nucleasa, ya sea para identificar diferentes regiones de SARS-CoV-2 o diferentes virus respiratorios.

Para avanzar hacia aplicaciones POC, acoplamos el paso de preamplificación isotérmica con oligos biotilados para producir amplicones marcados. Cuando se combina con CRISPR-Cas9 y sondas marcadas con FAM, esto permite la visualización colorimétrica de la detección mediante ensayos de flujo lateral (LFA) en tiras disponibles en el mercado. La lectura colorimétrica permite la interpretación de los resultados a simple vista, superando la necesidad de un fluorímetro. Detectamos con éxito SARS-CoV-2 a partir de muestras de pacientes en la configuración LFA, y cuando se combinó con RT-RPA multiplexada, se logró la detección de dos regiones distintas del virus en una sola prueba.

Además, la ausencia de actividad colateral en nuestra metodología permite el procesamiento de secuencias posteriores adicionales. Esto no es factible con las proteínas Cas12 o Cas13, ya que su actividad colateral, aunque útil para el diagnóstico, degradaría cualquier secuencia adicional en la reacción. Por lo tanto, también pretendemos explorar la capacidad de integración de señales de nuestro método de detección basado en CRISPR-Cas9. Demostramos que diseños de circuitos lógicos de ADN pueden procesar diferentes señales de SARS-CoV-2 detectadas por los complejos CRISPR. También nos propusimos mejorar nuestro sistema CRISPR-Cas9 para detectar tanto proteínas como ácidos nucleicos. Nos propusimos diseñar un ARN guía condicional que respondiera a la presencia de la proteína *spike* del SARS-CoV-2. Para ello, insertamos un aptámero en el ARN guía para bloquear la actividad de Cas9 en ausencia de la proteína. En presencia de la proteína *spike*, la interacción aptámero-proteína hace que el motivo de bloqueo sufra un cambio conformacional, liberando el ARN guía y activando Cas9. Aunque logramos con éxito el escenario de bloqueo utilizando las secuencias reguladoras, es necesario seguir trabajando para identificar una secuencia que

pueda inducir el cambio conformacional específico necesario para restaurar la actividad de Cas9 en presencia de la proteína *spike*.

En conjunto, esta plataforma de diagnóstico CRISPR-Cas9 permite una detección multiplexada en un solo tubo, complementando los métodos existentes basados en CRISPR, y ofreciendo un sistema extensible para aplicaciones en diagnóstico en el punto de atención y biocomputación.

RESUM

Els sistemes CRISPR-Cas es basen en un mecanisme del sistema immunitari adaptatiu que es troba en bacteris i arqueus. Funcionen utilitzant endonucleases guiades per ARN (proteïnes Cas) per tal de dirigir-se i reconèixer seqüències específiques d'àcids nucleics. Aquest reconeixement es fa en combinació amb un ARN guia, que permet una precisió i programabilitat de manera fàcil i ràpida. Aquestes característiques han fet que els sistemes CRISPR-Cas siguin revolucionaris en el camp de l'enginyeria genètica, permetent l'edició específica del genoma, assajos de regulació gènica i, desenvolupades en els darrers anys, aplicacions de diagnòstic.

Els mètodes de detecció d'àcids nucleics, com la qPCR, són la tècnica de diagnòstic de referència a la clínica degut a la seua alta sensibilitat i especificitat. No obstant això, aquestes tècniques solen requerir equips sofisticats, procediments que requereixen molt de temps i personal altament qualificat, fet que les fa poc adequades per al seu ús en contextos a gran escala o amb recursos limitats, com les pandèmies. Els brots recurrents de malalties causades per diferents virus, inclòs el nou virus respiratori SARS-CoV-2, suposen un repte per a la nostra societat a escala global. De cara al futur, hem de desenvolupar mètodes versàtils de detecció de virus que permeten diagnòstics ràpids i fiables, que superen les limitacions de les tècniques actuals i puguin utilitzar-se fàcilment fora del laboratori per a aplicacions en punts d'atenció (POC).

Els sistemes CRISPR-Cas han estat reorientats com a eines de diagnòstic d'àcids nucleics, fet possible per la capacitat d'algunes proteïnes Cas de realitzar un tall col·lateral no específic en reconèixer un objectiu. Aquestes plataformes es basen principalment en els efectors Cas12 i Cas13. El nostre objectiu és ampliar el conjunt d'eines de diagnòstic CRISPR-Cas desenvolupant una nova estratègia de detecció d'àcids nucleics basada en CRISPR-Cas9, el mode d'acció del qual es basa en el desplaçament de cadena en lloc de la catàlisi col·lateral, utilitzant la nucleasa Cas9 de *Streptococcus pyogenes*. Per a un procés de preamplificació donat, introduïm una balisa molecular adequada per produir un senyal fluorescent a l'interactuar amb el

complex CRISPR ternari. Mostrem que es poden detectar amplicons de DNA de SARS-CoV-2 generats a partir de mostres de pacients amb CRISPR-Cas9. També demostrem la capacitat de realitzar la detecció simultània de diferents amplicons de DNA amb la mateixa nucleasa, ja siga per identificar diferents regions de SARS-CoV-2 o diferents virus respiratoris.

Per avançar cap a aplicacions de punt d'atenció (POC), vam combinar el pas de preamplificació isotèrmica amb oligos biotinitats per produir amplicons etiquetats. Quan es combinen amb l'orientació CRISPR-Cas9 i sondes etiquetades amb FAM, això permet la visualització colorimètrica de la detecció mitjançant assajos de flux lateral (LFA) en tires comercials disponibles. La lectura colorimètrica permet la interpretació dels resultats a simple vista, superant la necessitat d'un fluorímetre. Vam detectar amb èxit el SARS-CoV-2 a partir de mostres de pacients en el sistema LFA, i quan es va combinar amb RT-RPA multiplexada, es va aconseguir la detecció de dues regions diferents del virus en una sola prova.

A més, l'absència d'activitat col·lateral en la nostra metodologia permet el processament de seqüències addicionals. Això no és factible amb les proteïnes Cas12 o Cas13, ja que la seva activitat col·lateral, tot i ser útil per a diagnòstics, degradaria qualsevol seqüència addicional en la reacció. Per tant, també ens proposem explorar la capacitat d'integració de senyals del nostre mètode de detecció basat en CRISPR-Cas9. Demostrem que els circuits lògics d'ADN dissenyats poden processar diferents senyals de SARS-CoV-2 detectats pels complexos CRISPR. També vam intentar millorar el nostre sistema CRISPR-Cas9 per detectar tant proteïnes com àcids nucleics. Ens vam proposar dissenyar un ARN guia condicional que respon a la presència de la proteïna *spike* del SARS-CoV-2. Per aconseguir-ho, vam inserir una seqüència d'aptàmer dins de l'ARN guia per bloquejar l'activitat de Cas9 en absència de la proteïna. En presència de la proteïna *spike*, la interacció aptàmer-proteïna fa que el motiu de bloqueig experimente un canvi conformacional, alliberant l'ARN guia i activant Cas9. Tot i que vam aconseguir amb èxit el bloqueig utilitzant les seqüències reguladores, es necessita més treball per identificar una seqüència que pugui induir el canvi conformacional específic necessari per restaurar l'activitat de Cas9 en presència de la proteïna *spike*.

Col·lectivament, aquesta plataforma de diagnòstic CRISPR-Cas9 permet una detecció multiplexada en un sol tub, complementant els mètodes existents basats en CRISPR i oferint un sistema extensible per a aplicacions en diagnòstics de punt d'atenció i biocomputació.

CHAPTER 1

GENERAL INTRODUCTION

CRISPR-CAS SYSTEMS

Clustered regularly interspaced short palindromic repeats (CRISPR) systems have revolutionized molecular biology by offering a highly versatile and programmable biotechnological toolkit with a wide range of applications. CRISPR has represented a groundbreaking shift within the field of genetic editing and beyond. Its presence was initially noted in 1987 when an unusual DNA structure of direct repeats separated by spacers with unique sequences was observed in *Escherichia coli* genome while examining genes associated with phosphate metabolism (Ishino *et al.*, 1987). Afterwards, early rough functional insight was provided after identifying those interspaced tandem repeats within the genomes of halophilic archaea from the Spanish Mediterranean coast (Mojica *et al.*, 1993, 1995). In parallel, CRISPR was detected in an increasing number of archaeal and bacterial genomes (Jansen *et al.*, 2002; Mojica *et al.*, 2000). The discovery that CRISPR spacers derive from preexisting sequences of bacteriophages, archaeal viruses, and plasmids, along with noticing those elements fail to infect the specific spacer-carrier host strain, shed light on the relationship between CRISPR and an acquired immunity against targeted foreign DNA (Bolotin *et al.*, 2005; Mojica *et al.*, 2005; Pourcel *et al.*, 2005). With only these initial observations, it would have been difficult to anticipate the revolutionary advances CRISPR would bring to scientific research.

The discovery that CRISPR-associated (Cas) proteins can be directed to a target DNA and provoke a double-stranded cleavage (Garneau *et al.*, 2010) was the first step in this revolution. This directed break is achieved by the pair formation of CRISPR RNAs (crRNAs) and *trans*-activating crRNA (tracrRNA), forming a mature RNA structure (Deltcheva *et al.*, 2011). The tracrRNA:crRNA duplex couples with Cas9 nuclease, assembling into a

catalytically active ribonucleoprotein, which will then be guided towards its DNA target and generate the cleavage. By engineering this tracrRNA:crRNA into a single guide RNA (sgRNA) chimera, it also acts as a directing-RNA inducing sequence-specific Cas9 dsDNA cleavage. Cas9 functions therefore as an RNA-guided DNA endonuclease (**Figure 1**) (Gasiunas *et al.*, 2012; Jinek *et al.*, 2012; Nishimasu *et al.*, 2014).

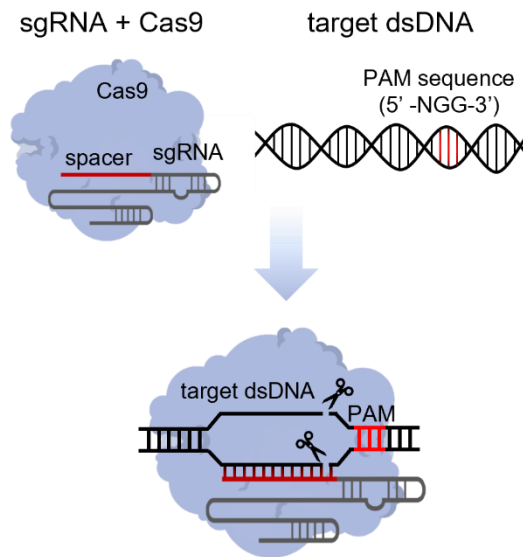


Figure 1. CRISPR-Cas9 mechanism of action. The sgRNA forms a complex with the Cas9 nuclease. Then, for a given dsDNA with a suitable PAM sequence (marked in red), the ribonucleoprotein is going to target the DNA by base complementarity between the spacer (marked in red) of the sgRNA and the target DNA. Afterwards, the nuclease is going to generate the double-stranded cleavage.

Target sequence recognition is accomplished through complementary base-pairings between the guide RNA and the target genome. It also relies on the presence of a short, conserved nucleotide sequence, located adjacent to the target region of the genome, known as the protospacer adjacent motif (PAM). The specific sequence and position of the PAM sequence varies within the CRISPR-Cas system; for example, in the *Streptococcus pyogenes* Cas9, the PAM consists of an NGG consensus sequence (Mojica *et al.*, 2009). PAM recognition is crucial for the binding and cleavage activities of Cas proteins. This recognition triggers RNA strand invasion along with local DNA

unwinding, resulting in the formation of an R-loop (Sternberg *et al.*, 2014; Szczelkun *et al.*, 2014). Hereafter, the subsequent precise cleavage of the target DNA is generated in a sequence-dependent manner. The Cas9 HNH nuclease domain cleaves the target DNA strand, while the RuvC domain cleaves the non-target strand; inducing a double-strand break at the specified genomic location (Jinek *et al.*, 2012). These findings highlighted the potential of the CRISPR-Cas systems to be exploited for gene targeting and genome editing applications in a programmable way.

CRISPR schemes evolved in numerous bacteria and archaea as adaptive immune systems playing a crucial role in protecting cells against viral infections (Bhaya *et al.*, 2011; Horvath and Barrangou, 2010). According to whole genome sequence analysis, CRISPR-Cas loci are found in the majority of archaea (276 of 324 analyzed archaeal species (85.2%)), and approximately 40% of bacteria (5,412 of 12,792 analyzed bacterial genomes (42.3%)) (Makarova *et al.*, 2020). Consequently, it can be expected that along organisms CRISPR-Cas systems show a remarkable diversity in architecture and organization. Thanks to advances in genomic approaches, ongoing identification of several Cas proteins is contributing to enlarge the CRISPR universe. The current CRISPR-Cas classification is composed of two main classes, six types and thirty-three subtypes. The class 1 CRISPR-Cas systems have multiple Cas proteins as effector modules, while class 2 systems encode single subunit effectors. Each class is divided into three types, each with further distinct subtypes. Type I, Type III and Type IV are included in class 1; and Type II, Type V and Type VI for class 2 (Makarova *et al.*, 2020) (**Figure 2**). Cas9 protein, the most commonly used Cas effector, belongs to class 2, Type II CRISPR-Cas systems (Doudna and Charpentier, 2014; Jiang and Doudna, 2017).

Because of its simplicity and ease of engineering, as well as their expanded functionality and capabilities due to newly discovered Cas proteins, these systems are now being repurposed for use in a variety of biotechnological fields. The most prominent and well-known applications are in genome editing, allowing scientists to modify genetic sequences in a precise manner (Cong *et al.*, 2013; Jinek *et al.*, 2013; Mali *et al.*, 2013). Besides gene editing, CRISPR systems are also instrumental in functional genomics. By

introducing mutations to the catalytic domains of Cas9, a non-functional variant known as dead Cas9 (dCas9) is generated. This variant lacks cleavage activity but retains its ability to bind to the target genome, which is valuable for regulating gene expression, and can be used for both selectively silencing or activating specific genes (Chavez *et al.*, 2015; Gilbert *et al.*, 2013). This same property can be utilized for setting tracking and imaging experiments by fusing green fluorescent protein (GFP) to dCas (Barrangou and Doudna, 2016; Chen *et al.*, 2013; Ishino *et al.*, 2018). The versatility of CRISPR technologies goes beyond traditional genetic and molecular biology insights, and recently, CRISPR systems have even been repurposed as nucleic acid detection tools (Kaminski *et al.*, 2021).

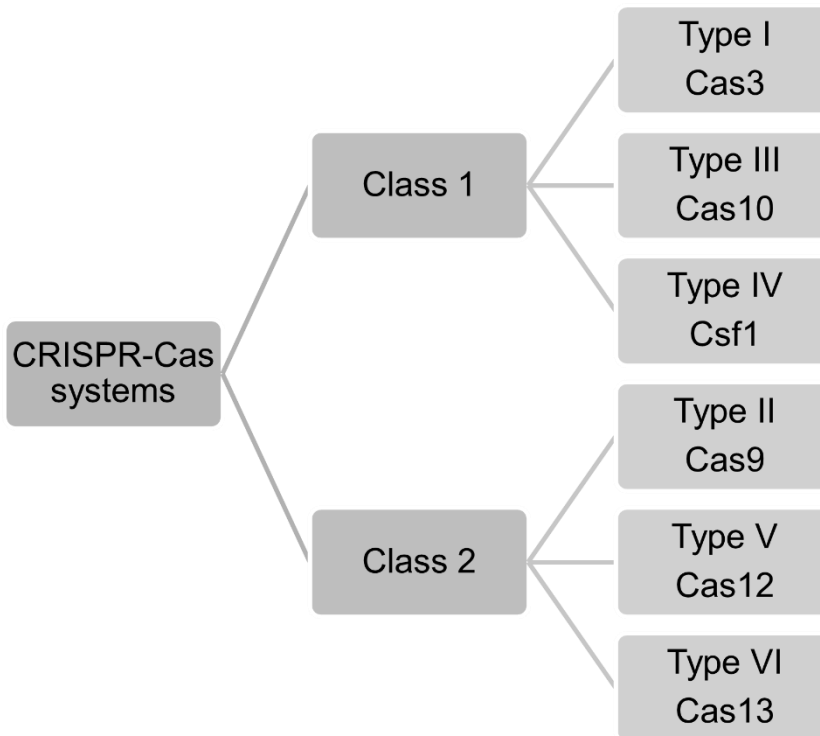


Figure 2. CRISPR-Cas systems classification. Cas effector module involved in crRNA and target binding and/or target cleavage are shown.

POINT-OF-CARE DIAGNOSTICS

Fast and confident diagnosis contributes to direct medical attention in terms of early therapeutic actions and guidance of the patient. Diagnostic techniques will differ depending on the tackled health issue. Immunoassays, enzyme assays, tissue and liquid biopsies or cytology analyzes are some examples of routine ways to manage health disorders. It is important to develop fast and non-invasive diagnostics techniques for enhancing management of the disease, prevent and control their spread and to respond to the high demand and emergence of diseases that are currently rising (Momčilović *et al.*, 2019).

During the twenty-first century, we have experienced a wave of severe infectious disease outbreaks. Recent coronavirus disease 2019 (COVID-19) pandemic has highlighted the challenges in diagnostics of viral infections, which contributes to mitigate the transmission of the virus. In addition, the 2003 severe acute respiratory syndrome coronavirus outbreak, the 2009 H1N1 Influenza virus pandemic (also known as swine flu), the 2012 Middle East respiratory syndrome coronavirus outbreak, the 2013-2016 Ebola virus outbreak in West Africa and the 2015 Zika virus disease epidemic are some notable examples of infectious diseases that have underscored the critical importance of advanced diagnostic capabilities (Baker *et al.*, 2022). It is important to note that the situation with infectious diseases is dynamic, and new outbreaks will keep taking place, making it necessary to continue to explore and implement cutting-edge diagnostic technologies. Currently, the gold-standard diagnostic technique of many diseases involves polymerase chain reaction (PCR) or variants of it, and, together with sequencing techniques, the disclosure of relevant mutations have enabled more accurate prognoses and epidemiological reconstructions (Kao *et al.*, 2014; Udugama *et al.*, 2020). Yet, isothermal amplification methods (*e.g.* recombinase polymerase amplification (RPA)) represent a suitable alternative to speed up the process and bypass the need of precise equipment, although it may lead to lower detection specificity due to non-specific amplification (Wang *et al.*, 2015; Zhao *et al.*, 2015). Still, alternative techniques are required to overcome the need for long procedures, expensive reagents and equipment, and skilled personnel while maintaining the diagnostic accuracy.

The ultimate goal of diagnostics is to serve populations and contribute towards a state of well-being beyond the laboratory itself. Therefore, there is a need to adapt current diagnostics technologies to be accessible and suitable for resource-limited areas and at-home environments. One possible way to assess such qualities is using the ASSURED criteria (affordable, sensitive, specific, user friendly, rapid and robust, equipment-free and deliverable to end users), established by the World Health Organization in 2003, for evaluating the suitability of diagnostic tests in a point-of-care (POC) scenario (Land *et al.*, 2019; Mahfouz, 2024).

Rapid antigen tests have emerged as an alternative diagnostic tool when a situation demands prompt and rapid identification. These tests directly detect viral components without the need for the amplification steps required for PCR. Therefore, they provide results within minutes and with no required infrastructure, making them particularly useful for home settings. The downside of these tests is that they show a lower sensitivity compared to molecular tests, and may fail to detect low amount of virus, potentially leading to false negative results in individuals with low viral loads or during the early stages of infection (Green and StGeorge, 2018; Peeling *et al.*, 2021). Moreover, their lack of sensitivity makes them inefficient in distinguishing single-base changes, making them unsuitable for identifying concerning mutations, which are crucial for tracking the spread of variant strains (Rao *et al.*, 2023). In addition, the design of reliable rapid antigen tests relies on conscientious optimization to ensure precision and consistency; the laboratory process to manufacture such test include several intricate steps. First, the selection of an antigen specific to the virus that is present in high concentrations during the infection phase. Next, assays are developed to detect its presence in patient samples. This usually relies on the design of binding molecules such antibodies, which will recognize and bind to the target antigen, facilitating the detection of the antigen in the patient sample. This is followed by format testing, manufacturing, scaling up and validation. It is important to ensure that these tests only detect the target antigen and show no cross reaction with similar molecules from other pathogens or substances present in the patient sample. Therefore, the process of creating reliable rapid

antigen tests is far from straightforward, and every laboratory protocol presents its own challenges which can influence test performance.

CRISPR-BASED DIAGNOSTICS

CRISPR-Cas systems emerge at this point as opportune molecular tools for conducting sensitive and specific nucleic acid detection. Their capabilities can overcome the limitations of diagnostic platforms, particularly when a massive intervention is required. CRISPR-based diagnostics build on the specificity, programmability, and user-friendly nature of CRISPR technology, with the goal of developing nucleic acid-based POC diagnostic tests suitable for routine clinical use, at-home testing, and field applications (Li *et al.*, 2019a).

The use of Cas proteins as nucleic acid detection tools gained attention after the discovery that certain Cas proteins display collateral catalytic activity upon target recognition. Cas13a (previously known as C2c2) is a class 2, Type VI system that encompasses RNA-targeting function, with a requirement for a (non-G) protospacer flanking site (PFS) following the RNA target site. Cas13 exhibits a nonspecific cleavage of other RNAs present in the sample after activation by the target (Abudayyeh *et al.*, 2016; East-Seletsky *et al.*, 2016). When coupled to an appropriately labelled RNA probe (*e.g.*, fluorophore-quencher when measuring fluorescence), a detection system is created. After recognition of a specified target, Cas13 performs a nonspecific cleavage, degrading the labelled probe, and separating quencher from fluorophore, which will produce a measurable fluorescence signal (**Figure 3**). The designed probe will only produce a signal when the specified sequence has been detected, since the collateral activity of Cas13 is only produced after activation by its target. Cas13a was then coupled with isothermal amplification to establish the first comprehensive and applicable CRISPR-Cas detection platform termed Specific High-Sensitivity Enzymatic Reporter UnLOCKing (SHERLOCK) (Gootenberg *et al.*, 2017). SHERLOCK shows fast DNA or RNA detection with attomolar sensitivity and single-base mismatch specificity. It has been applied to detect specific strains of Dengue

and Zika virus, as well as showed its utility for genotyping human DNA; identification of bacterial pathogens and detection of specific bacterial genes and distinguish mutations in cell-free tumor DNA.

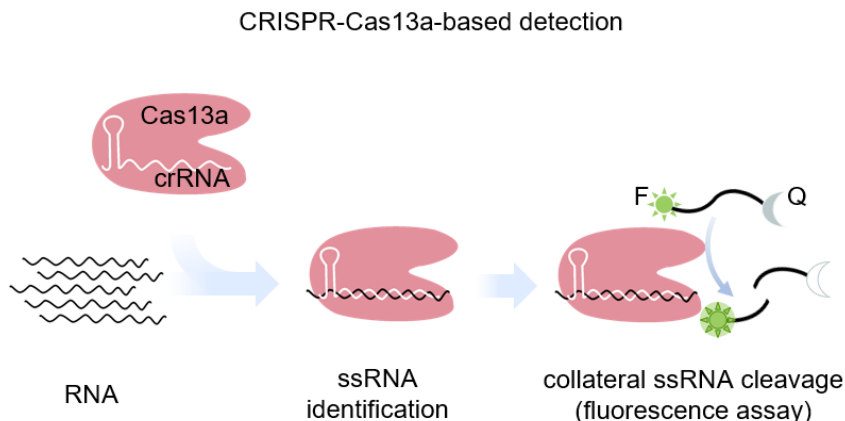


Figure 3. Schematic representation of CRISPR-Cas13a-based detection from RNA template target. The ssRNA probe is labelled with a fluorophore (F, sun icon) and a quencher (Q, moon icon).

Similarly, CRISPR-Cas12 has also been proven effective to detect nucleic acid sequences. Cas12a (also known as Cpf1) is an RNA-guided DNA endonuclease; class 2, Type V, which cleaves target DNA adjacent to a short T-rich PAM (TTTN) (Zetsche *et al.*, 2015a). Cas12a also processes single-stranded DNA after target recognition (Chen *et al.*, 2018; Li *et al.*, 2018a) (**Figure 4**). By combining Cas12a nonspecific cleavage with isothermal amplification, Chen *et al.* (2018) created a method named DNA endonuclease-targeted CRISPR *trans* reporter (DETECTR), achieving attomolar sensitivity for DNA detection. DETECTR has been successfully applied to detect human papillomavirus in patient samples. During the same period, other Cas12a-based technique termed HOLMES (for one-Hour Low-cost Multipurpose highly Efficient System) was described along with its usage in nucleic acid detection (Li *et al.*, 2018b). HOLMES was used to detect DNA and RNA viruses, enabling the distinction between virus strains and single nucleotide polymorphisms (SNP), showing attomolar sensitivity.

CRISPR-Cas12a-based detection

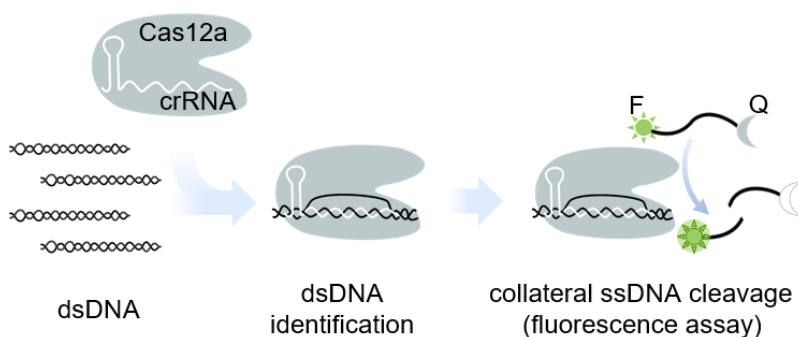


Figure 4. Schematic representation of CRISPR-Cas12a-based detection from dsDNA template target. The ssDNA probe is labelled with a fluorophore (F, sun icon) and a quencher (Q, moon icon).

Both platforms, SHERLOCK and DETECTR, are a couple examples of the vast capabilities of CRISPR-Cas systems, providing a powerful, rapid, and specific means for molecular diagnostics. While these work developments were the basis to prove the potential of CRISPR for diagnostic applications, subsequent research has been done to build upon these foundational technologies. As one example, CRISPR-Cas13 systems have been used for detecting human infecting RNA viruses directly from bodily fluids (Myhrvold *et al.*, 2018). They have also been able to detect the novel severe acute respiratory syndrome coronavirus 2 (SARS-CoV-2) without the need for a previous amplification step (Fozouni *et al.*, 2021; Shinoda *et al.*, 2021). When in combination with a droplet array assay, more than 4,500 crRNA-target pairs can be tested in a single array. This platform termed Combinatorial Arrayed Reactions for Multiplexed Evaluation of Nucleic acids (CARMEN), when used together with Cas13, can be exploited for scalable, multiplexed pathogen detection, even allowing the multiplexed identification of dozens of human immunodeficiency virus (HIV) drug-resistance mutations (Ackerman *et al.*, 2020). Beyond human concerning viruses, CRISPR-Cas detection tools have also been used successfully in discriminating SNPs in human cells, identifying pathogenic bacteria, detecting parasites, and detecting plant viruses, among some examples along the literature (Abudayyeh *et al.*, 2019; Li *et al.*, 2019b; Lee *et al.*, 2020; Marques *et al.*, 2022; Zhou *et al.*, 2020a).

Researchers have also explored the use of other Cas proteins that rely on collateral activity. Cas12f, previously denoted Cas14, is a novel class 2, Type V CRISPR-Cas system, which was discovered by environmental metagenomic sequencing analysis and is notable for its application to detection purposes. Cas12f contains from 400 to 700 amino acids, being two times smaller than Cas9, and it targets ssDNA cleavage without restrictive sequence requirements (Harrington *et al.*, 2018). Although a subsequent study has reported dsDNA cleavage activity in a PAM dependent manner (Karvelis *et al.*, 2020). Despite the lack of stringent PAM requirements, Cas12f is highly sensitive to mismatches in the middle of its target region making it an ideal candidate for nucleic acid detection applications, when a high-fidelity single-nucleotide resolution detection is desired. Similar to Cas12a, target recognition by Cas12f triggers collateral cleavage of ssDNA molecules. This collateral activity has been combined with isothermal amplification to develop DETECTR-Cas14, which offers better discrimination of SNPs in ssDNA compared to Cas12a. In addition, Cas3, a class 1, Type I system which shows highest activity for a AAG PAM sequence (Morisaka *et al.*, 2019), has been applied to the detection of SARS-CoV-2 and influenza virus (Yoshimi *et al.*, 2022). The researchers reported the discovery on Cas3 exhibiting nonspecific ssDNA cleavage after target-specific dsDNA cleavage and named the assay Cas3-Operated Nucleic Acid detectionN (CONAN).

A primary distinction between CRISPR type II (Cas9) systems and type V (Cas12) and type VI (Cas13) systems lies in the absence of non-specific collateral cleavage triggered by Cas9 on target recognition. The collateral cleavage renders Cas12 and Cas13 particularly suitable for biosensing applications, still Cas9 effectors have also been harnessed for molecular diagnostics. Very recently, it has been reported that crRNA- and tracrRNA-directed Cas9 shows *trans*-cleavage activity for single stranded substrates (Chen *et al.*, 2024). Yet, this collateral Cas9-based cleavage takes places under very specific conditions. Cas9 exhibits structure and sequence specific preferences for *trans*-cleavage substrates, with a particular preference for cleaving T- or C-rich ssDNA sequences. In addition, the use of chimeric sgRNA in place of crRNA and tracrRNA result in less efficient *trans*-cleavage

activity. Due to these specific conditions, Cas9 collateral activity was not widely known or utilized in earlier studies.

One of the earliest attempts in using CRISPR for nucleic acid detection was the development of a paper-based diagnostic platform for Zika virus. When coupled with Cas9, the researchers could discriminate among variants of the virus with single nucleotide resolution (Pardee *et al.*, 2016). To allow for strain-specific detection, they relied on the fact that Cas9 only cleaves its target when a PAM sequence is present. Mutations within the virus have a high chance of creating or destroying a PAM sequence; therefore, there exists strain-specific PAM sites that can be used for variant discrimination. In their approach, they include a trigger sequence of a synthetic toehold switch during the genome amplification. When the PAM is present in the tested sample, Cas9 will perform a dsDNA break, resulting in a truncated product that is unable to activate the sensor toehold switch. If the PAM is absent, Cas9 will not recognize the sequence and the full-length product will activate the sensor. They successfully applied this system to distinguish between the African and American Zika strains, since a PAM site only exists in the American variant sequences (**Figure 5**). Their development provided genotypic information on paper within a few hours, which, paired with the fact that Cas9 was compatible with the lyophilization process, made it suitable for field use. Another creative idea for applying CRISPR as a diagnostic tool was the development of an *in vitro* DNA detection system using a pair of dCas9 protein fused with halves of luciferase (Zhang *et al.*, 2017). In this system dCas9 is linked to the N- and C-terminal half of the luciferase enzyme, and each Cas protein is linked to a sgRNA targeting the upstream and downstream segment of a specific DNA sequence. Upon detection and binding of dCas9 of a given DNA complementary to the sgRNA sequences, luminescence is generated from the recovered activity of luciferase in its entirety. This system was applied to a *Mycobacterium tuberculosis* sample from an infected patient, yielding a 52-fold increase in luminescence in comparison to nonspecific *E. coli* genomic DNA. Other detection methods relying on Cas9-based methodology have been recently described. CAS-EXPAR (CRISPR-Cas9 triggered isothermal exponential amplification reaction) was designed for nucleic acid detection. This method utilizes directed site-specific cleavage of target by Cas9 to generate the primers to initiate the isothermal amplification.

The amplification process occurs cyclically, generating a large number of DNA copies, which are detected using real-time fluorescence monitoring. CAS-EXPAR showed attomolar sensitivity, high specificity, and rapid amplification kinetics (Huang *et al.*, 2018).

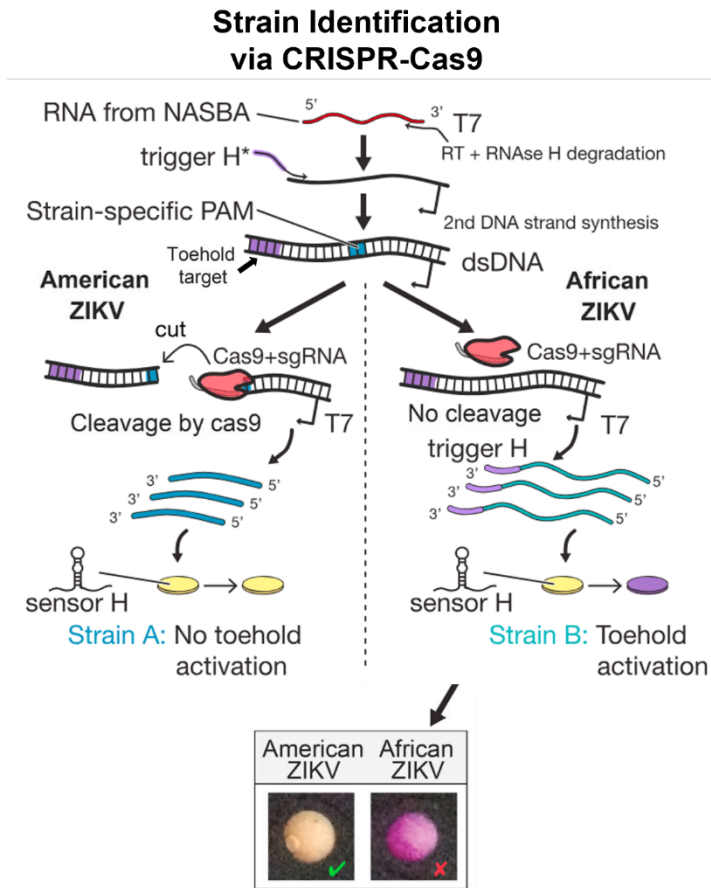


Figure 5. Strain identification of Zika virus (ZIKV) with CRISPR-Cas9. RNA is amplified with nucleic acid sequence-based amplification (NASBA) technology. A synthetic trigger sequence is appended to the amplified RNA for the toehold sensor (purple sequence). Then CRISPR-Cas9 reaction occurs. If a PAM sequence (blue) is present, Cas9 will cleavage the dsDNA with a truncated resulting amplicon that cannot activate the toehold sensor. In the absence of a PAM, a resulting full-length RNA containing the trigger can activate the toehold sensor which in turns produces a visible change in color (adapted from Pardee *et al.*, 2016).

Complementing these advancements, dCas9 has been employed for digital detection (Hajian *et al.*, 2019). In this technique, named CRISPR-Chip, dCas9 is immobilized on a graphene-based field-effect transistor. The binding of the target alters the transistor's electrical properties which can be measured as a change in current, facilitating label-free nucleic acid testing. Remarkably, this method can achieve femtomolar detection sensitivity without pre-amplification. Reported more recently, LEOPARD (leveraging engineered tracrRNAs and on-target DNAs for parallel RNA detection) enables simultaneous detection of different RNAs with single-base resolution (Jiao *et al.*, 2021). The team observed that cellular RNAs hybridized with the tracrRNA, resulting in the formation of “noncanonical” crRNAs (ncrRNAs). By reprogramming the tracrRNA to bind to cellular RNAs of interest, a transcript is converted into a functional guide RNA, directing Cas9 to a matching DNA target. Consequently, LEOPARD can report the presence of a specific RNA of interest based on DNA targeting cleavage, which can be revealed by gel electrophoresis or a Bioanalyzer. In addition to the methods mentioned, CRISPR-based diagnostics have numerous other innovative approaches and techniques being described. **Table 1** shows a comparison on the different Cas effector proteins mainly used for CRISPR diagnostic.

The remarkable progress in the CRISPR-based diagnostic field has inspired scientists to adapt these technologies for closer use in commercial and at-home settings. Towards suiting POC testing, researchers have managed to engineer CRISPR-Cas systems to produce colorimetric and other easily visible readout signals in the presence of specific target sequences. SHERLOCK and DETECTR use a fluorophore-quencher probe as reporter signal indicating the presence of the desired target, since due to the collateral activity activation upon presence of the target, the reporter will be degraded producing therefore the measurable fluorescence signal. Such reporter can be appropriately labelled to be exploited in immunochromatographic assays that run in commercial lateral flow strips, obtaining a visible readout (Gootenberg *et al.*, 2018; Myhrvold *et al.*, 2018). Visualization of the reaction is done by using a FAM-biotin reporter probe and the commercially available lateral flow strips. These strips are designed to capture entire reporter molecules at the first detection line, while the collateral activity generated upon target recognition by Cas12/Cas13 generates a signal at the second detection line.

Table 1. Comparison among the properties of some Cas proteins used for CRISPR diagnostics.

Effector protein	Cas3	Cas9	Cas12a	Cas12f	Cas13a-d
Class	1	2	2	2	2
Type	I	II	V	V	VI
Target	dsDNA	dsDNA	dsDNA	ssDNA, dsDNA	ssRNA
PAM	AAG	NGG	TTTN	rich 5' T/C	non G- PFS
Collateral activity	ssDNA	no*	ssDNA	ssDNA	ssRNA

*Cas9 has recently been shown to display collateral activity under very specific conditions (Chen *et al.*, 2024).

It has been reported rapid CRISPR-Cas12-based lateral flow assay (LFA) for the detection of SARS-CoV-2 infection from respiratory swab RNA extracts within less than 1 hour (Ali *et al.*, 2020; Broughton *et al.*, 2020). The CRISPR-Cas9 system can also be used in combination with probe reporters for LFA detection. By either incorporating a gold nanoparticle-DNA probe or labelling the Cas9 protein, it is possible to screen a variety of pathogens, including SARS-CoV-2, enabling for variant distinction and multiplexed detection (Ali *et al.*, 2021; Marsic *et al.*, 2021; Wang *et al.*, 2020; Xiong *et al.*, 2021). The integration of CRISPR-Cas-based detection with LFA is a promising approach for rapid and accessible nucleic acid detection. However, the mechanistic of these systems also introduces challenges since they may incorporate complicated components and there is a high rate of false positive results. Conditions of the assay must be carefully controlled, further complicating set-up optimization.

SIGNAL INTEGRATION BY CRISPR-CAS SYSTEMS

The programmability of CRISPR systems has allowed astonishing advances in research, holding promise for rapid and accessible nucleic acid detection. Yet, despite their remarkable capabilities, CRISPR-Cas systems are based on a simple fundamental principle. Cas proteins can potentially target any nucleic acid sequence by simply modifying the complementarity within the sgRNA and the target sequence. Despite relying on a straightforward principle, CRISPR-Cas systems can exhibit an intriguing capacity to process and respond to complex signals. Recognizing the potential for further enhancement, researchers are actively exploring the integration of multiple, potentially complex, signals to enhance the functionality of CRISPR-Cas systems.

One such avenue for advancement is incorporating CRISPR systems into biocomputational modules. Biocomputing involves utilizing biological systems or molecules to execute computational tasks, often leveraging DNA, RNA, proteins, or enzymes to mimic the operation of Boolean logic gates (**Figure 6**) (Katz, 2015). In these biomolecular logic gates, different reacting species act as input signals that are processed by various Boolean logic operations. The generated outputs are typically small molecules, optical signals (such as colorimetric or luminescent), or electrochemical signals. To digitize these chemical processes, the absence of an input trigger is designated as the logic 0 input, while logic 1 input is set at a specific concentration distinctly affecting the output signals for different combinations of 0 and 1 inputs. Biomolecular systems offer the possibility to assemble multi-step biocatalytic cascades of reactions, mimicking logic networks (Halamek *et al.*, 2010; Privman *et al.*, 2013) which have been used to perform arithmetic operations (Stojanović and Stefanović, 2003a), train a molecular automaton to play a game (Pei *et al.*, 2010; Stojanovic and Stefanovic, 2003b) or construct DNA small neural networks capable of making decisions (Qian *et al.*, 2011).

In particular, DNA computation has gained a lot of attention since its first demonstration to solve combinatorial problems (Adleman, 1994). The high

programmability of Watson-Crick base pairing, in combination with its easy synthesis, biocompatibility, and low cost, have spurred DNA computing to become a leading candidate for molecular computation (Fan *et al.*, 2020). In such DNA-based computational processes, specific DNA sequences are strategically designed to interact with each other in a programmable way. This interaction makes use of hybridization and branch migration in a process known as toehold-mediated strand displacement, which serves to exchange one strand of DNA (or RNA) with another one (Seelig *et al.*, 2006; Yurke *et al.*, 2000).

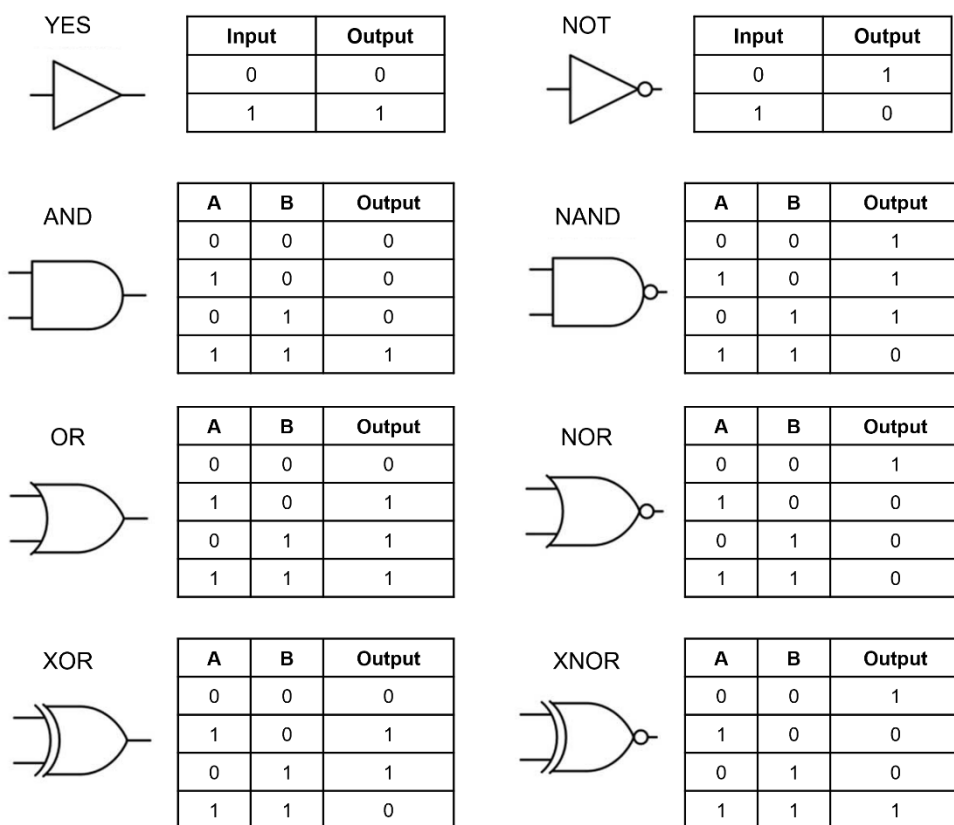


Figure 6. Summary of the common Boolean logic gate functions along with their truth tables, showing the output generated from a given set of inputs (adapted from Abels and Khisamutdinov, 2015).

In the strand displacement reaction, a DNA strand displaces another from a DNA duplex through base complementarity. A ssDNA molecule, referred to as the invading strand, binds to a short single-stranded overhanging complementary region known as “toehold” present in a DNA duplex. This binding initiates the branch migration process along the dsDNA, displacing one of the original strands and forming a new DNA duplex (Simmel *et al.*, 2019; Zhang and Winfree, 2009) (**Figure 7**). This mechanism has been instrumental in constructing multilayer digital logic circuitry (Qian and Winfree, 2011), smart bioanalysis sensors (Han *et al.*, 2012) and a variety of dynamic functions (Yin *et al.*, 2008).

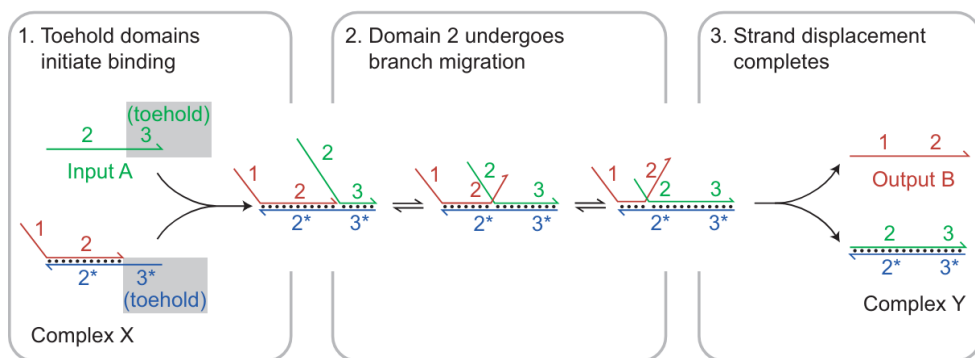


Figure 7. Overview of a toehold-mediated strand displacement reaction. ssDNA molecule A interacts with dsDNA complex X, facilitated by the toehold domain and the complementarity between 3 and 3* regions. The branch migration is then initiated, during which one strand domain displaces another with an identical sequence. After branch migration is completed, single strand B is released, and complex Y is formed (Zhang and Seelig, 2011).

While nucleic acid computation presents a powerful tool for advancing synthetic biology and practical applications, there is still work to be done to carry this field beyond the proof-of-concept stage. Integrating logic analysis with the programmability of CRISPR-Cas technology could lead to broadening the functionality of synthetic circuits, improving their computing flexibility and efficiency (Gander *et al.*, 2017; Nielsen and Voigt, 2014). Cas9 has shown to be instrumental in creating toehold-free DNA strand displacement logic circuits, implementing molecular converters for signal detection and amplification (Montagud-Martinez *et al.*, 2021). Also,

isothermal approaches for amplifying and detecting DNA have been developed using a CRISPR-Cas9-triggered nicking endonuclease-mediated strand displacement amplification method (Zhou *et al.*, 2018). Similarly, the same strand displacement principle with the cleavage activity of Cas12 has been combined to achieve multiplexed nucleic acid detection in several steps (Fu *et al.*, 2023). Conversely, principles from nucleic acid computation have also resulted in improvements to CRISPR systems, especially in constructing conditionally responsive systems, where different elements are engineered to respond to specific signals (Hanewich-Hollatz *et al.*, 2019; Jin *et al.*, 2019; Lin *et al.*, 2020).

By leveraging the capability for integrating signals, CRISPR systems can be indeed fine-tuned to respond to diverse stimuli, facilitating the development of strategies for precise conditional control regulation over CRISPR-Cas activity. This refers to the developments of methods applied to modulate the activity of CRISPR-Cas systems in a temporal and spatial manner. The conditional control can be directed to regulate Cas protein or sgRNA activity in response to specific signals, and it can help to minimize off-target effects and increase specificity and precision (Nuñez *et al.*, 2016; Richter *et al.*, 2017). Temporal control also allows to activate or deactivate Cas9 activity at specific time points. Split-Cas9 variants have been engineered to enable controllable assembly by a chemically inducible dimerization, or regaining activity when associating upon sgRNA binding (Wright *et al.*, 2015; Zetsche *et al.*, 2015b). Light can also induce dimerization to reconstitute the activity of split-Cas9 fragments (Nihongaki *et al.*, 2015). These approaches require two separate polypeptides, though alternative strategies to engineer such Cas proteins using only a single polypeptide are also being investigated. Current work in this area has been focused on using chemical, optical or thermal triggers. Alternatively, the insertion of a variety of ligand-binding domains allowed for Cas9 nucleases that are activated by the presence of a cell-permeable small molecule. The fusion of the nuclease to these domains disrupts Cas9 activity, whereas the presence of the ligand restores its activity through conformational changes that trigger protein splicing or by nuclear translocation, allowing the reconstitution of the complex with the sgRNA. (Davis *et al.*, 2015; Liu *et al.*, 2016a; Nguyen *et al.*, 2016). Optical control of

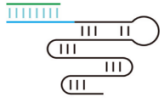
Cas9 function can be achieved using a photolabile caging group inserted into a lysine residue. The photocaged form of the amino acid results in a non-functional protein, and upon UV irradiation, the caged amino acid is liberated and Cas9 becomes active again (Hemphill *et al.*, 2015). Furthermore, while screening engineered Cas9 variants activated by blue light, Ritcher *et al.*, 2016 also identified a temperature-sensitive variant with robust activity at 29 °C but negligible activity at 37 °C.

In addition to modulating the Cas protein, another effective strategy for controlling CRISPR-Cas systems involves targeting the sgRNA itself. By directly modulating the availability, conformation, or interaction with other elements of the sgRNA, researchers can exert precise and dynamic regulation over the targeting specificity and activity of the CRISPR system. This approach complements the modulation of Cas proteins and offers additional flexibility in fine-tuning CRISPR functionality. Because sgRNA is target-dependent, its regulation has the potential to independently regulate each target, offering so-called orthogonal regulation, allowing its use in multiplexing scenarios. This strategy has been approached by engineering synthetic antisense RNA to sequester and inactivate the sgRNA in a tunable way (**Figure 8.a**) (Lee *et al.*, 2016). Inserting a back-fold extension to the 5' end of the sgRNA yields the formation of a spacer blocking hairpin (SBH). The SBH loop can be replaced with conditional RNA-cleaving units, generating inducible SHB designs that can control CRISPR activity in the presence of specific inducers (**Figure 8.b**) (Ferry *et al.*, 2017). Indeed, by incorporating ligand-responsive self-cleaving catalytic RNAs (aptazymes) between the spacer and blocked sequence, small-molecule control of sgRNA structure and genome engineering activity can be achieved (**Figure 8.c**) (Tang *et al.*, 2017). Light-dependent sgRNAs can also be constructed, made by blocking the guide sequence with a complementary oligonucleotide containing photocleavable groups (**Figure 8.d**). Upon light trigger the complementary oligonucleotides are destroyed, resulting in release of the sgRNA and restoration of Cas9 activity (Jain *et al.*, 2016). The introduction of caged nucleobases into the sgRNA sequence also leads to rapid restoration of CRISPR function upon light activation (**Figure 8.e**) (Zhou *et al.*, 2020b). Cas9 can also be deactivated with photocleavable sgRNA by the incorporation of a single photocleavable 2-nitrobenzyl modification in the

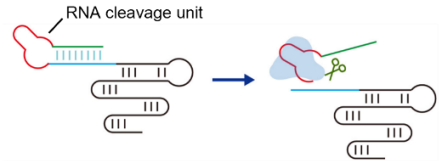
middle of the guide sequence. Light triggers the sgRNA cleavage and deactivation, yielding fast and near complete inhibition on CRISPR function (**Figure 8.f**) (Zou *et al.*, 2021). Toehold riboswitches (Green *et al.*, 2014) can also be incorporated into sgRNA scaffolds offering conditional control. In this design, the toehold-strand is added as a stem-loop structure sequestering the sgRNA spacer. Upon trigger strand interaction, the toehold strand is displaced and the sgRNA becomes activated (**Figure 8.g**) (Siu and Chen, 2019).

In addition, aptamers, single-stranded nucleic acid with a defined structure that can specifically bind a target with high affinity, can be designed as a conformational switching motif to engineer ligand-responsive systems (Nutiu and Li, 2003). Liu *et al.* (2016b) included ligand-responsive riboswitches in the sgRNA, which is blocked and inactive until the binding of a specific ligand which renders the guide sequence accessible (**Figure 8.h**). The insertion of an aptamer into the sgRNA stem loops was employed to develop a new method for small-molecule control of CRISPR-Cas9 function. The ligand binding could either stabilize or destabilize the functional sgRNA conformation, compromising the Cas9 binding (**Figure 8.i**). This method can be used to both activate and deactivate the CRISPR function in response to a small molecule (Kundert *et al.*, 2019). Another strategy has been followed by extending the 3' end of the sgRNA with both a blocking and an aptamer as a triggering motif, which involves no significant modification of the sgRNA skeleton (**Figure 8.j**) (Lin *et al.*, 2019). These strategies are useful for a wide range of applications in many scenarios; there are already a large number of aptamer-ligand pairs described and currently available; and new aptamers for specific molecules of interest can be routinely selected through systematic evolution of ligands by exponential enrichment (SELEX) (Ni *et al.*, 2020; Zhang *et al.*, 2019).

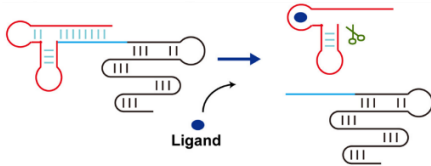
a Antisense RNA spacer-blocking



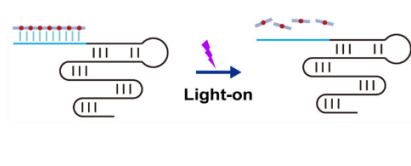
b Spacer-blocking hairpin



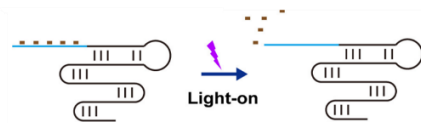
c Aptamer-based ribozyme



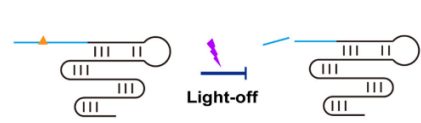
d Photocleavable ssDNA



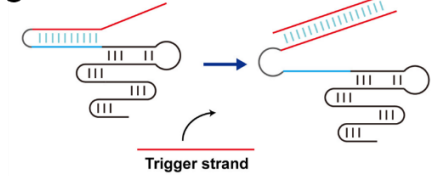
e Photocaged nucleobases



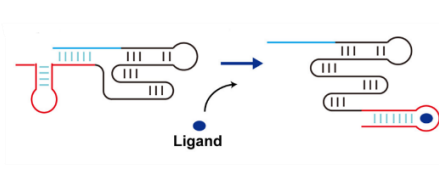
f Photocleavable sgRNA



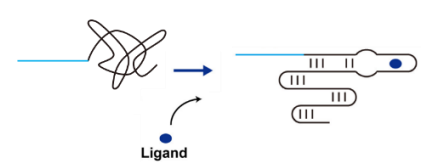
g Toehold-gated guide RNA



h Aptamer-based riboswitch



i Ligand-activated guide RNA



j Ligand-activated guide RNA (extending 3' end)

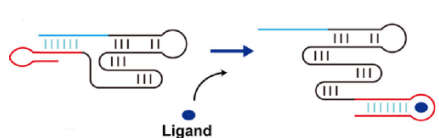


Figure 8. sgRNA engineering strategies to conditionally control CRISPR-Cas9 (adapted from Hu *et al.*, 2023).

MOTIVATION FOR EXPANDING THE CRISPR TOOLKIT

Further developing the diagnostic capabilities of CRISPR technologies represents a promising avenue for creating accurate and economical diagnostic methods, in this thesis we explore this potential for CRISPR-Cas9. By harnessing Cas9's precision and programmability, we aim to develop a novel diagnostic tool that is accurate, rapid, and can be readily deployed in various settings.

Traditional CRISPR-diagnostic methods described in the literature predominantly rely on non-specific collateral activity, which, while effective, can limit the scope of their applications due to its inherent non-specificity. We propose leveraging the properties of the Cas9 effector to overcome these limitations. Thanks to the absence of general collateral cleavage activity in sgRNA-Cas9, simultaneous detection of different targets can be easily achieved in a rapid way. This also allows for additional sequences to be utilized in downstream processing, enabling us to move beyond the single detection paradigm. This development will facilitate more sophisticated diagnostic and biocomputational applications, such as multiplexed detection and the integration of logic circuits within diagnostic assays. Ultimately, our vision is to enhance the versatility and utility of CRISPR-based diagnostics, making them applicable in both clinical and field settings.

REFERENCES

- Abels SG, Khisamutdinov EF (2015) Nucleic acid computing and its potential to transform silicon-based technology. *DNA and RNA Nanotechnol* 2, 13-22.
- Abudayyeh OO, Gootenberg JS, Kellner MJ, Zhang F (2019) Nucleic acid detection of plant genes using CRISPR-Cas13. *The CRISPR journal* 2, 165-171.
- Abudayyeh OO, Gootenberg JS, Konermann S, Joung J, Slaymaker IM, *et al.* (2016) C2c2 is a single-component programmable RNA-guided RNA-targeting CRISPR effector. *Science* 353, aaf5573.
- Ackerman CM, Myhrvold C, Thakku SG, Freije CA, Metsky HC, *et al.* (2020) Massively multiplexed nucleic acid detection with Cas13. *Nature* 582, 277-282.
- Adleman LM (1994) Molecular computation of solutions to combinatorial problems. *Science* 266, 1021-1024.
- Ali Z, Aman R, Mahas A, Rao GS, Tehseen M, *et al.* (2020) iSCAN: An RT-LAMP-coupled CRISPR-Cas12 module for rapid, sensitive detection of SARS-CoV-2. *Virus Res* 288, 198129.
- Ali Z, Sánchez E, Tehseen M, Mahas A, Marsic T, *et al.* (2021) Bio-SCAN: A CRISPR/dCas9-based lateral flow assay for rapid, specific, and sensitive detection of SARS-CoV-2. *ACS Synth Biol* 11, 406-419.
- Baker RE, Mahmud AS, Miller IF, Rajeev M, Rasambainarivo F, *et al.* (2022) Infectious disease in an era of global change. *Nat Rev Microbiol* 20, 193-205.
- Barrangou R, Doudna JA (2016) Applications of CRISPR technologies in research and beyond. *Nat Biotechnol* 34, 933-941.
- Bhaya D, Davison M, Barrangou R (2011) CRISPR-Cas systems in bacteria and archaea: versatile small RNAs for adaptive defense and regulation. *Annu Rev Genet* 45, 273-297.

- Bolotin A, Quinquis B, Sorokin A, Ehrlich SD (2005) Clustered regularly interspaced short palindrome repeats (CRISPRs) have spacers of extrachromosomal origin. *Microbiology* 151, 2551–2561.
- Broughton JP, Deng X, Yu G, Fasching CL, Servellita V, *et al.* (2020) CRISPR-Cas12- based detection of SARS-CoV-2. *Nat Biotechnol* 38, 870–874.
- Chavez A, Scheiman J, Vora S, Pruitt BW, Tuttle M, *et al.* (2015) Highly efficient Cas9-mediated transcriptional programming. *Nat Methods* 12, 326-328.
- Chen B, Gilbert LA, Cimini BA, Schnitzbauer J, Zhang W, *et al.* (2013) Dynamic imaging of genomic loci in living human cells by an optimized CRISPR/Cas system. *Cell* 155, 1479-1491.
- Chen J, Chen Y, Huang L, Lin X, Chen H, *et al.* (2024) Trans-nuclease activity of Cas9 activated by DNA or RNA target binding. *Nat Biotechnol*, 1-11.
- Chen JS, Ma E, Harrington LB, Da Costa M, Tian X, *et al.* (2018) CRISPR-Cas12a target binding unleashes indiscriminate single-stranded DNase activity. *Science* 360, 436-439.
- Cong L, Ran FA, Cox D, Lin S, Barretto R, *et al.* (2013) Multiplex genome engineering using CRISPR/Cas systems. *Science* 339, 819-823.
- Davis KM, Pattanayak V, Thompson DB, Zuris JA, Liu DR (2015) Small molecule-triggered Cas9 protein with improved genome-editing specificity. *Nat Chem Biol* 11, 316-318.
- Deltcheva E, Chylinski K, Sharma CM, Gonzales K, Chao Y, *et al.* (2011) CRISPR RNA maturation by trans-encoded small RNA and host factor RNase III. *Nature* 471, 602-607.
- Doudna JA, Charpentier E (2014) The new frontier of genome engineering with CRISPR-Cas9. *Science* 346, 1258096.

- East-Seletsky A, O'Connell MR, Knight SC, Burstein D, Cate JH, *et al.* (2016). Two distinct RNase activities of CRISPR-C2c2 enable guide-RNA processing and RNA detection. *Nature* 538, 270-273.
- Fan D, Wang J, Wang E, Dong S (2020) Propelling DNA computing with materials' power: Recent advancements in innovative DNA logic computing systems and smart bio-applications. *Adv Sci* 7, 2001766.
- Ferry QR, Lyutova R, Fulga TA (2017) Rational design of inducible CRISPR guide RNAs for de novo assembly of transcriptional programs. *Nat Commun* 8, 14633.
- Fozouni P, Son S, Díaz de León Derby M, Knott GJ, Gray CN, *et al.* (2021) Amplification-free detection of SARS-CoV-2 with CRISPR-Cas13a and mobile phone microscopy. *Cell* 184, 323-333.
- Fu J, Zhang L, Long Y, Liu Z, Meng G, *et al.* (2023) Multiplexed CRISPR-Based Nucleic Acid Detection Using a Single Cas Protein. *Anal Chem* 95, 16089-16097.
- Gander MW, Vrana JD, Voje WE, Carothers JM, Klavins E (2017) Digital logic circuits in yeast with CRISPR-dCas9 NOR gates. *Nat Commun* 8, 15459.
- Garneau JE, Dupuis MÈ, Villion M, Romero DA, Barrangou R, *et al.* (2010) The CRISPR/Cas bacterial immune system cleaves bacteriophage and plasmid DNA. *Nature* 468, 67-71.
- Gasiunas G, Barrangou R, Horvath P, Siksnyš V (2012) Cas9-crRNA ribonucleoprotein complex mediates specific DNA cleavage for adaptive immunity in bacteria. *PNAS* 109, E2579-E2586.
- Gilbert LA, Larson MH, Morsut L, Liu Z, Brar GA, *et al.* (2013) CRISPR-mediated modular RNA-guided regulation of transcription in eukaryotes. *Cell* 154, 442-451.
- Gootenberg JS, Abudayyeh OO, Kellner MJ, Joung J, Collins JJ, Zhang F (2018) Multiplexed and portable nucleic acid detection platform with Cas13, Cas12a, and Csm6. *Science* 360, 439-444.

- Gootenberg JS, Abudayyeh OO, Lee JW, Essletzbichler P, Dy AJ, *et al.* (2017) Nucleic acid detection with CRISPR-Cas13a/C2c2. *Science* 356, 438-442.
- Green AA, Silver PA, Collins JJ, Yin P (2014) Toehold switches: de-novo-designed regulators of gene expression. *Cell* 159, 925-939.
- Green DA, StGeorge K (2018) Rapid antigen tests for influenza: rationale and significance of the FDA reclassification. *J Clin Microbiol* 56, 10-1128.
- Hajian R, Balderston S, Tran T, DeBoer T, Etienne J, *et al.* (2019) Detection of unamplified target genes via CRISPR-Cas9 immobilized on a graphene field-effect transistor. *Nat Biomed Eng* 3, 427-437.
- Halamek J, Bocharova V, Chinnapareddy S, Windmiller JR, Strack G, *et al.* (2010) Multi-enzyme logic network architectures for assessing injuries: digital processing of biomarkers. *Mol Biosyst* 6, 2554-2560.
- Han D, Zhu Z, Wu C, Peng L, Zhou L, *et al.* (2012) A logical molecular circuit for programmable and autonomous regulation of protein activity using DNA aptamer-protein interactions. *J Am Chem Soc* 134, 20797-20804.
- Hanewich-Hollatz MH, Chen Z, Hochrein LM, Huang J, Pierce NA (2019) Conditional guide RNAs: programmable conditional regulation of CRISPR/Cas function in bacterial and mammalian cells via dynamic RNA nanotechnology. *ACS Cent Sci* 5, 1241-1249.
- Harrington LB, Burstein D, Chen JS, Paez-Espino D, Ma E, *et al.* (2018) Programmed DNA destruction by miniature CRISPR-Cas14 enzymes. *Science* 362, 839-842.
- Hemphill J, Borchardt EK, Brown K, Asokan A, Deiters A (2015) Optical control of CRISPR/Cas9 gene editing. *J Am Chem Soc* 137, 5642-5645.
- Horvath P, Barrangou R (2010) CRISPR/Cas, the immune system of bacteria and archaea. *Science* 327, 167-170.
- Hu LF, Li YX, Wang JZ, Zhao YT, Wang Y (2023) Controlling CRISPR-Cas9 by guide RNA engineering. *Wiley Interdiscip Rev RNA* 14, e1731.

- Huang M, Zhou X, Wang H, Xing D (2018) Clustered regularly interspaced short palindromic repeats/Cas9 triggered isothermal amplification for site-specific nucleic acid detection. *Anal Chem* 90, 2193-2200.
- Ishino Y, Krupovic M, Forterre P (2018) History of CRISPR-Cas from encounter with a mysterious repeated sequence to genome editing technology. *J Bacteriol* 200, 10-1128.
- Ishino Y, Shinagawa H, Makino K, Amemura M, Nakata A (1987) Nucleotide sequence of the *iap* gene, responsible for alkaline phosphatase isozyme conversion in *Escherichia coli*, and identification of the gene product. *J Bacteriol* 169, 5429-5433.
- Jain PK, Ramanan V, Schepers AG, Dalvie NS, Panda A, *et al.* (2016) Development of light-activated CRISPR using guide RNAs with photocleavable protectors. *Angew Chem Int Ed Engl* 55, 12440-12444.
- Jansen R, Embden JDV, Gaastra W, Schouls LM (2002) Identification of genes that are associated with DNA repeats in prokaryotes. *Mol Microbiol* 43, 1565-1575.
- Jiang F, Doudna JA (2017) CRISPR–Cas9 structures and mechanisms. *Annu Rev Biophys* 46, 505-529.
- Jiao C, Sharma S, Dugar G, Peeck NL, Bischler T, *et al.* (2021) Noncanonical crRNAs derived from host transcripts enable multiplexable RNA detection by Cas9. *Science* 372, 941-948.
- Jin M, Garreau de Loubresse N, Kim Y, Kim J, Yin P (2019) Programmable CRISPR-Cas repression, activation, and computation with sequence-independent targets and triggers. *ACS Synth Biol* 8, 1583-1589.
- Jinek M, Chylinski K, Fonfara I, Hauer M, Doudna JA, Charpentier E (2012) A programmable dual-RNA-guided DNA endonuclease in adaptive bacterial immunity. *Science* 337, 816-821.
- Jinek M, East A, Cheng A, Lin S, Ma E, Doudna J (2013) RNA-programmed genome editing in human cells. *elife* 2, e00471.

- Kaminski MM, Abudayyeh OO, Gootenberg JS, Zhang F, Collins JJ (2021) CRISPR-based diagnostics. *Nat Biomed Eng* 5, 643-656.
- Kao RR, Haydon DT, Lycett SJ, Murcia PR (2014) Supersize me: how whole-genome sequencing and big data are transforming epidemiology. *Trends Microbiol* 22, 282-291.
- Karvelis T, Bigelyte G, Young JK, Hou Z, Zedaveinyte R, *et al.* (2020) PAM recognition by miniature CRISPR–Cas12f nucleases triggers programmable double-stranded DNA target cleavage. *Nucleic Acids Res* 48, 5016-5023.
- Katz E (2015) Biocomputing—Tools, aims, perspectives. *Curr Opin Biotechnol* 34, 202-208.
- Kundert K, Lucas JE, Watters KE, Fellmann C, Ng AH, *et al.* (2019) Controlling CRISPR-Cas9 with ligand-activated and ligand-deactivated sgRNAs. *Nat Commun* 10, 2127.
- Land KJ, Boeras DI, Chen XS, Ramsay AR, Peeling RW (2019) REASSURED diagnostics to inform disease control strategies, strengthen health systems and improve patient outcomes. *Nat Microbiol* 4, 46-54.
- Lee RA, Puig HD, Nguyen PQ, Angenent-Mari NM, Donghia NM, *et al.* (2020) Ultrasensitive CRISPR-based diagnostic for field-applicable detection of Plasmodium species in symptomatic and asymptomatic malaria. *PNAS* 117, 25722-25731.
- Lee YJ, Hoynes-O'Connor A, Leong MC, Moon TS (2016) Programmable control of bacterial gene expression with the combined CRISPR and antisense RNA system. *Nucleic Acids Res* 44, 2462-2473.
- Li L, Li S, Wu N, Wu J, Wang G, *et al.* (2019b) HOLMESv2: a CRISPR-Cas12b-assisted platform for nucleic acid detection and DNA methylation quantitation. *ACS Synth Biol* 8, 2228-2237.

- Li SY, Cheng QX, Liu JK, Nie XQ, Zhao GP, Wang J (2018a) CRISPR-Cas12a has both cis-and trans-cleavage activities on single-stranded DNA. *Cell Res* 28, 491-493.
- Li SY, Cheng QX, Wang JM, Li XY, Zhang ZL, Gao S, *et al.* (2018b) CRISPR-Cas12a-assisted nucleic acid detection. *Cell Discov* 4, 20.
- Li Y, Li S, Wang J, Liu G (2019a) CRISPR/Cas systems towards next-generation biosensing. *Trends Biotechnol* 37, 730-743.
- Lin B, An Y, Meng L, Zhang H, Song J, *et al.* (2019) Control of CRISPR-Cas9 with small molecule-activated allosteric aptamer regulating sgRNAs. *Chem Commun* 55, 12223-12226.
- Lin J, Liu Y, Lai P, Ye H, Xu L (2020) Conditional guide RNA through two intermediate hairpins for programmable CRISPR/Cas9 function: building regulatory connections between endogenous RNA expressions. *Nucleic Acids Res* 48, 11773-11784.
- Liu KI, Ramli MNB, Woo CWA, Wang Y, Zhao T, *et al.* (2016a) A chemical-inducible CRISPR-Cas9 system for rapid control of genome editing. *Nature Chem Biol* 12, 980-987.
- Liu Y, Zhan Y, Chen Z, He A, Li J, *et al.* (2016b) Directing cellular information flow via CRISPR signal conductors. *Nat Methods* 13, 938-944.
- Mahfouz M (2024) Revolutionizing Point-of-Care Diagnostics via CRISPR Systems. *ACS Synth Biol* 13, 411-412.
- Makarova KS, Wolf YI, Iranzo J, Shmakov SA, Alkhnbashi OS, *et al.* (2020) Evolutionary classification of CRISPR-Cas systems: a burst of class 2 and derived variants. *Nat Rev Microbiol* 18, 67-83.
- Mali P, Yang L, Esvelt KM, Aach J, Guell M, *et al.* (2013) RNA-guided human genome engineering via Cas9. *Science* 339, 823-826.
- Marques MC, Sanchez-Vicente J, Ruiz R, Montagud-Martinez R, Márquez-Costa R, *et al.* (2022) Diagnostics of infections produced by the plant

- viruses TMV, TEV, and PVX with CRISPR-Cas12 and CRISPR-Cas13. *ACS Synth Biol* 11, 2384-2393.
- Marsic T, Ali Z, Tehseen M, Mahas A, Hamdan S, Mahfouz M (2021) Vigilant: an engineered VirD2-Cas9 complex for lateral flow assay-based detection of SARS-CoV2. *Nano Lett* 21, 3596-3603.
- Mojica FJ, Díez-Villaseñor C, García-Martínez J, Almendros C (2009) Short motif sequences determine the targets of the prokaryotic CRISPR defence system. *Microbiol* 155, 733-740.
- Mojica FJ, Díez-Villaseñor C, Soria E, Juez G (2000) Biological significance of a family of regularly spaced repeats in the genomes of Archaea, Bacteria and mitochondria. *Mol Microbiol*,36, 244-246.
- Mojica FJ, Díez-Villaseñor CS, García-Martínez J, Soria E (2005) Intervening sequences of regularly spaced prokaryotic repeats derive from foreign genetic elements. *J Mol Evol* 60, 174-182.
- Mojica FJ, Juez G, Rodríguez-Valera F (1993) Transcription at different salinities of *Haloferax mediterranei* sequences adjacent to partially modified PstI sites. *Mol Microbiol* 9, 613-621.
- Mojica FJM, Ferrer C, Juez G, Rodríguez-Valera F (1995) Long stretches of short tandem repeats are present in the largest replicons of the *Archaea Haloferax mediterranei* and *Haloferax volcanii* and could be involved in replicon partitioning. *Mol Microbiol* 17, 85-93.
- Momčilović S, Cantacessi C, Arsić-Arsenijević V, Otranto D, Tasić-Otašević S (2019) Rapid diagnosis of parasitic diseases: current scenario and future needs. *Clin Microbiol Infect* 25, 290-309.
- Montagud-Martinez R, Heras-Hernandez M, Goiriz L, Daros JA, Rodrigo G (2021) CRISPR-mediated strand displacement logic circuits with toehold-free DNA. *ACS Synth Biol* 10, 950-956.
- Morisaka H, Yoshimi K, Okuzaki Y, Gee P, Kunihiro Y, *et al.* (2019) CRISPR-Cas3 induces broad and unidirectional genome editing in human cells. *Nat Commun* 10, 5302.

- Myhrvold C, Freije CA, Gootenberg JS, Abudayyeh OO, Metsky HC, *et al.* (2018) Field-deployable viral diagnostics using CRISPR-Cas13. *Science* 360, 444-448.
- Nguyen DP, Miyaoka Y, Gilbert LA, Mayerl SJ, Lee BH, *et al.* (2016) Ligand-binding domains of nuclear receptors facilitate tight control of split CRISPR activity. *Nat Commun* 7, 12009.
- Ni S, Zhuo Z, Pan Y, Yu Y, Li F, *et al.* (2020) Recent progress in aptamer discoveries and modifications for therapeutic applications. *ACS Appl Mater Interfaces* 13, 9500-9519.
- Nielsen AA, Voigt CA (2014) Multi-input CRISPR/C as genetic circuits that interface host regulatory networks. *Mol Syst Biol* 10, 763.
- Nihongaki Y, Kawano F, Nakajima T, Sato M (2015) Photoactivatable CRISPR-Cas9 for optogenetic genome editing. *Nat Biotechnol* 33, 755-760.
- Nishimasu H, Ran FA, Hsu PD, Konermann S, Shehata SI, *et al.* (2014) Crystal structure of Cas9 in complex with guide RNA and target DNA. *Cell* 156, 935-949.
- Nuñez JK, Harrington LB, Doudna JA (2016) Chemical and biophysical modulation of Cas9 for tunable genome engineering. *ACS Chem Biol*, 11, 681-688.
- Nutiu R, Li Y (2003) Structure-switching signaling aptamers. *J Am Chem Soc* 125, 4771-4778.
- Pardee K, Green AA, Takahashi MK, Braff D, Lambert G, *et al.* (2016) Rapid, low-cost detection of Zika virus using programmable biomolecular components. *Cell* 165, 1255-1266.
- Peeling RW, Olliaro PL, Boeras DI, Fongwen N (2021) Scaling up COVID-19 rapid antigen tests: promises and challenges. *Lancet Infect Dis* 21, e290-e295.
- Pei R, Matamoros E, Liu M, Stefanovic D, Stojanovic MN (2010) Training a molecular automaton to play a game. *Nat Nanotechnol* 5, 773-777.

- Pourcel C, Salvignol G, Vergnaud G (2005) CRISPR elements in *Yersinia pestis* acquire new repeats by preferential uptake of bacteriophage DNA, and provide additional tools for evolutionary studies. *Microbiology* 151, 653-663.
- Privman V, Zavalov O, Halámková L, Moseley F, Halánek J, *et al.* (2013) Networked enzymatic logic gates with filtering: New theoretical modeling expressions and their experimental application. *J Phys Chem B* 117, 14928-14939.
- Qian L, Winfree E (2011) Scaling up digital circuit computation with DNA strand displacement cascades. *Science* 332, 1196-1201.
- Qian L, Winfree E, Bruck J (2011) Neural network computation with DNA strand displacement cascades. *Nature* 475, 368-372.
- Rao A, Westbrook A, Bassit L, Parsons R, Fitts E, *et al.* (2023) Sensitivity of rapid antigen tests against SARS-CoV-2 Omicron and Delta variants. *J Clin Microbiol* 61, e00138-23.
- Richter F, Fonfara I, Bouazza B, Schumacher CH, Bratovič M, *et al.* (2016) Engineering of temperature- and light-switchable Cas9 variants. *Nucleic Acids Res* 44, gkw930.
- Richter F, Fonfara I, Gelfert R, Nack J, Charpentier E, *et al.* (2017) Switchable Cas9. *Curr Opin Biotechnol* 48 119-126.
- Seelig G, Soloveichik D, Zhang DY, Winfree E (2006) Enzyme-free nucleic acid logic circuits. *Science* 314, 1585-1588.
- Shinoda H, Taguchi Y, Nakagawa R, Makino A, Okazaki S, *et al.* (2021) Amplification-free RNA detection with CRISPR-Cas13. *Commun Biol* 4, 476.
- Simmel FC, Yurke B, Singh HR (2019) Principles and applications of nucleic acid strand displacement reactions. *Chem Rev* 119, 6326-6369.
- Siu KH, Chen W (2019) Riboregulated toehold-gated gRNA for programmable CRISPR-Cas9 function. *Nat Chem Biol* 15, 217-220.

- Sternberg SH, Redding S, Jinek M, Greene EC, Doudna JA (2014) DNA interrogation by the CRISPR RNA-guided endonuclease Cas9. *Biophys J* 106, 695a.
- Stojanović MN, Stefanović D (2003a) Deoxyribozyme-based half-adder. *J Am Chem Soc* 125, 6673-6676.
- Stojanovic MN, Stefanovic D (2003b) A deoxyribozyme-based molecular automaton. *Nat Biotechnol* 21, 1069-1074.
- Szczelkun MD, Tikhomirova MS, Sinkunas T, Gasiunas G, Karvelis T, *et al.* (2014) Direct observation of R-loop formation by single RNA-guided Cas9 and Cascade effector complexes. *PNAS* 111, 9798-9803.
- Tang W, Hu JH, Liu DR (2017) Aptazyme-embedded guide RNAs enable ligand-responsive genome editing and transcriptional activation. *Nat Commun* 8, 15939.
- Udugama B, Kadhiresan P, Kozlowski HN, Malekjahani A, Osborne M, *et al.* (2020). Diagnosing COVID-19: the disease and tools for detection. *ACS nano* 14, 3822-3835.
- Wang DG, Brewster JD, Paul M, Tomasula PM (2015) Two methods for increased specificity and sensitivity in loop-mediated isothermal amplification. *Molecules* 20, 6048-6059.
- Wang X, Xiong E, Tian T, Cheng M, Lin W, *et al.* (2020) Clustered regularly interspaced short palindromic repeats/Cas9-mediated lateral flow nucleic acid assay. *ACS nano* 14, 2497-2508.
- Wright AV, Sternberg SH, Taylor DW, Staahl BT, Bardales JA, *et al.* (2015) Rational design of a split-Cas9 enzyme complex. *PNAS* 112, 2984-2989.
- Xiong E, Jiang L, Tian T, Hu M, Yue H, *et al.* (2021) Simultaneous dual-gene diagnosis of SARS-CoV-2 based on CRISPR/Cas9-mediated lateral flow assay. *Angew Chem Int Ed Engl* 60, 5307-5315.
- Yin P, Choi HM, Calvert CR, Pierce NA (2008) Programming biomolecular self-assembly pathways. *Nature* 451, 318-322.

- Yoshimi K, Takeshita K, Yamayoshi S, Shibumura S, Yamauchi Y, *et al.* (2022) CRISPR-Cas3-based diagnostics for SARS-CoV-2 and influenza virus. *Isience* 25, 103830.
- Yurke B, Turberfield AJ, Mills JAP, Simmel FC, Neumann JL (2000) A DNA-fuelled molecular machine made of DNA. *Nature* 406, 605-608.
- Zetsche B, Gootenberg JS, Abudayyeh OO, Slaymaker IM, Makarova KS, *et al.* (2015a) Cpf1 is a single RNA-guided endonuclease of a class 2 CRISPR-Cas system. *Cell* 163, 759-771.
- Zetsche B, Volz SE, Zhang F (2015b) A split-Cas9 architecture for inducible genome editing and transcription modulation. *Nat Biotechnol* 33, 139-142.
- Zhang DY, Seelig G (2011) Dynamic DNA nanotechnology using strand-displacement reactions. *Nat Chem* 3, 103-113.
- Zhang DY, Winfree E (2009) Control of DNA strand displacement kinetics using toehold exchange. *J Am Chem Soc* 131, 17303-17314
- Zhang Y, Lai BS, Juhas M (2019) Recent advances in aptamer discovery and applications. *Molecules* 24, 941.
- Zhang Y, Qian L, Wei W, Wang Y, Wang B, *et al.* (2017) Paired design of dCas9 as a systematic platform for the detection of featured nucleic acid sequences in pathogenic strains. *ACS Synth Biol* 6, 211-216.
- Zhao Y, Chen F, Li Q, Wang L, Fan C (2015) Isothermal amplification of nucleic acids. *Chem Rev* 115, 12491-12545.
- Zhou J, Yin L, Dong Y, Peng L, Liu G, *et al.* (2020a) CRISPR-Cas13a based bacterial detection platform: Sensing pathogen *Staphylococcus aureus* in food samples. *Anal Chim Acta* 1127, 225-233.
- Zhou W, Brown W, Bardhan A, Delaney M, Ilk AS, *et al.* (2020b) Spatiotemporal control of CRISPR/Cas9 function in cells and zebrafish using light-activated guide RNA. *Angew Chem Int Ed Engl* 59, 8998-9003.

Zhou W, Hu L, Ying L, Zhao Z, Chu PK, Yu XF (2018) A CRISPR–Cas9-triggered strand displacement amplification method for ultrasensitive DNA detection. *Nat Commun* 9, 5012.

Zou RS, Liu Y, Wu B, Ha T (2021) Cas9 deactivation with photocleavable guide RNAs. *Mol Cell* 81, 1553-1565.

CHAPTER 2

OBJECTIVES

CRISPR-Cas systems have shown to be a highly versatile tool, offering numerous solutions to biotechnological problems. The incorporation of CRISPR technologies as diagnostic tools represents a significant advancement towards addressing the unmet needs of existing diagnostic technologies. However, there is still room for improvement especially when it comes to scalability and specificity. This thesis aims to enlarge the CRISPR toolkit by achieving the following objectives:

1. Develop a new diagnostic tool based on Cas9-triggered strand displacement.
2. Employ CRISPR-Cas9-based detection mechanism coupled to lateral flow assay producing a colorimetric visible readout, suitable for point-of-care testing.
3. Explore CRISPR-Cas9 potential for integrating multiple different signals, especially related to biocomputation and conditional control.

CHAPTER 3

Multiplexable Virus Detection by CRISPR-Cas9-Mediated Strand Displacement

This work has been published in a peer-reviewed journal.

See the full citation:

Márquez-Costa R, Montagud-Martinez R, Marques MC, Albert E, Navarro D, Daros JA, Ruiz R, Rodrigo G (2023) Multiplexable and biocomputational virus detection by CRISPR-Cas9-mediated strand displacement. *Analytical Chemistry* 95: 9564-9574

<https://doi.org/10.1021/acs.analchem.3c01041>

My contribution to this work:

I designed the nucleic acid sequences and performed most of the experiments under the supervision of G. Rodrigo. I analyzed the data and contributed to the figures preparation and writing of the manuscript.

1. INTRODUCTION

Infectious diseases defy the modern lifestyle of our societies, and it is increasingly evident that better and handier detection methods of viruses and bacteria would facilitate their control. Of note, the coronavirus disease 2019 (COVID-19) pandemic caused by severe acute respiratory syndrome coronavirus 2 (SARS-CoV-2) (Zhu *et al.*, 2020) has highlighted the challenges in diagnostics of viral infections. A fast and confident diagnostic tool contributes to significantly reducing the transmission of the virus in the community and allows early therapeutic actions that can mitigate acute outcomes of infection. Currently, a reverse transcription quantitative polymerase chain reaction (RT-qPCR) is the gold-standard diagnostic technique of infectious diseases in the clinic due to its high sensitivity and specificity (Yang and Rothman, 2004). However, when a rapid and massive intervention is required, such as in a pandemic context, alternative techniques that can bypass, at least in part, the need for expensive equipment and well-trained personnel are highly required (Mina *et al.*, 2020).

Clustered regularly interspaced short palindromic repeats (CRISPR) systems are being repurposed in recent years for diagnostic applications (Chen *et al.*, 2018; Gootenberg *et al.*, 2017). Owing to the ability of some CRISPR-associated (Cas) proteins to display a collateral catalytic activity upon target recognition, a sensitive and specific nucleic acid detection is possible. In combination with isothermal amplification techniques (Zhao *et al.*, 2015), sensitivities at the attomolar scale (*i.e.*, about one copy per microliter) and specificities at one nucleotide resolution have been achieved, atop of bypassing the dependence on qPCR equipment. In this regard, the use of CRISPR systems may represent a suitable alternative for the diagnostics of infectious diseases in the clinic and also in the field. Notably, these systems have been already applied to detect SARS-CoV-2 in clinical samples (Broughton *et al.*, 2020). Indeed, different assays based on CRISPR-Cas12 (Broughton *et al.*, 2020; Ding *et al.*, 2020; Xiong *et al.*, 2020) or CRISPR-Cas13 (Arizti-Sanz *et al.*, 2020; Fozouni *et al.*, 2021; Patchesung *et al.*, 2020) have been implemented for the detection of SARS-CoV-2 (even the direct detection of the virus without preamplification has been possible with the

Leptotrichia buccalis Cas13a nuclease (Fozouni *et al.*, 2021)). However, the multiplexed detection remains challenging due to the nonspecificity of that collateral catalytic activity. Certainly, sensing different elements at a time can be of utility for determining the presence of coinfecting pathogens or even for genotyping and identifying diverse mutations.

To overcome this limitation, orthogonal Cas proteins can be employed to achieve multiplexed nucleic acid detection in a single reaction (*e.g.*, by using a Cas12 to target DNA and a Cas13 to target RNA) (Gootenberg *et al.*, 2018). Nevertheless, the number of nucleic acids that can be detected simultaneously is limited by the number of different Cas proteins involved in the assay. The use of droplets constitutes an alternative to distribute the detection by performing specific reactions in different compartments, thereby allowing a multiplexed detection with just one CRISPR system (Ackerman *et al.*, 2020), in addition to descending the limit of detection (Tian *et al.*, 2021). Moreover, a recent development exploited the formation of noncanonical CRISPR RNAs for multiplexed RNA detection with Cas9 revealed by gel electrophoresis (Jiao *et al.*, 2021). In any case, we still need to develop further methods that are easy to implement for multiplexed nucleic acid detection, especially to achieve point-of-care applications in emergency scenarios.

In this work, we present a novel nucleic acid detection approach based on CRISPR-Cas9 aimed at fulfilling the aforementioned gap. We exploited the absence of the collateral catalytic activity of *Streptococcus pyogenes* Cas9 to develop a simple procedure based on CRISPR-mediated strand displacement (Montagud-Martinez *et al.*, 2021) and fluorogenic molecular beacons (Tyagi and Kramer, 1996) that allows a direct multiplexed detection of nucleic acids in a single tube. We called this platform COLUMBO (CRISPR-Cas9 R-loop usage for molecular beacon opening). First, we demonstrate that this can be applied to detect SARS-CoV-2. Second, we demonstrate a simultaneous detection of three different genomic regions of this coronavirus, as well as the potential application of detecting three different viruses in the sample or even discriminating SARS-CoV-2 variants without the need for sequencing.

2. RESULTS

2.1 Rational Design of COLUMBO

COLUMBO requires a preamplification step to generate a suitable double-stranded DNA fragment from the nucleic acid of interest (DNA or RNA). This can be done by PCR or by an alternative method running isothermally, such as recombinase polymerase amplification (RPA) (Piepenburg *et al.*, 2006). In this work, we decided to use standard primers, such as the Charité E-Sarbeco primers and the Centers for Disease Control and Prevention (CDC) N1 and N2 primers for SARS-CoV-2. Nothing prevents using other primers. Importantly, the amplified DNA molecule needs to harbor a protospacer adjacent motif (PAM) for Cas9 binding (NGG). The occurrence of a PAM sequence for Cas9 is a minimal requirement that can be met in many cases, as it occurs in the E and N gene amplicons. The position of the PAM sequence within the DNA amplicon determines the length of the single guide RNA (sgRNA) spacer. In principle, spacers of 20-40 nt should be adequate. Then, the sequence-specific detection is accomplished thanks to interfacing a CRISPR-Cas9 reaction with an appropriately designed molecular beacon (single-stranded DNA, ssDNA) folding into a stem-loop structure. Once the R-loop is formed, the nontargeted DNA strand that has been displaced can interact with other nucleic acids supplied in *trans* (Richardson *et al.*, 2016). Previously, we showed that this mechanism is instrumental to engineer toehold-free DNA circuits for logic computation (Montagud-Martinez *et al.*, 2021). The precise sequence of the displaced strand conditions the sequence and secondary structure of the beacon. If it is rich in GC, the beacon can be designed with a shorter stem. The dynamic range of the beacon is uncertain *a priori*, so functional screening could be performed. Here, the interaction of the beacon with the displaced strand causes the reconfiguration of the former separating the fluorophore from the quencher, thereby producing a fluorescent signal (**Figure 1**).

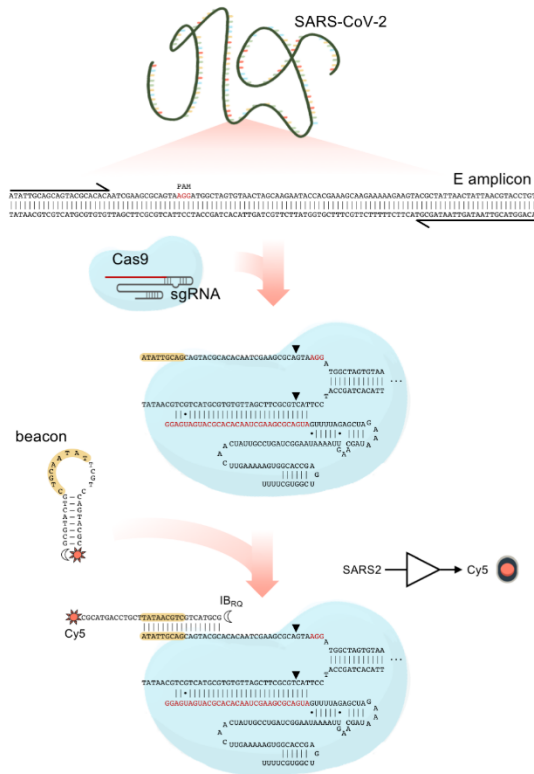


Figure 1. SARS-CoV-2 detection through a CRISPR-Cas9-based strand displacement reaction. Schematics of the global reaction of amplification and detection of a DNA product from SARS-CoV-2 E gene (PCR primers drawn at the ends), containing a PAM (shown in red) for Cas9 recognition. A preassembled CRISPR-Cas9 ribonucleoprotein targeting the amplicon (sgRNA spacer marked in red) was then able to displace a strand so that the molecular beacon could interact with and change its conformation (seed region for this interaction marked in yellow). The molecular beacon was labelled with the fluorophore Cy5 (sun icon) in the 3' end and the dark quencher IB_{RQ} (moon icon) in the 5' end. Wobble base pairs denoted by dots.

We envisioned a system in which the PAM-distal region of the displaced strand is responsible for the interaction with the beacon. The R-loop needs to be open in the PAM-distal end for the beacon to interact efficiently with the displaced strand. Otherwise, the displaced strand has not sufficient freedom. This interaction is seeded by the pairing of some nucleotides located in the loop of the beacon with the complementary nucleotides located in the 5' end

of the displaced strand, ensuring a low activation energy barrier (Rodrigo *et al.*, 2013a). The beacon is not fully complementary to the displaced strand (only one-half binds to it). Moreover, to limit the potential interaction of the beacon with the sgRNA, the spacer of the sgRNA excludes the seed region of the displaced strand. The spacer also harbors a mutation in the 5' end region to form a wobble base pair with the targeted DNA strand (Chen *et al.*, 2017). The R-loop opens spontaneously at the PAM-distal region as a result of a low melting temperature, thereby exposing the 5' end of the displaced strand to the solvent. Consequently, the beacon only opens when the ternary CRISPR complex (DNA-sgRNA-Cas9) is formed (**Figure 2**).

2.2 SARS-CoV-2 Detection with COLUMBO

Using the Charité (Berlin) E-Sarbeco primers (Vogels *et al.*, 2020), we generated a suitable DNA amplicon for COLUMBO by PCR from a test sample based on the SARS-CoV-2 E gene. The amplified material was purified to remove elements potentially interfering with the molecular beacon. An sgRNA was designed to exploit a PAM located at an appropriate position (**Figure 1**), *in vitro* transcribed from a DNA template, and assembled with a Cas9 given from a commercial preparation. In turn, a molecular beacon appropriately designed was chemically synthesized, labelling its 3' end with the fluorophore cyanine 5 (Cy5) and its 5' end with the dark quencher Iowa Black RQ (IB_{RQ}). Then, we added the sgRNA-Cas9 ribonucleoprotein to the reaction to target the amplified DNA (detection of the nucleic acid of interest) and the beacon to produce a red fluorescent signal upon interaction with the displaced strand in the PAM-distal region. Remarkably, COLUMBO displayed good performance, with a dynamic range of more than 3-fold change in red fluorescence and no apparent opening of the beacon in response to the DNA amplicon or the sgRNA alone (**Figure 3.a**).

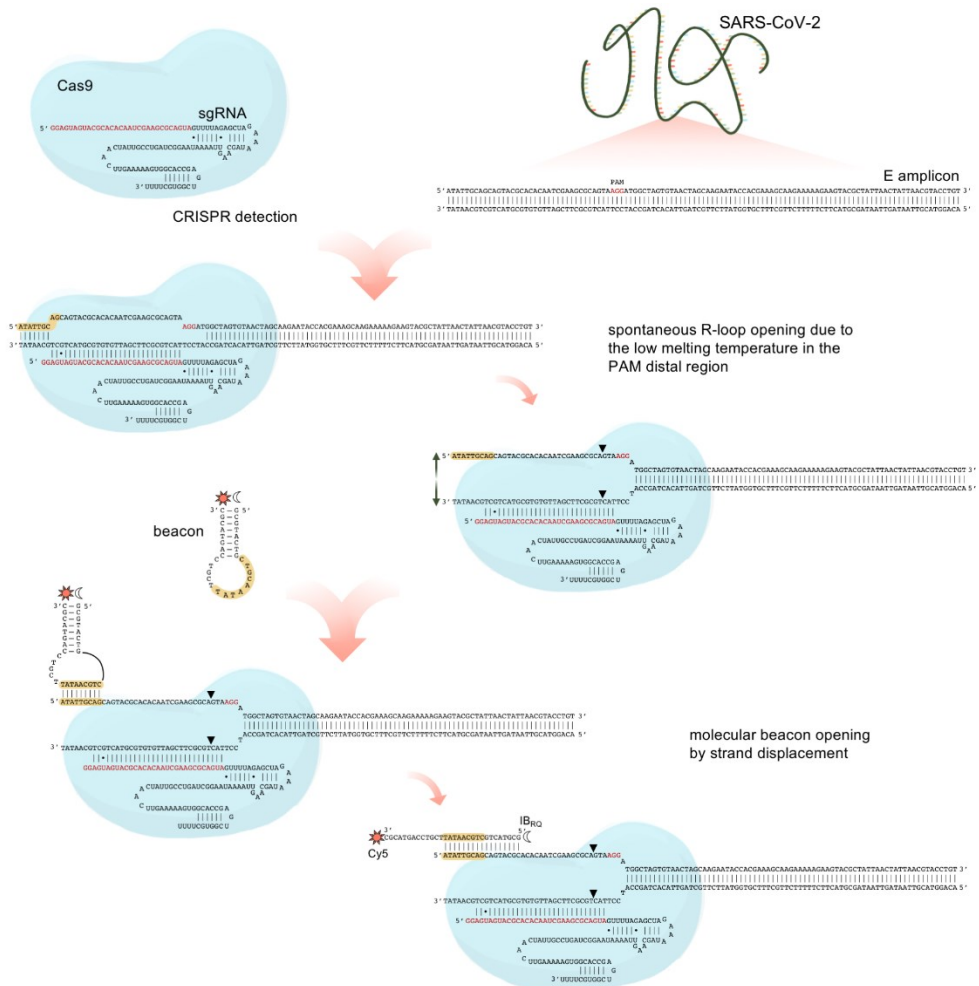


Figure 2. Detailed schematics of nucleic acid detection through CRISPR-Cas9-based strand displacement. In this example, a DNA amplicon from SARS-CoV-2 E gene was generated, containing a PAM (shown in red) for Cas9 recognition. A preassembled CRISPR-Cas9 ribonucleoprotein targeting the amplicon (sgRNA spacer marked in red) could then be used for sequence specific detection. The spacer starts by GG as it is *in vitro* transcribed by the T7 polymerase. The resulting R-loop was opened by the PAM-distal region due to a low melting temperature in the DNA end (in this example, 7 base pairs). The displaced strand could interact with a properly designed molecular beacon (seed regions marked in yellow), which opens afterwards. The molecular beacon was labelled with the fluorophore Cy5 (sun icon) in the 3' end and the dark quencher Iowa Black RQ (moon icon) in the 5' end.

The ability of the beacon to interact with the displaced strand was also assessed by agarose gel electrophoresis (**Figure 3.b**). Furthermore, we performed a set of reactions with increasing concentrations of the DNA amplicon, observing proportionality between the input and output signals (**Figure 3.c**). Thus, COLUMBO might be used to quantify a given DNA in the sample ranging from the nanomolar scale.

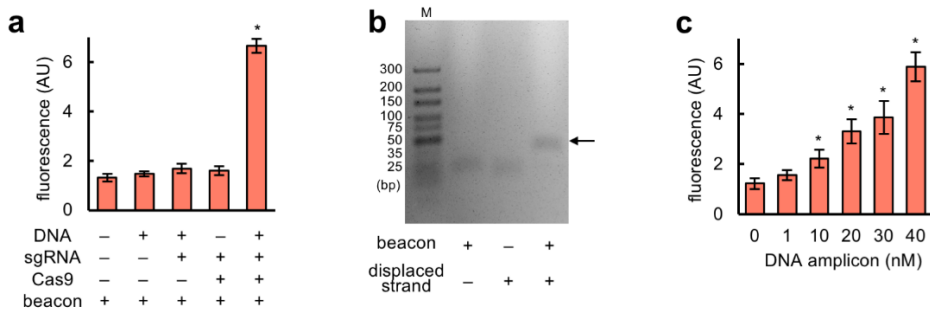


Figure 3. SARS-CoV-2 detection through a CRISPR-Cas9-based strand displacement reaction. a) Fluorescence-based characterization of the detection; amplifications performed by PCR. b) Gel electrophoretic assay to reveal the interaction between the molecular beacon and the displaced strand from the DNA amplicon (the arrow marks the intermolecular complex). M, molecular marker. c) Effect of the DNA amplicon concentration on the output fluorescence signal. Error bars correspond to standard deviations ($n = 3$). *Statistical significance with test samples (Welch's t -test, two-tailed $P < 0.05$).

Next, we tested the ability of using RPA instead of PCR to generate the DNA amplicon in combination with COLUMBO, as this is important to achieve point-of-care applications. Our results indicate that both methods are suitable, having used the very same primers (**Figure 4**). A slightly higher fluorescent signal in the presence of the target DNA was produced after PCR, while the preamplification process was faster with RPA.

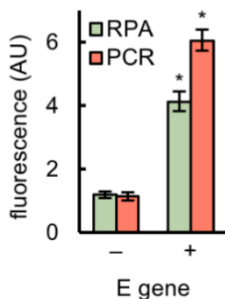


Figure 4. SARS-CoV-2 detection through a CRISPR-Cas9-based strand displacement reaction. Detection of the DNA amplicon generated by PCR or RPA (isothermal method). Error bars correspond to standard deviations ($n = 3$). *Statistical significance with test samples (Welch’s t -test, two-tailed $P < 0.05$).

In terms of sensitivity, 1 copy/ μL in the sample was detected irrespective of the amplification method (**Figure 5**).

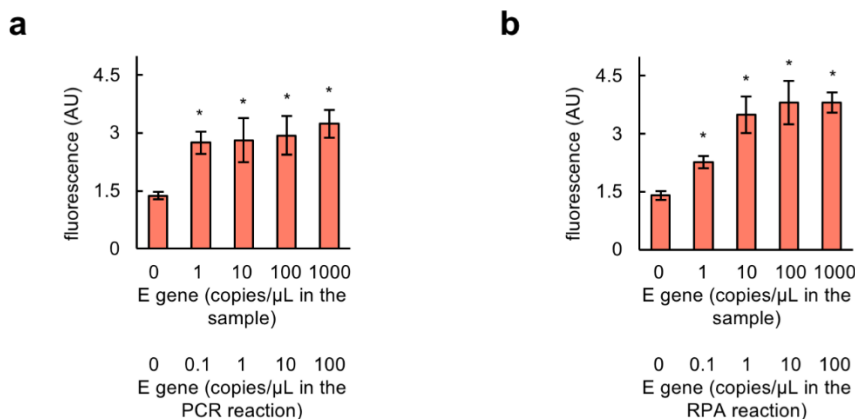


Figure 5. Limit of detection assays. a) Fluorescence-based characterization of the detection with COLUMBO-PCR. b) Fluorescence-based characterization of the detection with COLUMBO-RPA. Test samples containing the SARS-CoV-2 E gene at different concentrations were used. Error bars correspond to standard deviations ($n = 3$). *Statistical significance (Welch’s t -test, two-tailed $P < 0.05$).

In addition, we inspected the impact of the catalytic activity of Cas9 on the performance of COLUMBO. To this end, we used three different versions of Cas9: the wild-type nuclease, the Cas9 H840A nickase (Cas9n), which only cleaves the nontargeted strand, and the catalytically dead Cas9 protein (dCas9), which does not produce any cleavage (Jinek *et al.*, 2012). Both Cas9 and Cas9n produced a substantial fold change in fluorescence upon detection, although higher in the case of Cas9 (**Figure 6**). However, dCas9 failed in reaching such a performance, despite a significant differential readout was still possible. Arguably, the cleavage of the nontargeted strand confers more translational and rotational freedom to facilitate the interaction with the beacon (Manghi and Destainville, 2016). We also found Cas9 and Cas9n to have equal activity on displacing that strand, but lower in the case of dCas9 (**Figure 7**).

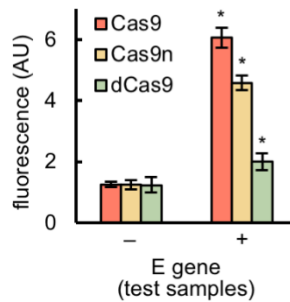


Figure 6. SARS-CoV-2 detection through a CRISPR-Cas9-based strand displacement reaction. Effect of different versions of Cas9 (Cas9, Cas9n, or dCas9) on the output signal. Error bars correspond to standard deviations ($n = 3$). *Statistical significance with test samples (Welch's t -test, two-tailed $P < 0.05$).

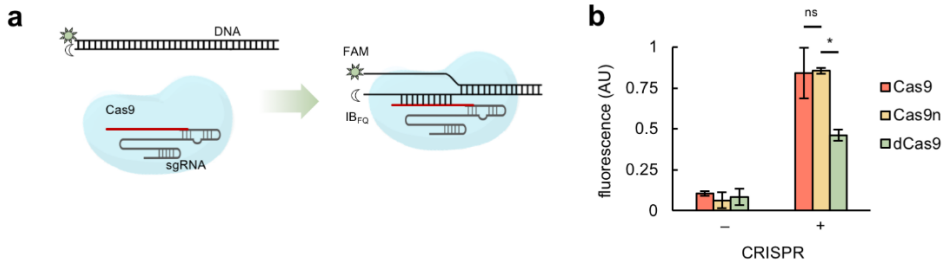


Figure 7. Activity assessment of Cas9 versions. a) Schematics of a test to assess the DNA targeting activity of a CRISPR-Cas9 ribonucleoprotein. The targeted DNA was labelled with a fluorophore (FAM) and quencher (Iowa Black FQ). Upon targeting, the fluorophore is separated from the quencher, then producing a fluorescence signal. b) Fluorescence-based characterization with different Cas9 versions (Cas9, Cas9n, and dCas9). Error bars correspond to standard deviations ($n = 3$). *Statistical significance (Welch's t -test, two-tailed $P < 0.05$). ^{ns}Not statistically significant.

Motivated by these results, we decided to apply COLUMBO to detect SARS-CoV-2 in patient samples. Nasopharyngeal swabs from people diagnosed as positive or negative in viral infection by RT-qPCR in the hospital were collected (Torres *et al.*, 2021). We reconfirmed the infections by RT-qPCR in our lab (**Figure 8.a**). After RT-PCR amplification with the Charité E-Sarbeco primers (without RNA extraction), COLUMBO displayed marked differential readouts that were useful to discriminate the presence of the virus (**Figure 8.b**). These results demonstrate the potential suitability of COLUMBO to perform clinical diagnostics in a simple and effective way.

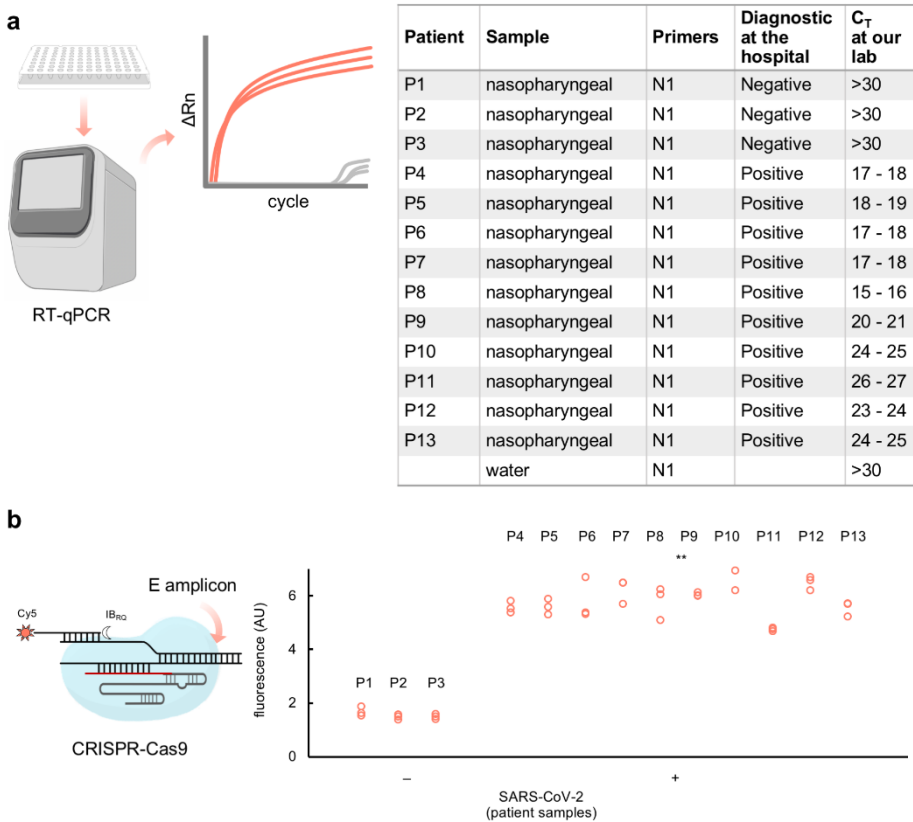


Figure 8. RT-qPCR characterization of patient samples. a) Characteristics of the different patient samples used in this work, including the cycle threshold (C_T) value (N gene). b) Fluorescence-based characterization of all samples with COLUMBO-PCR (E gene). **Overall statistical significance (Welch's *t*-test, two-tailed *P* < 0.001).

2.3 Evaluation of Modifications of COLUMBO

Because the beacon interacts in the PAM-distal region and the R-loop needs to open at that point, the forward primer (with respect to the PAM) overlaps with the region targeted by the beacon. Therefore, the primer may interfere in the detection reaction. This was solved by purifying the amplified material. To avoid the purification step after the preamplification reaction, the region targeted by the molecular beacon should distinguish from those targeted by the primers and the sgRNA. In this regard, a strategy based on cleaving the

resulting DNA amplicon in the PAM-distal region with a restriction enzyme was devised (**Figure 9**).

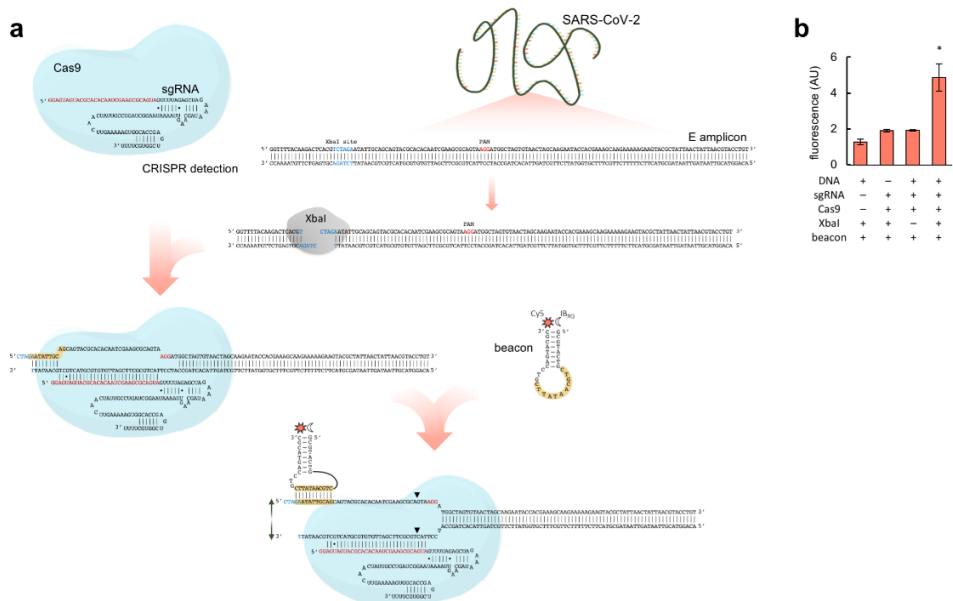


Figure 9. Nucleic acid detection through CRISPR-Cas9-based strand displacement with no prior purification. a) Schematics of the global reaction of amplification and detection of a DNA product from SARS-CoV-2 E gene, containing a PAM (shown in red) for Cas9 recognition and the XbaI restriction site (shown in blue). XbaI was used to cleave the amplicon in the PAM-distal region. A preassembled CRISPR-Cas9 ribonucleoprotein targeting the cleaved amplicon (sgRNA spacer marked in red) was then able to displace a strand so that the molecular beacon could interact with and change its conformation (seed region for this interaction marked in yellow). The molecular beacon was labelled with the fluorophore Cy5 (sun icon) in the 3' end and a dark quencher (moon icon) in the 5' end. In this way, the purification step was avoided because the primer and the beacon target different regions. b) Fluorescence-based characterization of the detection with no prior purification, incubating at the same time the CRISPR-Cas9 ribonucleoprotein, the beacon, and the restriction enzyme (XbaI). Error bars correspond to standard deviations ($n = 3$). *Statistical significance (Welch's t -test, two-tailed $P < 0.05$).

In this way, the forward primer (with respect to the PAM) and the beacon do not significantly overlap. A particular restriction site can be introduced with the primer or be present in the original sequence. In principle, different

restriction enzymes may be used. Here, we used XbaI, which has good efficiency in our reaction buffer. We designed a new primer to amplify the SARS-CoV-2 E gene. We achieved a successful detection with no apparent leakage following this approach (dynamic range of more than 2.5-fold in red fluorescence). In addition, we investigated the use of the PAM-proximal region of the displaced strand to interact with the molecular beacon. A new beacon targeting the N1 amplicon was designed. We found a significant opening of the beacon as a result of the interaction, but we also noticed an unwanted interaction with the sgRNA, which reduced the net dynamic range of the system (**Figure 10**).

2.4 Multiplexed SARS-CoV-2 Detection with COLUMBO

We then moved forward to perform the simultaneous detection of different genomic regions of SARS-CoV-2. This is important to minimize the rate of false positives. The CDC N1 and N2 primers (Vogels *et al.*, 2020) were used together with the Charité E-Sarbeco primers to generate three different DNA amplicons by PCR from a test sample based on the SARS-CoV-2 N and E genes. Suitable PAMs were found in these amplicons (**Figure 11**).

We designed the corresponding sgRNAs and molecular beacons according to the aforementioned specifications. The new beacons to detect the N1 and N2 amplicons were labelled with the fluorophores carboxyfluorescein (FAM) and carboxytetramethylrhodamine (TAMRA), respectively, in their 3' end and with the dark quencher Iowa Black FQ (IB_{FQ}) in their 5' end (**Figure 12**). No significant interferences were observed when using simultaneously these three fluorophores (**Figure 13**).

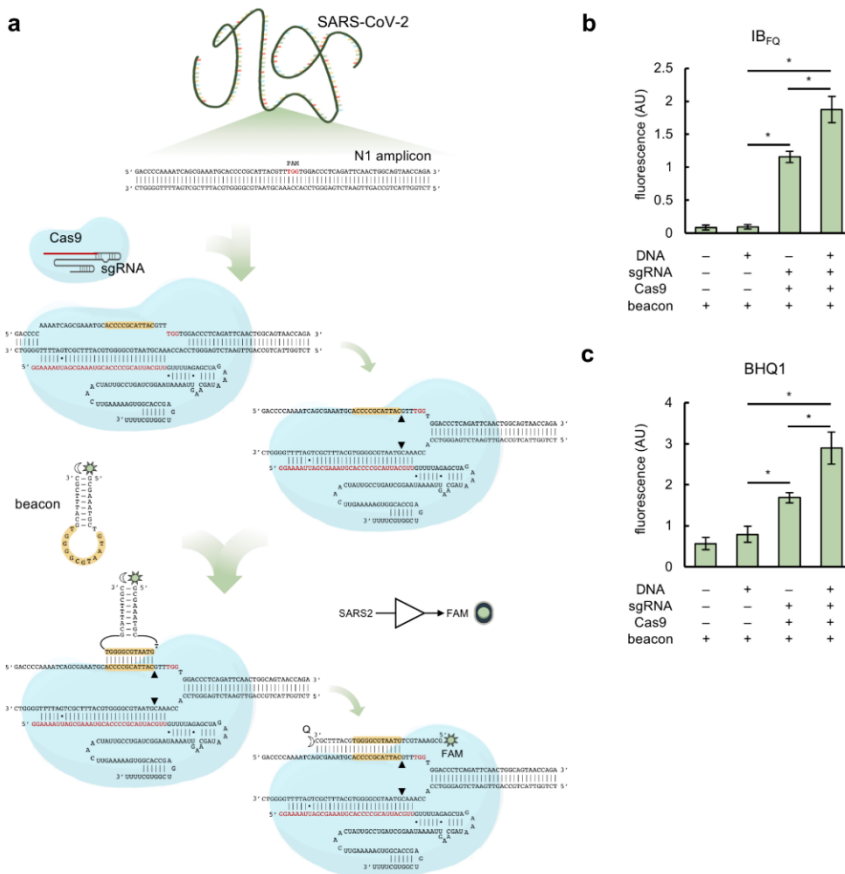


Figure 10. Nucleic acid detection through CRISPR-Cas9-based strand displacement in the PAM-proximal region. a) Schematics of the global reaction of amplification and detection of a DNA product from SARS-CoV-2 N gene (N1 region), containing a PAM (shown in red) for Cas9 recognition. A preassembled CRISPR-Cas9 ribonucleoprotein targeting the amplicon (sgRNA spacer marked in red) was then able to displace a strand so that the molecular beacon could interact with (in the PAM-proximal region) and change its conformation (seed region for this interaction marked in yellow). The molecular beacon was labelled with the fluorophore FAM (sun icon) in the 5' end and a dark quencher (moon icon) in the 3' end. b,c) Fluorescence-based characterization of the detection; amplifications performed by PCR. A high signal was observed in absence of the DNA amplicon and presence of the CRISPR-Cas9 ribonucleoprotein, indicating an unwanted interaction between the sgRNA with the beacon (as in this case the sgRNA spacer contains the seed region). In b) the quencher IB_{FQ} was used, while in c) the quencher BHQ1 was used. Error bars correspond to standard deviations ($n = 3$). *Statistical significance (Welch's t -test, two-tailed $P < 0.05$).

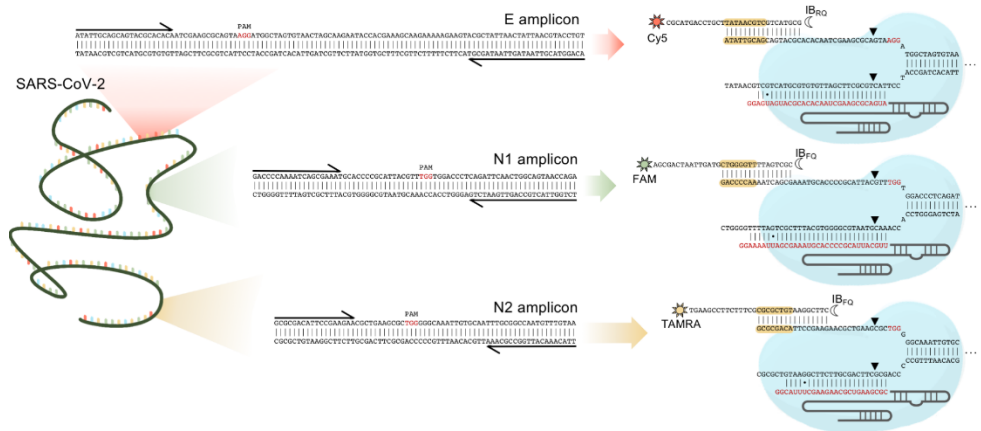


Figure 11. Multiplexed SARS-CoV-2 detection through CRISPR-Cas9-based strand displacement reactions. Schematics of the global reactions of amplification and detection of three different DNA products from SARS-CoV-2 (from E and N genes, PCR primers drawn at the ends), containing each a PAM (shown in red) for Cas9 recognition. Preassembled CRISPR-Cas9 ribonucleoproteins targeting the amplicons (sgRNA spacers marked in red) and appropriate molecular beacons were used for the detection (seed regions for the beacon-displaced strand interaction marked in yellow). The molecular beacons were labelled with Cy5 and IB_{RQ} (for E detection), FAM and IB_{FQ} (for N1 detection), and TAMRA and IB_{FQ} (for N2 detection). Wobble base pairs denoted by dots.

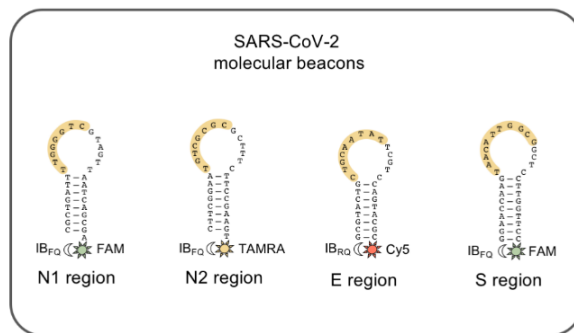


Figure 12. Secondary structures of the designed molecular beacons (stem-loop folding) to detect SARS-CoV-2, labelled with the corresponding fluorophores (sun icons; FAM, TAMRA, or Cy5) in the 3' end and dark quenchers (moon icons; IB_{FQ} or IB_{RQ}) in the 5' end. The seed region to interact with the displaced strand is marked in yellow.

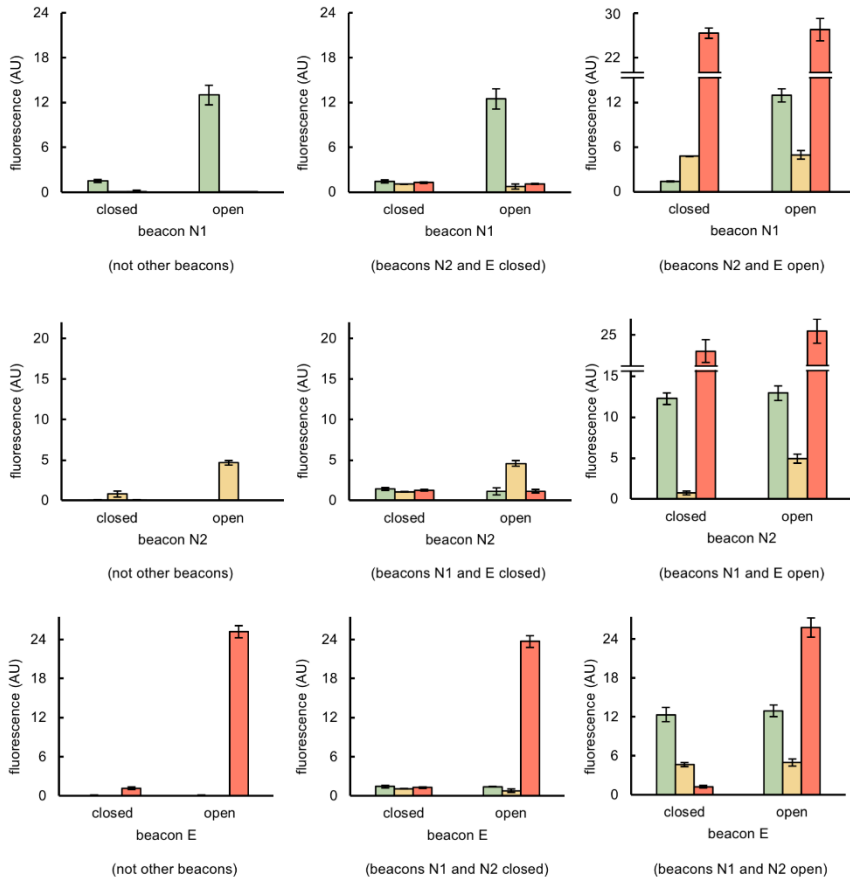


Figure 13. Fluorescence-based characterization of the performance of the molecular beacons to detect SARS-CoV-2 when they work alone or in the presence of other beacons. Open beacons obtained by hybridization with appropriate oligonucleotides. Error bars correspond to standard deviations ($n = 3$). Effect of other beacons not statistically significant (one-way ANOVA test, independent samples, $P > 0.05$).

Notably, COLUMBO allowed the precise detection of the different genomic regions having performed a series of combinatorial amplifications, with a minimal 3-fold change in relative fluorescence (**Figure 14.a**). In addition, we performed a multiplexed RT-PCR amplification over patient samples with all primers. COLUMBO gave a positive signal in the three fluorescence channels in the case of patients diagnosed as infected by SARS-CoV-2 in the hospital (**Figure 14.b**).

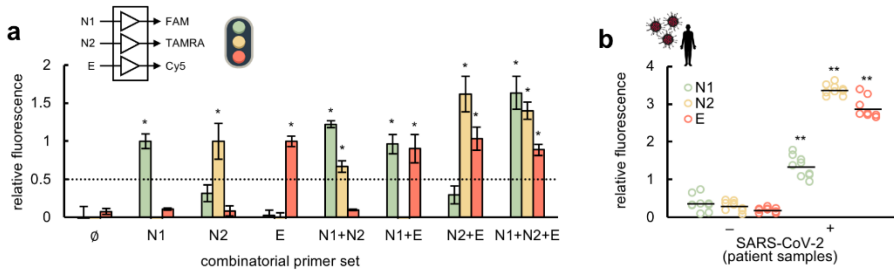


Figure 14. Multiplexed SARS-CoV-2 detection through CRISPR-Cas9-based strand displacement reactions. a) Fluorescence-based characterization of the detection by performing amplifications with combinatorial sets of primers by PCR. The detection threshold (given by the dotted line) was set to 0.5, indicating that the difference in relative fluorescence was more than 2-fold. b) Multiplexed detection of SARS-CoV-2 in patient samples (6 patients, 3 reactions per patient); amplifications performed by RT-PCR. Error bars correspond to standard deviations ($n = 3$). *Statistical significance with test samples (Welch's t -test, two-tailed $P < 0.05$, and relative fluorescence > 0.5). **Statistical significance with patient samples (Welch's t -test, two-tailed $P < 0.001$)

Furthermore, we investigated the possibility of using DETECTR (DNA endonuclease-targeted CRISPR *trans* reporter) (Chen *et al.*, 2018) in combination with COLUMBO to perform multiplexed detections. The structure of the molecular beacon together with a low concentration regime for Cas12a would prevent a premature degradation of the beacon as a result of the collateral catalytic activity of this nuclease upon targeting. Alternatively, a molecular beacon of RNA could be used. We focused on detecting the DNA amplicon generated with the CDC N1 primers with DETECTR, noting that it contains a PAM for Cas12a binding (TTTV) (Broughton *et al.*, 2020), and the amplicon generated with the Charité E-Sarbeco primers with COLUMBO (**Figure 15.a**). A suitable sgRNA was *in vitro* transcribed and assembled with the *Acidaminococcus sp.* Cas12a for DETECTR. After multiplexed RT-PCR or RT-RPA amplification over patient samples, we found that COLUMBO and DETECTR can work together to detect different SARS-CoV-2 genes (**Figure 15.b**).

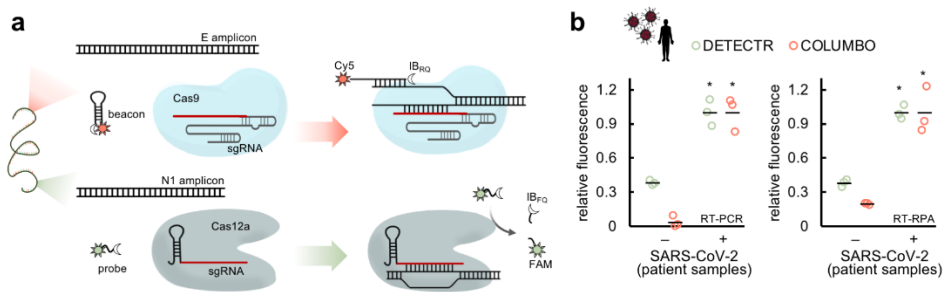


Figure 15. Multiplexed SARS-CoV-2 detection through CRISPR-Cas9-based strand displacement reactions in combination with Cas12a DETECTR. a) Schematics of the reaction of detection with COLUMBO and DETECTR of two different DNA products from SARS-CoV-2 (from E and N genes). A ssDNA probe labelled with FAM and IB_{FQ} was used for DETECTR (for N1 detection). b) Fluorescence-based characterization of the detection by performing multiplexed amplifications by RT-PCR or RT-RPA (2 patients, 3 reactions per patient). Error bars correspond to standard deviations ($n = 3$). *Statistical significance with patient samples (Welch's t -test, two-tailed $P < 0.05$).

2.5 Differential Virus Detection with COLUMBO

We assessed the ability of COLUMBO to detect simultaneously different viruses in the sample. Such a multiplexed detection is important because it may allow performing differential diagnostics in the future and uncovering mixed infections. We focused on three different coronaviruses: SARS-CoV-2, SARS-CoV-1, and Middle East respiratory syndrome coronavirus (MERS-CoV) (da Costa *et al.*, 2020). The CDC N1 primers were considered for SARS-CoV-2, new primers were designed for SARS-CoV-1, and previously designed primers were taken for MERS-CoV (Lu *et al.*, 2014). We checked that each pair of primers only aligns with the cognate genome. Suitable PAMs were found in the corresponding amplicons (**Figure 16**). We then designed new sgRNAs and beacons to detect SARS-CoV-1 (signal from fluorophore TAMRA) and MERS-CoV (signal from fluorophore Cy5) (**Figure 17**). The low GC content of the protospacer regions in these cases forced the design of beacons with larger stems in order to ensure intra- and intermolecular stability.

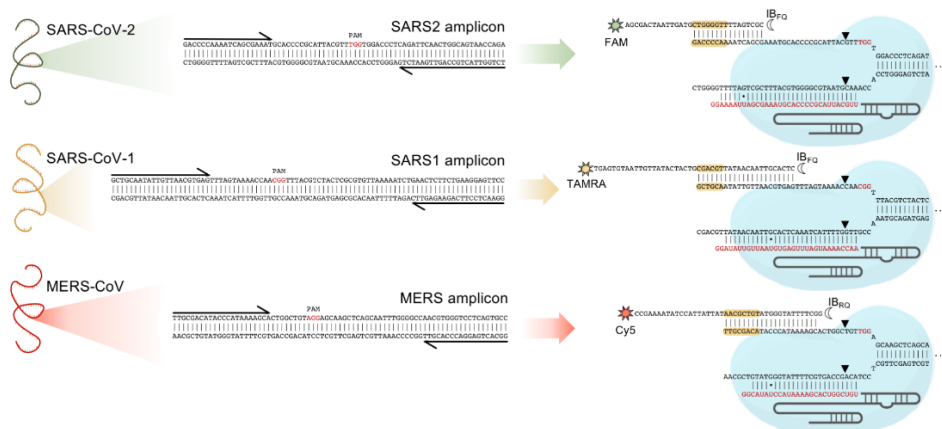


Figure 16. Multiplexed coronavirus detection through CRISPR-Cas9-based strand displacement reactions. Schematics of the global reactions of amplification and detection of DNA products from SARS-CoV-2, SARS-CoV-1, and MERS-CoV (PCR primers drawn at the ends), containing a PAM each (shown in red) for Cas9 recognition. Preassembled CRISPR-Cas9 ribonucleoproteins targeting the amplicons (sgRNA spacers marked in red) and appropriate molecular beacons were used for the detection (seed regions for the beacon-displaced strand interaction marked in yellow). The molecular beacons were labelled with FAM and IB_{FQ} (for SARS-CoV-2 detection), TAMRA and IB_{FQ} (for SARS-CoV-1 detection), and Cy5 and IB_{RQ} (for MERS-CoV detection). Wobble base pairs denoted by dots.

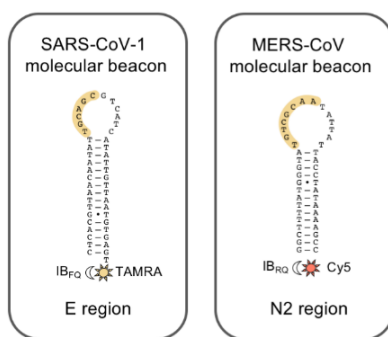


Figure 17. Secondary structures of the designed molecular beacons (stem-loop folding) to detect SARS-CoV-1 and MERS-CoV, labelled with the corresponding fluorophores (sun icons; TAMRA or Cy5) in the 3' end and dark quenchers (moon icons; IB_{FQ} or IB_{RQ}) in the 5' end. The seed region to interact with the displaced strand is marked in yellow. Wobble base pairs denoted by dots.

Notably, COLUMBO allowed the precise detection of the different DNA amplicons added in a combinatorial way, with a minimal 2.4-fold change in relative fluorescence as before (**Figure 18.a**). In addition, we performed a multiplexed RT-PCR amplification over patient samples with all primers. COLUMBO gave a positive signal only in the green fluorescence channel, corresponding to SARS-CoV-2, in the case of patients diagnosed as infected in the hospital (**Figure 18.b**). These results indicate that COLUMBO is a suitable method to achieve a direct multiplexed detection of nucleic acids with no need for gel electrophoresis, in contrast to previous work (Jiao *et al.*, 2021).

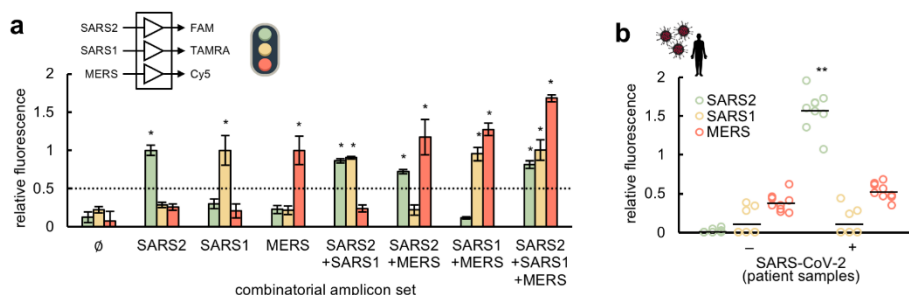


Figure 18. Multiplexed coronavirus detection through CRISPR-Cas9-based strand displacement reactions. a) Fluorescence-based characterization of the detection by working with combinatorial sets of DNA amplicons. The detection threshold (given by the dotted line) was set to 0.5, indicating that the difference in relative fluorescence was more than 2-fold. b) Differential detection of SARS-CoV-2 in patient samples (6 patients, 3 reactions per patient); amplifications performed by RT-PCR. Error bars correspond to standard deviations ($n = 3$). *Statistical significance with test samples (Welch's t -test, two-tailed $P < 0.05$, and relative fluorescence > 0.5). **Statistical significance with patient samples (Welch's t -test, two-tailed $P < 0.001$).

Next, we tested if COLUMBO, in addition to detecting SARS-CoV-2, can reveal specific mutations. This would be important to provide a cost-effective genetic perspective about the transmission dynamics in the pandemic (du Plessis *et al.*, 2021). We first generated different E gene amplicon variants harboring substitution mutations in the PAM or the protospacer and measure the detection activity (**Figure 19**). Mutations in the PAM would compromise the binding of the Cas protein, while mutations in the protospacer the binding

of the beacon (in the PAM-distal region) and the sgRNA (in the PAM-proximal region). These results show that the native Cas9 is only able to discriminate mutations in the PAM, while the HiFi Cas9 is able to discriminate mutations in the PAM and the protospacer, so this latter nuclease seems better suited for applications in which the detection of variants is required.

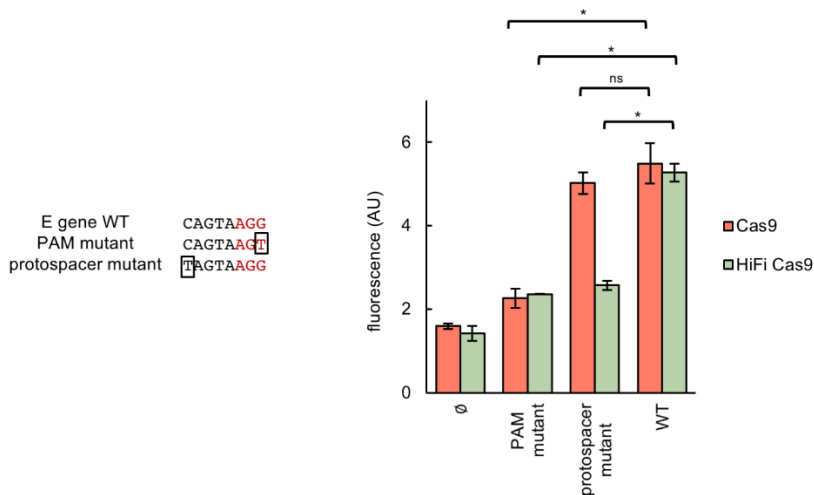


Figure 19. Detection of substitution mutations through CRISPR-Cas9-based strand displacement. Fluorescence-based characterization of E gene variant detection with the native Cas9 and HiFi Cas9. On the left, substitution mutations are framed (PAM shown in red). Error bars correspond to standard deviations ($n = 3$). *Statistical significance (Welch's t -test, two-tailed $P < 0.05$). ^{ns}Not statistically significant.

Then, we hypothesized that it could be possible to perform a multiplexed detection with two sgRNAs, one targeting a conserved region to confirm the infection by SARS-CoV-2 and another targeting a mutable region to identify a specific viral genotype (**Figure 20.a**). As a proof of concept, we here focused on the H69-V70 deletion of six nucleotides in the S gene (S-delH69-V70) identified in the Alpha variant (Meng *et al.*, 2021). Using test samples containing the E and S/S-delH69-V70 amplicons, the intended multiplexed detection was successfully accomplished, indicating that the corresponding sgRNA does not interact with the wild-type S amplicon (**Figure 20.b**).

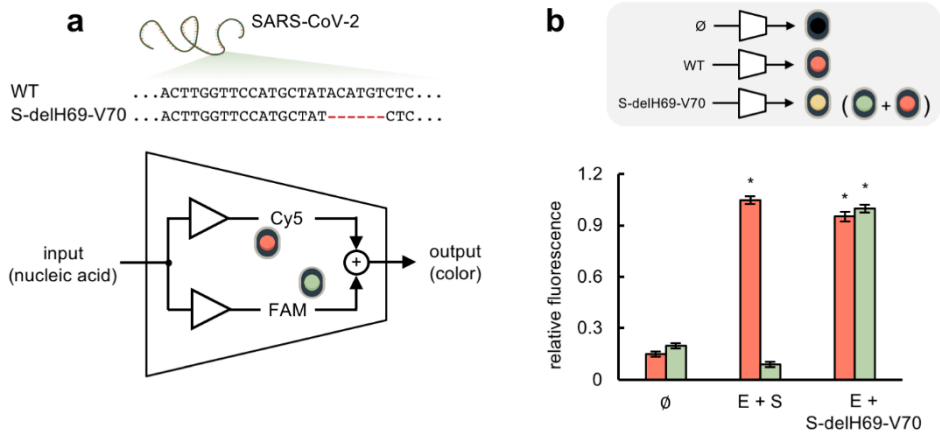


Figure 20. Mutant SARS-CoV-2 detection through CRISPR-Cas9-based strand displacement reactions. a) Schematics of an electronic circuit implementing a molecular program for detection: if the sample is free of SARS-CoV-2, there is no light signal; if it contains the wild-type SARS-CoV-2, a red signal is obtained (only from Cy5); if it contains a SARS-CoV-2 that carries the mutation S-delH69-V70, red and green signals are obtained (from Cy5 and FAM), *i.e.*, a “yellow” signal. b) Fluorescence-based characterization of the detection by working directly with DNA amplicons: none, E and S (simulating the wild-type SARS-CoV-2), and E and S-delH69-V70 (simulating a mutant SARS-CoV-2, Alpha variant). Error bars correspond to standard deviations ($n = 3$). *Statistical significance with test samples (Welch’s t -test, two-tailed $P < 0.05$).

We also considered a deletion of three nucleotides in the N gene (N-delQ9) identified in a Delta variant sublineage (Wang *et al.*, 2022), which we were able to detect in a multiplexed fashion using test samples containing the E and N1/N1-delQ9 amplicons (**Figure 21**). These examples suggest that, provided suitable sgRNAs and beacons are designed, COLUMBO could be applied to identify further SARS-CoV-2 mutants to limit the use of sequencing.

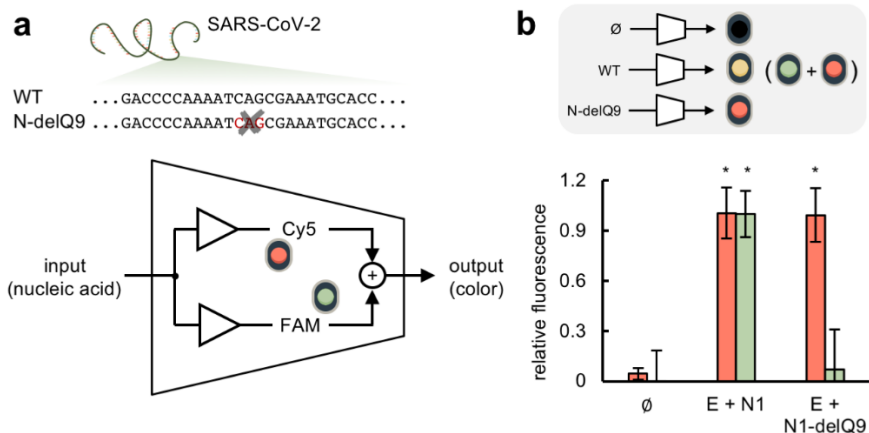


Figure 21. Mutant SARS-CoV-2 detection through CRISPR-Cas9-based strand displacement. a) Schematics of an electronic circuit implementing a molecular program for detection: if the sample is free of SARS-CoV-2, there is no light signal; if it contains the wild-type SARS-CoV-2, a “yellow” signal is obtained (merging the signals from Cy5 and FAM); if it contains a SARS-CoV-2 that carries the mutation N-delQ9, a red signal is obtained (only from Cy5). b) Fluorescence-based characterization of the detection by working directly with DNA amplicons: none, E and N1 (simulating the wild-type SARSCoV-2), and E and N1-delQ9 (simulating a mutant SARS-CoV-2). Error bars correspond to standard deviations ($n = 3$). *Statistical significance (Welch’s t -test, two-tailed $P < 0.05$).

3. DISCUSSION

We have enlarged the CRISPR-based detection toolkit with the CRISPR-Cas9 system on which COLUMBO relies. As in the case of SHERLOCK (specific high-sensitivity enzymatic reporter unlocking) (Gootenberg *et al.*, 2017) and DETECTR (Chen *et al.*, 2018), a preamplification process is required. However, COLUMBO is based on strand displacement (hybridization) and not on a collateral catalytic activity. That is, the sgRNA-Cas9 ribonucleoprotein gives the specificity of the detection by targeting the resulting DNA amplicon, and the interaction between the displaced DNA strand and a molecular beacon gives the fluorescence readout. Consequently, different DNA amplicons can be detected with the same nuclease (Cas9) and without the need for complex setups to run parallel microreactions (Ackerman

et al., 2020; Tian *et al.*, 2021), which is an advance in terms of broad usability and standardization. Remarkably, we have applied this novel approach with success to detect SARS-CoV-2 in patient samples, thereby envisioning a diagnostic potential. We also showed that COLUMBO and DETECTR can work together, a feature that is important to boost the intricacy in CRISPR diagnostics.

In our designer scheme, the native Cas9 from *S. pyogenes* is exploited, but the use of engineered versions of Cas9 with enhanced specificity (Slaymaker *et al.*, 2016) could make the detection of virus variants with subtle specific mutations more plausible. COLUMBO might be run after RT-qPCR completion as a simple virus genotyping step in order to complement the quantitative detection in the clinic with relevant information for patient prognosis and epidemiological surveillance. Further work should also refine the approach to make it even more streamlined (*i.e.*, joining amplification and detection). On the other hand, increasing developments on portable fluorescence microscopy coupled to mobile phones, already applied to detect SARS-CoV-2 (Fozouni *et al.*, 2021; Ning *et al.*, 2021), are appealing and might be used to characterize our CRISPR-Cas9 reactions. A cell-free expression system might also be interfaced to achieve a detection with a colorimetric readout (Pardee *et al.*, 2016), given that strand displacement allows nucleic acid conversion (Montagud-Martinez *et al.*, 2021). This would enable point-of-care diagnostics and field-deployable testing.

Finally, we envision the application of computational methods to automate the sequence design of the different nucleic acid species that COLUMBO requires, given a series of energetic and structural specifications (Rodrigo *et al.*, 2013b; Zadeh *et al.*, 2011). This would allow ending with species with suitable intra- and intermolecular stability, while minimizing undesired cross-interactions (*e.g.*, between the molecular beacon and the sgRNA). One limitation of COLUMBO is the sometimes-moderate dynamic range of the fluorescence signal, which may make it difficult to achieve an accurate detection of the virus, especially in the case of multiplexing. In this regard, the combination of computational sequence design with systematic functional screening might allow optimizing the system. In addition, computational methods might contribute to the engineering of more complex nucleic acid

circuits not only to detect a specific sequence, but to perform a logic computation from multiple input signals (*e.g.*, to inform about the presence of two or more viruses in the sample with just one fluorophore) (Seelig *et al.*, 2006). Within this extended diagnostic framework, the activity of the sgRNAs might be conditional to the presence or absence of further strands to have an additional layer of operation (Li *et al.*, 2019). All in all, due to its specificity, multiplexing capability, compatibility, and easy usage, we expect COLUMBO to provide exciting prospects in the field of viral diagnostics.

4. MATERIALS AND METHODS

4.1 Test Samples

For single detection, a test sample was generated with a plasmid containing the SARS-CoV-2 E gene (IDT) at 10^3 copies/ μL (different dilutions down to 1 copy/ μL were also made). Additional test samples were generated for multiplexed detection. First, a test sample was generated by mixing two plasmids containing the SARS-CoV-2 N and E genes (IDT) each at 10^3 copies/ μL . Second, different combinatorial samples of three DNA amplicons from different viruses were prepared. The DNA amplicon from SARS-CoV-2 was generated by PCR from the aforementioned plasmid with the CDC N1 primers, and the DNA amplicons from SARS-CoV-1 and MERS-CoV were chemically synthesized (IDT). Third, two DNA amplicons from the S gene, one being the wild-type version and another carrying the amino acid H69-V70 deletion, (Meng *et al.*, 2021) and a DNA amplicon from the N gene carrying the CAG deletion at position 28298 (deleting the ninth residue Q) (Wang *et al.*, 2022) were chemically synthesized. Sequences are provided in **Data set Table 1**.

4.2 Clinical Samples

Nasopharyngeal swabs corresponding to infected and noninfected patients with SARS-CoV-2 (RT-qPCR diagnostics) were obtained from the Clinic University Hospital of Valencia (Spain). Samples were inactivated through the action of proteinase K followed by a heat shock (5 min at 60 °C) before proceeding. No RNA extraction was performed. The ethical committee of the Clinic University Hospital approved this study (order #2020/221).

4.3 Primers

The CDC N1 and N2 primers were used to amplify two different N gene regions from SARS-CoV-2, and the Charité E-Sarbeco primers were used to amplify one E gene region (Vogels *et al.*, 2020). The Charité E-Sarbeco primers were used for both PCR and RPA, while the CDC N1 primers were only used for PCR. Longer primers targeting the N1 region were designed for RPA. Primers to amplify the S gene were also designed here. In addition, a genomic region from SARS-CoV-1 could be amplified with newly designed primers, and a region from MERS-CoV could be amplified with the previously designed MERS-related N2 primers (Lu *et al.*, 2014). Sequences are provided in **Data set Table 2**.

4.4 CRISPR Elements

Three versions of *S. pyogenes* Cas9 were used (from IDT): the wild-type nuclease (Cas9), the Cas9 H840A nickase (Cas9n), and the catalytically dead Cas9 protein (dCas9) (Jinek *et al.*, 2012). *Acidaminococcus sp.* Cas12a (from IDT) was also used to implement DETECTR reactions. In addition, sgRNAs were generated by *in vitro* transcription with the TranscriptAid T7 high yield transcription kit (Thermo) from DNA templates. sgRNAs were then purified

by using the RNA clean and concentrator column (Zymo) and quantified in a NanoDrop. Sequences are provided in **Data set Table 3**.

4.5 Molecular Beacons

Different DNA oligonucleotides folding into a stem-loop structure and appropriately labelled were designed to hybridize with the displaced DNA strands from the CRISPR reactions. These probes were designed to have a seed region in the loop and of high GC content, as well as a melting temperature higher than 50 °C (**Figure 22** shows a computational study on the size of the seed region). The correct folding and hybridization ability (with the target DNA, but not with the sgRNA) were checked with NUPACK (Zadeh *et al.*, 2011). Molecular beacons targeting the PAM-distal region were labelled in their 5' end with a dark quencher (IB_{FQ} or IB_{RQ}) and in their 3' end with a fluorophore (FAM, TAMRA, or Cy5). When targeting the PAM-proximal region, the beacon was labelled in its 5' end with FAM and its 3' end with IB_{FQ} or Black Hole Quencher 1 (BHQ1). To ensure appropriate folding, molecular beacons were heated at 95 °C for 2 min and then cooled slowly to 25 °C prior to their use in the CRISPR reactions. Sequences provided in the **Data set Table 4**.

4.6 Nucleic Acid Amplification by PCR

With test samples, 250 nM of forward and reverse primers, 200 µM dNTPs (NZYTech), 0.02 U/µL Phusion high-fidelity DNA polymerase (Thermo), 1× Phusion buffer, and 2 µL of sample were mixed for a total volume of 20 µL (adjusted with RNase-free water). The protocol was 98 °C for 30 s for denaturation, followed by 35 cycles of 98 °C for 10 s, 62 °C for 10 s, and 72 °C for 5 s for amplification. With patient samples, the TaqPath 1-step RT-qPCR master mix, CG (Applied) was used with 250 nM of forward and reverse primers and 4 µL of sample. The protocol was 50 °C for 15 min for RT, then 95 °C for 2 min for denaturation, followed by 35 cycles of 95 °C for

15 s and 62 °C for 60 s for amplification. In the case of multiplexed amplifications, each primer pair was also used at 250 nM. Reactions were incubated in a thermocycler (Eppendorf). PCR products were purified by using a DNA clean and concentrator column (Zymo) by centrifugation.

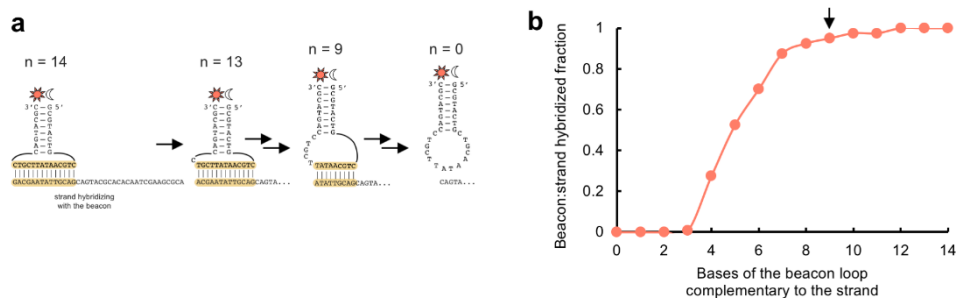


Figure 22. Computational analysis of the energy barrier associated with the interaction of the beacon. a) Schematics of the hybridization between a beacon and a given strand. The beacon for the SARS-CoV-2 E gene was considered (fixed). Different sequences (based on the E gene) were generated to interact with the beacon, starting from one that interacts with the full-length loop (seed region of 14 nt, $n = 14$) and ending with one that does not interact with the loop (no seed region, $n = 0$). b) Molar fraction of the hybridized species (beacon:strand) as a function of the size of the seed region (*i.e.*, the number of bases of the beacon loop that are complementary to the strand). NUPACK was used considering DNA parameters and a concentration of 40 nM for both species. The arrow marks the sequence corresponding to the actual design.

4.7 Nucleic Acid Amplification by RPA

The TwistAmp basic kit (TwistDX) was used. With test samples, 480 nM of forward and reverse primers was added to 29.5 μL of rehydration buffer for a total volume of 45.4 μL (adjusted with RNase-free water). With patient samples, 500 U RevertAid (Thermo) and 50 U RNase inhibitor (Thermo) were added to the mix. In the case of multiplexed amplifications, each primer pair was used at 240 nM. The TwistAmp basic reaction pellet was resuspended with the resulting volume, and then 2 μL of the sample was added. To start the reaction, 7 mM magnesium acetate was added. Reactions

were incubated at 42 °C for 30 min in a thermomixer (Eppendorf), shaking 10 s at 300 rpm every 2 min. In principle, shaking is not required for RPA to work. However, in our hands, we found better amplifications with shaking, especially in the case of clinical samples. In some cases, RPA reactions without shaking produced no observable bands when revealed in a gel. RPA products were purified by using the DNA clean and concentrator column by centrifugation.

4.8 CRISPR-Cas9-Based Detection

CRISPR reactions were performed in 1× TAE buffer pH 8.5 (Invitrogen), 0.05% Tween 20 (Merck), and 12.5 mM MgCl₂ (Merck) at a final volume of 20 µL. The CRISPR-Cas9 ribonucleoprotein, previously assembled at room temperature for 30 min, was added at 100 nM. In the case of test samples, 40 nM of amplified DNA (otherwise specified) was used per reaction. In the case of patient samples, 2 or 6 µL of amplified product was used per reaction for single or multiplexed detection. For the limit of detection assays, 2 µL of purified PCR product was used (5 µL in the case of RPA). Reactions were incubated at 37 °C for 20 min in a thermomixer (Eppendorf). The molecular beacon (beacons) was (were) added afterward at 100 nM, followed by 5 min incubation at 37 °C. The beacons could also be added at the beginning of the CRISPR reaction to simplify the approach, obtaining similar results (**Figure 23**). For the multiplexed detection of the E and S-delH69-V70 amplicons, 200 nM of ribonucleoprotein targeting the S-delH69-V70 amplicon was used, and the two beacons were added at the beginning.

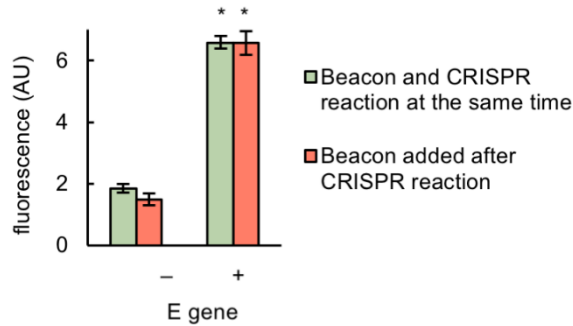


Figure 23. Fluorescence-based characterization of the detection when the beacon is added at the beginning of the CRISPR reaction. Error bars correspond to standard deviations ($n = 3$). *Statistical significance (Welch's t -test, two-tailed $P < 0.05$).

4.9 Activity assessment of different Cas9 versions

A suitable dsDNA molecule, whose sequence is GGCTAAAGAGGAAGAGGACATGGTGAATTCGTA ACT, was labelled with a fluorophore (FAM, in 5') and a quencher (Iowa Black FQ, in 3') in the PAM-distal ends. A suitable sgRNA, whose spacer is GGCUAAAGAGGAAGAGGACA, was used to perform the CRISPR reactions. These were done in 1x TAE buffer pH 8.5 (Invitrogen), 0.05% Tween 20 (Merck), and 12.5 mM MgCl₂ (Merck) at a final volume of 20 μ L. The sgRNACas9 ribonucleoprotein was added at 100 nM and the labelled dsDNA at 20 nM. Here, Cas9, Cas9n, and dCas9 were used. Reactions were incubated at 37 °C for 20 min in a thermomixer (Eppendorf).

4.10 CRISPR-Cas9-based detection with no prior purification

From test samples containing the SARS-CoV-2 E gene, DNA amplicons were generated by PCR as already indicated, this time with 45 cycles. Then, 6 μ L of non-purified sample was used in the CRISPR reaction. This was performed in 1x TAE buffer pH 8.5 (Invitrogen), 0.05% Tween 20 (Merck), and 12.5 mM MgCl₂ (Merck), with the sgRNA-Cas9 ribonucleoprotein at 100 nM, the

molecular beacon at 100 nM, and XbaI at 0.5 U/ μ L, for a final volume of 20 μ L. Reactions were incubated at 37 °C for 20 min in a thermomixer (Eppendorf).

4.11 Combined CRISPR-Cas9- and CRISPR-Cas12a-Based Detection

CRISPR reactions were performed in 1 \times TAE buffer pH 8.5 (Invitrogen), 0.05% Tween 20 (Merck), and 12.5 mM MgCl₂ (Merck) at a final volume of 20 μ L. The CRISPR-Cas9 and CRISPR-Cas12a ribonucleoproteins, previously assembled at room temperature for 30 min, were added at 100 and 1.33 nM, respectively. The ssDNA probe for CRISPR-Cas12a (TTATT, labelled in its 5' end with the fluorophore FAM and in its 3' end with the dark quencher I_BFQ) was also added at 100 nM. From patient samples, 4 μ L of the amplified product was used per reaction for multiplexed detection. Reactions were incubated at 37 °C for 20 min in a thermomixer (Eppendorf). The molecular beacon was added afterward at 100 nM, followed by a 5 min incubation at 37 °C.

4.12 Single-point mutation detection with CRISPR-Cas9

Different E gene amplicon variants harboring substitution mutations in the PAM or the protospacer (in the seed region, *i.e.*, the PAM-proximal region) were chemically synthesized (IDT). Wild-type Cas9 and HiFi Cas9 from IDT were used. According to IDT, HiFi Cas9 has similar on-target potency to wild-type Cas9, but with significantly reduced off-target effects, then allowing for precise targeting. CRISPR reactions were performed as already indicated.

4.13 RT-qPCR

The TaqPath 1-step RT-qPCR master mix, CG was used. 2 μL of sample was mixed with 500 nM of forward and reverse primers (CDC N1), 250 nM of ssDNA probe (provided by IDT to detect the N gene), and 5 μL of the master mix for a total volume of 20 μL (adjusted with RNase-free water) in a fast microplate (Applied). Reactions were performed in a QuantStudio 3 equipment (Thermo) with this protocol: incubation at 25 °C for 2 min for uracil-N glycosylation, followed by 50 °C for 15 min for RT, followed by an inactivation step at 90 °C for 2 min, then followed by 40 cycles of amplification at 90 °C for 3 s and 60 °C for 30 s.

4.14 Gel Electrophoresis

Nucleic acid amplification (from plasmid or viral genome) was confirmed by gel electrophoresis (see examples in **Figure 24**). For that, 2 μL of amplified product was used. Gel electrophoresis was also used to confirm the interaction between the molecular beacon and the displaced strand from the DNA amplicon (ssDNA molecule). For that, the nucleic acid species were introduced at 7.5 μM each in 20 μL of the CRISPR reaction buffer and were incubated for 30 min at room temperature. Samples were loaded on a 3% agarose gel prepared with 0.5 \times TBE buffer, which was run for 45 min at room temperature (110 V). Gels were stained using RealSafe (Durviz). The GeneRuler ultralow range DNA ladder (10-300 bp, Thermo) was used as a marker.

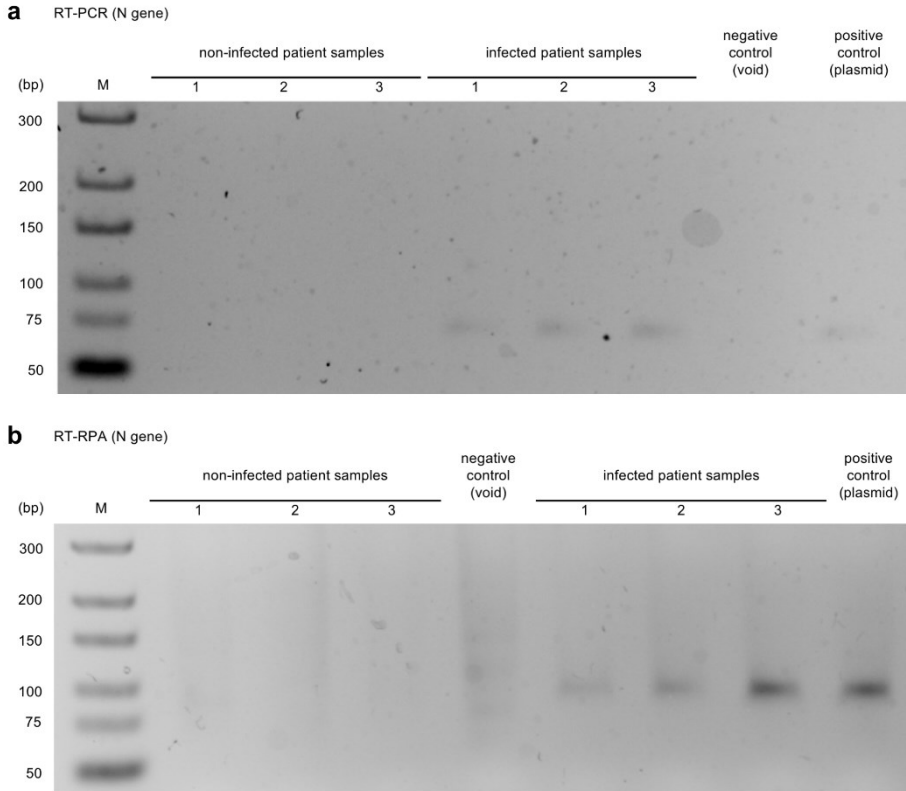


Figure 24. Gel electrophoretic assay to reveal the viral genome amplification. a) Amplification of SARS-CoV-2 (N gene) over patient samples by RT-PCR. b) Amplification of SARS-CoV-2 (N gene) over patient samples by RT-RPA. Due to the RPA buffer composition, we noted that the migration of the fragment in the gel was slower. M, molecular marker (GeneRuler ultra-low range DNA ladder).

4.15 Fluorometry

Reaction volumes were loaded in a black 384-well microplate with clear bottom (Falcon), which was then placed in a fluorometer (Varioskan Lux, Thermo) to measure green, orange, and red fluorescence (measurement time of 100 ms, automatic range, and top optics). For FAM, excitation was at 495/12 nm and emission at 520/12 nm (green); for TAMRA, excitation was at 557/12 nm and emission at 583/12 nm (orange); and for Cy5, excitation was at 645/12 nm and emission at 670/12 nm (red). Fluorescence values were

represented as absolute or relative. For the latter, the fluorescence values of the closed-form beacons were subtracted to correct the signals, which were then normalized by appropriate reference values. In the case of multiplexed reactions for the simultaneous detection of different SARS-CoV-2 genes or different coronaviruses, the normalization was with respect to the positive case where only one amplicon is present. In the case of reactions for mutant SARS-CoV-2 detection or combining Cas9 and Cas12a, the normalization was with respect to the positive case where all amplicons are present.

4.16 Data set

Table 1. List of amplicons used in this work.

Amplicons			
Virus	Gene	Region	Sequence 5' - 3'
SARS-CoV-2	Nucleocapsid	N1	GACCCCAAATCAGCGAAATGCACCCC GCATTACGTTTGGTGGACCCTCAGATT CAACTGGCAGTAACCAGA
SARS-CoV-2	Nucleocapsid	N1 (RPA)	GACCCCAAATCAGCGAAATGCACCCC GCATTACGTTTGGTGGACCCTCAGATT CAACTGGCAGTAACCAGAATGGAGAAC
SARS-CoV-2	Nucleocapsid	N1- delQ9	GACCCCAAATCGAAATGCACCCCGCA TTACGTTTGGTGGACCCTCAGATTCAA CTGGCAGTAACCAGA
SARS-CoV-2	Nucleocapsid	N2	TTACAAACATTGGCCGCAAATTGCACA ATTTGCCCCAGCGCTTCAGCGTTCTT CGGAATGTGCGGC
SARS-CoV-2	Envelope	E	ACAGGTACGTTAATAGTTAATAGCGTA CTTCTTTTTCTTGCTTTCGTGGTATTC TTGCTAGTTACACTAGCCATCCTTACT GCGCTTCGATTGTGTGCGTACTGCTGC AATAT
SARS-CoV-2	Spike	S	CGCCAATGTTACTTGGTTCATGCTAT ACATGTCTCTGGGACCAATGGTACTAA GAGGTTTGATAACCCTGTCCT
SARS-CoV-2	Spike	S- delH69- V70	CGCCAATGTTACTTGGTTCATGCTAT CTCTGGGACCAATGGTACTAAGAGGTT TGATAACCCTGTCCT
SARS-CoV-1	Envelope	E	GCTGCAATATTGTTAACGTGAGTTTAG TAAAACCAACGGTTTACGTCTACTCGC GTGTTAAAAATCTGAACTCTTCTGAAG GAGTTCC
MERS-CoV	Nucleocapsid	N2	GGCACTGAGGACCCACGTTGGCCCCAA ATTGCTGAGCTTGCTCCTACAGCCAGT GCTTTTATGGGTATGTGCGCAA

Table 2. List of primers used in this work.

Primers			
Virus	Gene	Primer	Sequence 5' - 3'
SARS-CoV-2	Nucleocapsid	N1 Forward	GACCCCAAAATCAGCGAAAT
SARS-CoV-2	Nucleocapsid	N1 Reverse	TCTGGTTACTGCCAGTTGAATCTG
SARS-CoV-2	Nucleocapsid	N1 (RPA) Forward	GACCCCAAAATCAGCGAAATGCACCCC GCA
SARS-CoV-2	Nucleocapsid	N1 (RPA) Reverse	GTTCTCCATTCTGGTTACTGCCAGTTG AAT
SARS-CoV-2	Nucleocapsid	N2 Forward	TTACAAACATTGGCCGCAAA
SARS-CoV-2	Nucleocapsid	N2 Reverse	GCGCGACATTCCGAAGAA
SARS-CoV-2	Envelope	E Forward	ACAGGTACGTTAATAGTTAATAGCGT
SARS-CoV-2	Envelope	E Reverse	ATATTGCAGCAGTACGCACACA
SARS-CoV-2	Envelope	E (XbaI) Reverse	GGTTTTACAAGACTCACGTCTAGAATA TTG
SARS-CoV-2	Spike	S Forward	CGCCAATGTTACTTGGTTCCATG
SARS-CoV-2	Spike	S Reverse	AGGACAGGGTTATCAAACCTC
SARS-CoV-1	Envelope	E Forward	GCTGCAATATTGTTAACGTGAG
SARS-CoV-1	Envelope	E Reverse	GGAACTCCTTCAGAAGAGTTC
MERS-CoV	Nucleocapsid	N2 Forward	GGCACTGAGGACCCACGTT
MERS-CoV	Nucleocapsid	N2 Reverse	TTGCGACATACCCATAAAAGCA

Table 3. List of sgRNAs used in this work.

sgRNAs			
Virus	Gene	Region	Sequence 5' - 3'
SARS-CoV-2	Nucleocapsid	N1	GGAAAAUUAGCGAAAUGCACCCCGCAU UACGUUGUUUUAGAGCUAGAAAUAGCA AGUUAAAAUAAGGCUAGUCCGUUAUCA ACUUGAAAAAGUGGCACCGAGUCGGUG CUUUU
SARS-CoV-2	Nucleocapsid	N2	GGCAUUUCGAAGAACGCUGAAGCGCGU UUUAGAGCUAGAAAUAGCAAGUUAAAA UAAGGCUAGUCCGUUAUCAACUUGAAA AAGUGGCACCGAGUCGGUGCUUUU
SARS-CoV-2	Envelope	E	GGAGUAGUACGCACACAAUCGAAGCGC AGUAGUUUUAGAGCUAGAAAUAGCAAG UUAAAAUAAGGCUAGUCCGUUAUCAAC UUGAAAAAGUGGCACCGAGUCGGUGCU UUU
SARS-CoV-2	Spike	S-delH69-V70	GGUAUUACUUGGUUCCAUGCUAUCUCG UUUUAGAGCUAGAAAUAGCAAGUUAAA AUAAGGCUAGUCCGUUAUCAACUUGAA AAAGUGGCACCGAGUCGGUGCUUUU
SARS-CoV-1	Envelope	E	GGUAUUUGUUAAUGUGAGUUUAGUAAA ACCAAGUUUUAGAGCUAGAAAUAGCAA GUAAAAUAAGGCUAGUCCGUUAUCA CUUGAAAAAGUGGCACCGAGUCGGUGC UUUU
MERS-CoV	Nucleocapsid	N2	GGCAUAUCCAUAAAAGCACUGGCUGUG UUUUAGAGCUAGAAAUAGCAAGUUAAA AUAAGGCUAGUCCGUUAUCAACUUGAA AAAGUGGCACCGAGUCGGUGCUUUU

Table 4. List of molecular beacons used in this work.

Beacons				
Virus	Gene	(5'-) Quencher	Fluorophore (-3')	Sequence 5' - 3'
SARS-CoV-2	Nucleocapsid	Iowa Black FQ	FAM	CGCTGATTTTGGGG TCGTAGTTAATCAG CGA
SARS-CoV-2	Nucleocapsid	Iowa Black FQ	TAMRA	CTTCGGAATGTCCG GCGCTTTCTTCCGA AGT
SARS-CoV-2	Envelope	Iowa Black RQ	CY5	GCGTACTGCTGCAA TATTCGTCCAGTAC GC
SARS-CoV-2	Spike	Iowa Black FQ	FAM	GGAACCAAGTAACA TTGGCGGCTCCTTG GTTCC
SARS-CoV-1	Envelope	Iowa Black FQ	TAMRA	CTCACGTTAACAAT ATTGCAGCGTCATC ATATTGTTAATGTG AGT
MERS-CoV	Nucleocapsid	Iowa Black RQ	CY5	GGCTTTTATGGGTA TGTCGCAATATTAT TACCTATAAAAGCC
Virus	Gene	(5'-) Fluorophore	Quencher (-3')	Sequence 5' - 3'
SARS-CoV-2	Nucleocapsid (PAM-proximal)	FAM	Iowa Black FQ	GCGAAATGCTGTAA TGCGGGGTGCATTT CGC
SARS-CoV-2	Nucleocapsid (PAM-proximal)	FAM	Black Hole Quencher 1	GCGAAATGCTGTAA TGCGGGGTGCATTT CGC

5. REFERENCES

- Ackerman CM, Myhrvold C, Thakku SG, Freije CA, Metsky HC, *et al.* (2020) Massively multiplexed nucleic acid detection with Cas13. *Nature* 582, 277-282.
- Arizti-Sanz J, Freije CA, Stanton AC, Petros BA, Boehm CK, *et al.* (2020) Streamlined inactivation, amplification, and Cas13-based detection of SARS-CoV-2. *Nat Commun* 11, 5921.
- Broughton JP, Deng X, Yu G, Fasching CL, Servellita V, *et al.* (2020) CRISPR-Cas12-based detection of SARS-CoV-2. *Nat Biotechnol* 38, 870-874.
- Chen F, Ding X, Feng Y, Seebeck T, Jiang Y, Davis GD (2017) Targeted activation of diverse CRISPR-Cas systems for mammalian genome editing via proximal CRISPR targeting. *Nat Commun* 8, 14958.
- Chen JS, Ma E, Harrington LB, Da Costa M, Tian X, *et al.* (2018) CRISPR-Cas12a target binding unleashes indiscriminate single-stranded DNase activity. *Science* 360, 436-439.
- da Costa VG, Moreli ML, Saivish MV (2020) The emergence of SARS, MERS and novel SARS-2 coronaviruses in the 21st century. *Arch Virol* 165, 1517-1526.
- Ding X, Yin K, Li Z, Lalla RV, Ballesteros E, *et al.* (2020) Ultrasensitive and visual detection of SARS-CoV-2 using all-in-one dual CRISPR-Cas12a assay. *Nat Commun* 11, 4711.
- du Plessis L, McCrone JT, Zarebski AE, Hill V, Ruis C, *et al.* (2021) Establishment and lineage dynamics of the SARS-CoV-2 epidemic in the UK. *Science* 371, 708-712.
- Fozouni P, Son S, Diaz de Leon Derby M, Knott GJ, Gray CN, *et al.* (2021) Amplification-free detection of SARS-CoV-2 with CRISPR-Cas13a and mobile phone microscopy. *Cell* 184, 323-333.

- Gootenberg JS, Abudayyeh OO, Kellner MJ, Joung J, Collins JJ, Zhang F (2018) Multiplexed and portable nucleic acid detection platform with Cas13, Cas12a, and Csm6. *Science* 360, 439-444.
- Gootenberg JS, Abudayyeh OO, Lee JW, Essletzbichler P, Dy AJ, *et al.* (2017) Nucleic acid detection with CRISPR-Cas13a/C2/c2. *Science* 356, 438-442.
- Jiao C, Sharma S, Dugar G, Peeck NL, Bischler T, *et al.* (2021) Noncanonical crRNAs derived from host transcripts enable multiplexable RNA detection by Cas9. *Science* 372, 941-948.
- Jinek M, Chylinski K, Fonfara I, Hauer M, Doudna JA, Charpentier E (2012) A programmable dual-RNA-guided DNA endonuclease in adaptive bacterial immunity. *Science* 337, 816-821.
- Li Y, Teng X, Zhang K, Deng R, Li J (2019) RNA strand displacement responsive CRISPR/Cas9 system for mRNA sensing. *Anal Chem* 91, 3989-3996.
- Lu X, Whitaker B, Sakthivel SKK, Kamili S, Rose LE, *et al.* (2014) Real-time reverse transcription-PCR assay panel for Middle East respiratory syndrome coronavirus. *J Clin Microbiol* 52, 67-75.
- Manghi M, Destainville N (2016) Physics of base-pairing dynamics in DNA. *Phys Rep* 631, 1-41.
- Meng B, Kemp SA, Papa G, Datir R, Ferreira IA, *et al.* (2021) Recurrent emergence of SARS-CoV-2 spike deletion H69/V70 and its role in the Alpha variant B.1.1.7. *Cell Rep* 35, 109292.
- Mina MJ, Parker R, Larremore DB (2020) Rethinking Covid-19 test sensitivity – A strategy for containment. *N Engl J Med* 383, e120.
- Montagud-Martinez R, Heras-Hernandez M, Goiriz L, Daros JA, Rodrigo G (2021) CRISPR-mediated strand displacement logic circuits with toehold-free DNA. *ACS Synth Biol* 10, 950-956.

- Ning B, Yu T, Zhang S, Huang Z, Tian D, *et al.* (2021) A smartphone-read ultrasensitive and quantitative saliva test for COVID-19. *Sci Adv* 7, eabe3703.
- Pardee K, Green AA, Takahashi MK, Braff D, Lambert G, *et al.* (2016) Rapid, low-cost detection of Zika virus using programmable biomolecular components. *Cell* 165, 1255-1266.
- Patchesung M, Jantarug K, Pattama A, Aphicho, K, Suraritdechachai S, *et al.* (2020) Clinical validation of a Cas13-based assay for the detection of SARS-CoV-2 RNA. *Nat Biomed Eng* 4, 1140-1149.
- Piepenburg O, Williams CH, Stemple DL, Armes NA (2006) DNA detection using recombination proteins. *PLoS Biol* 4, e204.
- Richardson CD, Ray GJ, DeWitt MA, Curie GL, Corn JE (2016) Enhancing homology-directed genome editing by catalytically active and inactive CRISPR-Cas9 using asymmetric donor DNA. *Nat Biotechnol* 34, 339-344.
- Rodrigo G, Landrain TE, Majer E, Daros JA, Jaramillo A (2013b) Full design automation of multi-state RNA devices to program gene expression using energy-based optimization. *PLoS Comput Biol* 9, e1003172.
- Rodrigo G, Landrain TE, Shen S, Jaramillo A (2013a) A new frontier in synthetic biology: automated design of small RNA devices in bacteria. *Trends Genet* 29, 529-536.
- Seelig G, Soloveichik D, Zhang DY, Winfree E (2006) Enzyme-free nucleic acid logic circuits. *Science* 314, 1585-1588.
- Slaymaker IM, Gao L, Zetsche B, Scott DA, Yan WX, Zhang F (2016) Rationally engineered Cas9 nucleases with improved specificity. *Science* 351, 84-88.
- Tian T, Shu B, Jiang Y, Ye M, Liu L, *et al.* (2021) An ultralocalized Cas13a assay enables universal and nucleic acid amplification-free single-molecule RNA diagnostics. *ACS Nano* 15, 1167-1178.

- Torres I, Qualai J, Albert E, Bueno F, Huntley D, *et al.* (2021) Real-life evaluation of a rapid extraction-free SARS-CoV-2 RT-PCR assay (COVID-19 PCR Fast-L) for the diagnosis of COVID-19. *J Med Virol* 93, 5233-5235.
- Tyagi S, Kramer FR (1996) Molecular beacons: probes that fluoresce upon hybridization. *Nat Biotechnol* 14, 303-308.
- Vogels CB, Brito AF, Wyllie AL, Fauver JR, Ott IM, *et al.* (2020) Analytical sensitivity and efficiency comparisons of SARS-CoV-2 RT-qPCR primer-probe sets. *Nat Microbiol* 5, 1299-1305.
- Wang H, Jean S, Wilson SA, Lucyshyn JM, McGrath S, *et al.* (2022) A deletion in the N gene of SARS-CoV-2 may reduce test sensitivity for detection of SARS-CoV-2. *Diagn Microbiol Infect Dis* 102, 115631.
- Xiong D, Dai W, Gong J, Li G, Liu N, *et al.* (2020) Rapid detection of SARS-CoV-2 with CRISPR-Cas12a. *PLoS Biol* 18, e3000978.
- Yang S, Rothman RE (2004) PCR-based diagnostics for infectious diseases: uses, limitations, and future applications in acute-care settings. *Lancet Infect Dis* 4, 337-348.
- Zadeh JN, Steenberg CD, Bois JS, Wolfe BR, Pierce MB, *et al.* (2011) NUPACK: analysis and design of nucleic acid systems. *J Comput Chem* 32, 170-173.
- Zhao Y, Chen F, Li Q, Wang L, Fan C (2015) Isothermal amplification of nucleic acids. *Chem Rev* 115, 12491-12545.
- Zhu N, Zhang D, Wang W, Li X, Yang B, *et al.* (2020) A novel coronavirus from patients with pneumonia in China, 2019. *N Engl J Med* 382, 727-733.

CHAPTER 4

Pathogen detection by CRISPR-Cas9-mediated strand displacement in a lateral flow assay

This work has not been published in a scientific journal yet.

My contribution to this work:

I performed the experiments in collaboration with lab colleagues under the supervision of G. Rodrigo. I contributed to data analyses, figures preparation and writing of the manuscript.

1. INTRODUCTION

Nucleic acid detection has become a standard approach for precise disease diagnosis thanks to the rapid advancement of genetic and genomic sequencing technologies (Boyd, 2013). For infectious diseases, accurately identifying the causative pathogen is essential for implementing the correct treatment and containment strategies, requiring in most cases multiplexed reactions (Fox, 2007). Also, developing and deploying surveillance platforms to track pathogen spread is increasingly important. In the case of non-transmissible diseases, detecting key genetic variations and biomarkers can enable early intervention before symptoms appear and the condition worsens (Gilboa *et al.*, 2020). Apart from clinical diagnostics, nucleic acid detection with high specificity and sensitivity is vital for applications in epidemiological surveillance, agricultural biosecurity, environmental monitoring, and biodefense.

Currently, polymerase chain reaction (PCR) methods, together with sequencing techniques, is the cornerstone of diagnostics across various fields due to its high sensitivity and specificity (Yang and Rothman, 2004). However, the coronavirus disease 2019 (COVID-19) pandemic (Kumar *et al.*, 2021) has underscored the need for diagnostic tools beyond PCR; ones that do not require expensive equipment or specialized training, hence facilitating large-scale screening programs. According to the World Health Organization, these new tools should be affordable, sensitive, specific, user-friendly, rapid, equipment-free, and deliverable (ASSURED) (Mabey *et al.*, 2004). These characteristics make them ideal for point-of-care (POC) testing and use in low-resource settings. Notably, by increasing testing capacity through a combination of complementary methods, better outcomes in disease prevention and community-level mitigation could be achieved (Larremore *et al.*, 2021).

In recent times, systems based on clustered regularly interspaced short palindromic repeats (CRISPR) have found innovative applications in the realm of specific and sensitive nucleic acid detection (Kaminski *et al.*, 2021). These ribonucleoprotein-based systems are archetype because of their

programmable sequence specificity, diverse binding and cleavage mechanisms, and compatibility with advanced nanobiotechnological developments. Pioneering work disclosed the *trans*-cleavage activity of the nucleases Cas12a and Cas13a (on single-stranded DNA and RNA, respectively) (Gootenberg *et al.*, 2017; Chen *et al.*, 2018), which was exploited to produce a suitable readout upon target recognition in combination with an isothermal pre-amplification step. Recombinase polymerase amplification (RPA) (Piepenburg *et al.*, 2006) is particularly favored for its simplicity in design and execution, though other amplification methods could also be employed (Zhao *et al.*, 2015).

The resulting CRISPR-based approach allows detections with single nucleotide specificity and attomolar sensitivity. Of note, the single-stranded DNA (ssDNA) reporter employed upon CRISPR-Cas12 or CRISPR-Cas13 detection assays can be labelled accordingly to utilize immunochromatographic assays that use commercially available lateral flow strips for their resolution (Broughton *et al.*, 2020; Gootenberg *et al.*, 2018; Marques *et al.*, 2022). Lateral flow assays (LFA) are characterized by their simplicity, speed, and cost-effectiveness (Bahadır and Sezgintürk, 2016). Lateral flow devices can differentiate between intact and cleaved reporter in CRISPR-Cas12/13 detection strategies. For successful collateral cleavage CRISPR-Cas-based-LFA, several factors must be considered, including the quality of the reporter (which depends on the chosen nuclease), sample application, and the correct quantity of reporter for intuitive result readout (Deng *et al.*, 2021). However, in these applications with commercially available strips the control line is used as the test line and *viceversa*, which greatly reduces the sensitivity of the technique and favors the occurrence of false positives (Liu *et al.*, 2021; Posthuma-Trumpie *et al.*, 2009).

CRISPR-Cas-based detection strategies with no collateral activity mechanism have also been harnessed in combination with LFA devices. CASLFA (CRISPR-Cas9-mediated lateral flow nucleic acid assay) (Wang *et al.*, 2020), FELUDA (*Francisella novicida* Cas9 editor linked uniform detection assay) (Azhar *et al.*, 2021), Bio-SCAN (biotin-coupled specific CRISPR-based assay for nucleic acid detection) (Ali *et al.*, 2021), and Vigilant (VirD2-dCas9 guided and LFA-coupled nucleic acid test) (Marsic *et al.*, 2021) are methods

that have been developed to exploit LFA kits, relying on RPA and CRISPR-Cas9. These techniques depend on the formation of a suitable CRISPR-Cas9-DNA complex carrying specific labels. In particular, CASLFA utilizes a biotinylated primer and a gold nanoparticle-linked oligonucleotide probe. In subsequent studies, CASLFA design was further improved for the simultaneous detection of different targeted regions in specially designed lateral flow strips (Xiong *et al.*, 2021). FELUDA uses a biotinylated primer and fluorescein-labelled single guide RNA (sgRNA), Bio-SCAN employs a fluorescein-labelled primer and a biotinylated dCas9, and Vigilant combines a biotinylated primer with a dCas9-relaxase fusion attached to a fluorescein-labelled oligonucleotide.

In the aforementioned diagnostic schemes, the test line, which is more sensitive than the control line, provides the readout. They have demonstrated limits of detection ranging from attomolar to femtomolar within approximately one hour and are capable of discriminating small genetic variations. Of note, they have been effectively applied to detect pathogens such as SARS-CoV-2, African swine fever virus, and *Listeria monocytogenes*. However, these methods require the modification of either the sgRNA or the nuclease, which prevents a widespread and cost-effective application. In addition, it would be beneficial to perform a multiplexed detection of different species in the same reaction with the CRISPR-Cas9 system to then be resolved in a commercially available LFA. This would enable the rapid creation of necessary tests to meet high and dynamic demand quickly.

Recently, we developed a novel nucleic acid detection method based on CRISPR-Cas9-mediated strand displacement, which we called COLUMBO (CRISPR-Cas9 R-loop usage for molecular beacon opening) (Márquez-Costa *et al.*, 2023). This method allowed a multiplexed detection in a single tube, thereby complementing the existing CRISPR-based diagnostic techniques. Nonetheless, it relies on the generation of a fluorescence signal upon nucleic acid recognition, which precludes its pervasive application in POC settings. In this work, we report the modification of COLUMBO aimed to use LFAs to resolve the detection. To this end, we employed biotin- and digoxigenin-labelled primers for the pre-amplification step and fluorescein-labelled probes for the CRISPR-Cas9-mediated strand displacement reactions. Our results

show that a rapid and streamline procedure implemented with attainable reagents allows the multiplexed detection of different species and displays ASSURED diagnostic potential.

2. RESULTS

2.1 Working principle and design of the Cas9-mediated detection LFA

We aimed to develop a nucleic acid detection platform with target-specific binding given by the CRISPR-Cas9 system via LFA for proper POC testing. We modified our recently developed COLUMBO method (Márquez-Costa *et al.*, 2023) to detect a nucleic acid of interest on commercially available lateral flow technology using gold particles. This allows us to obtain a readout without the need for a fluorimeter. The LFA detection requires the target to be labelled by both FAM and biotin. We designed biotin-labelled primers to amplify a suitable double-stranded DNA fragment from a pathogen's gene region of interest. Samples from patients are then labelled with biotin upon RT-RPA amplification. Then, sequence-specific detection is achieved by interfacing a CRISPR-Cas9 reaction, and a FAM-labelled probe is included in the reaction. The FAM-labelled probe hybridizes with the displaced strand from the Cas9 reaction. When the nucleic acid of interest is present in the sample, such elements are assembled, and the resulting structure (biotin-DNA + Cas9-sgRNA + FAM-probe) is both biotin and FAM-labelled, meaning it can be detected using commercially available strips (**Figure 1**).

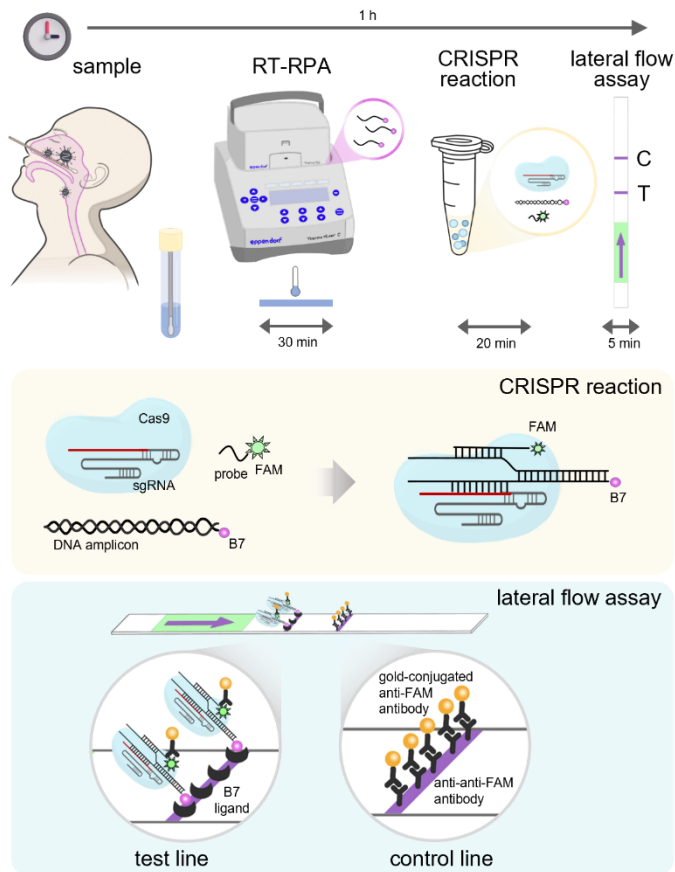


Figure 1. Schematics of the intended reaction with times. First a nasopharyngeal swab is obtained from patient samples. The collected samples are then amplified by RT-RPA with biotin (B7)-primers, yielding biotin-labelled amplicons. Then CRISPR-Cas9 reaction is interfaced. Cas9 recognizes and target the DNA amplicon and a FAM-labelled probe is going to hybridize with the generated displaced strand. At this point there is a complex probe-CRISPR-Cas9-DNA amplicon that is both FAM and biotin labelled. Upon sample addition in the sample application area of the dipstick, the gold-labelled FAM-specific antibodies bind the FAM-biotin complex. Then, the gold complexes travel through the membrane. The test line (T) is coated with biotin-ligand molecules, capturing only the biotin-target complexes, which will generate a red-blue band over the time. Unbound gold particles will continue migrating over the control line (C) containing anti-anti-FAM antibodies which will form a colored control band.

2.2 Validation of the platform with test SARS-CoV-2 samples

We evaluated the ability of the system to properly detect the N1 and E region from SARS-CoV-2. These experiments are focused on test samples generated from commercially available SARS-CoV-2 genome. After RT-PCR amplification for labelling the generated amplicons with biotin, we run a combinatorial set of the reactions with CRISPR-Cas9 elements and run the lateral flow reaction. The test line appeared within 3 minutes, finding only a positive value when all the reaction elements were present, and no apparent color change in the test line in response to isolated elements (**Figure 2**).

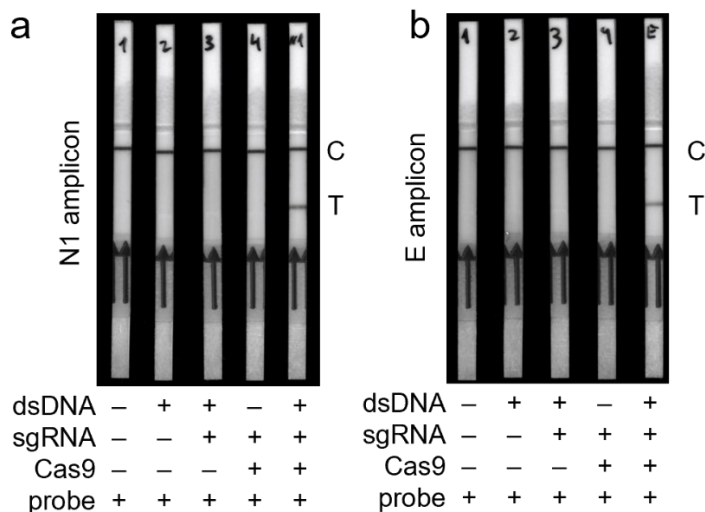


Figure 2. SARS-CoV-2 detection through a CRISPR-Cas9-based LFA reaction. a) LFA characterization of the detection for N1 amplicon. b) LFA characterization of the detection for E amplicon. (C) control line, (T) test line.

We varied the concentration of the DNA amplicon, finding proportionality between the input and the output signal (**Figure 3**).

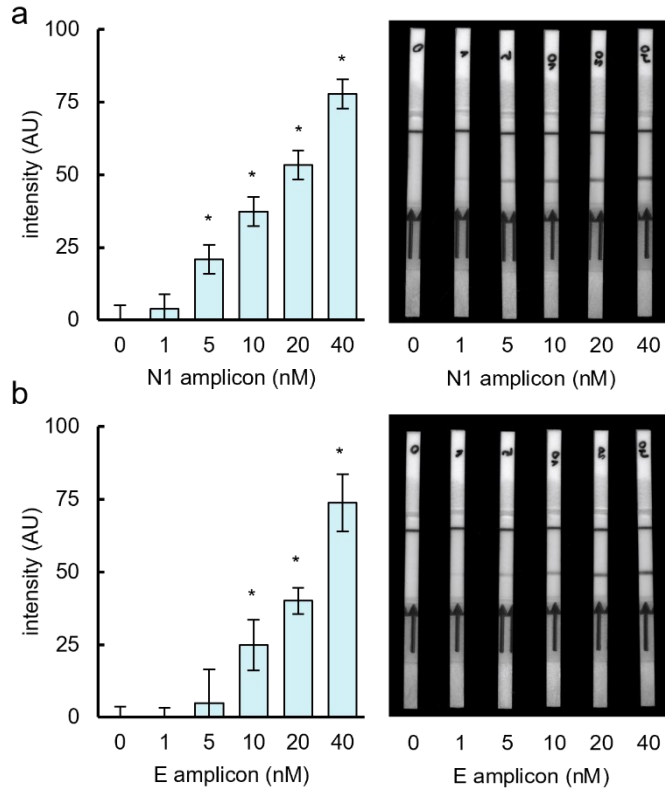


Figure 3. Effect of the DNA amplicon concentration on the output band intensity readout. Quantification of the band intensity is displayed on the left, lateral flow strips photos are displayed on the right. a) CRISPR-Cas9-based detection LFA performed for N1 amplicon. b) CRISPR-Cas9-based detection LFA performed for E amplicon. Error bars correspond to standard deviations ($n = 3$). *Statistical significance (Welch's t -test, two-tailed $P < 0.05$; determined with respect to the first condition).

We also inspected the impact of different versions of Cas9: the wild-type Cas9, HiFi Cas9 (characterized by showing significantly reduced off-target effects compared to the wild-type), the Cas9 H840A nickase (Cas9_n, which only cleaves the non-targeted strand), and the catalytically dead Cas9 protein (dCas9, which does not produce any cleavage but retains binding activity). All different Cas9 versions successfully produced a distinguishable colored test line in the presence of all elements, demonstrating the robustness of the method (**Figure 4**).

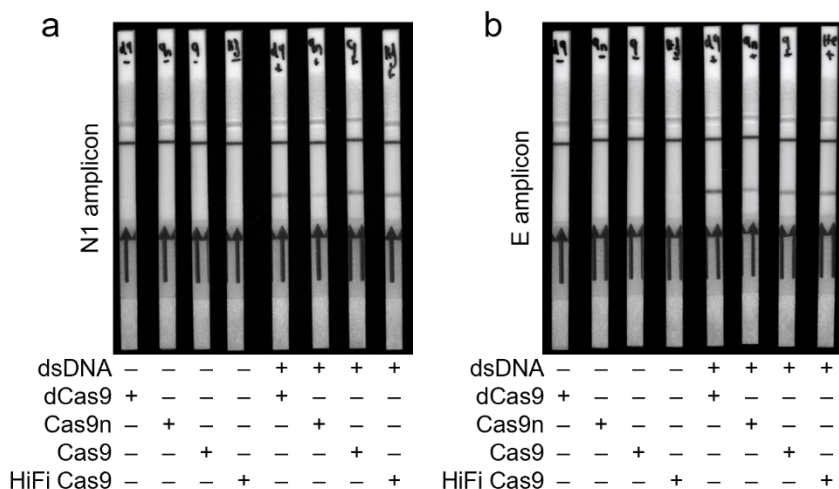


Figure 4. Effect of different versions of Cas9 (dCas9, Cas9n, Cas9 or HiFi Cas9) on the output signal. a) N1 amplicon targeted with different versions of Cas9. b) E amplicon targeted with different versions of Cas9.

Furthermore, we assessed how sensitive the detection assay was in discerning single-base mutations. To determine it, we set up reactions using Cas9 and HiFi Cas9 with the sgRNA and the probe designed to target the WT E amplicon. Then tested the ribonucleoprotein-probe complex against different single-base mutants of the E amplicon (**Figure 5**). The results show that both the native Cas9 and the HiFi Cas9 are only able to discriminate mutations in the PAM region in the LFA. None of them were able to discriminate mutations in the protospacer region.

In addition, we aimed to compare the output generated with our Cas9 reaction approach with a reaction using Cas12. We ran CRISPR-Cas12a reactions using a fluorescein and biotin-labelled ssDNA molecule as a probe. We obtained inconsistent results with Cas12 reactions, showing false positive results when running negative tests. No false results were observed with Cas9 (**Figure 6**).

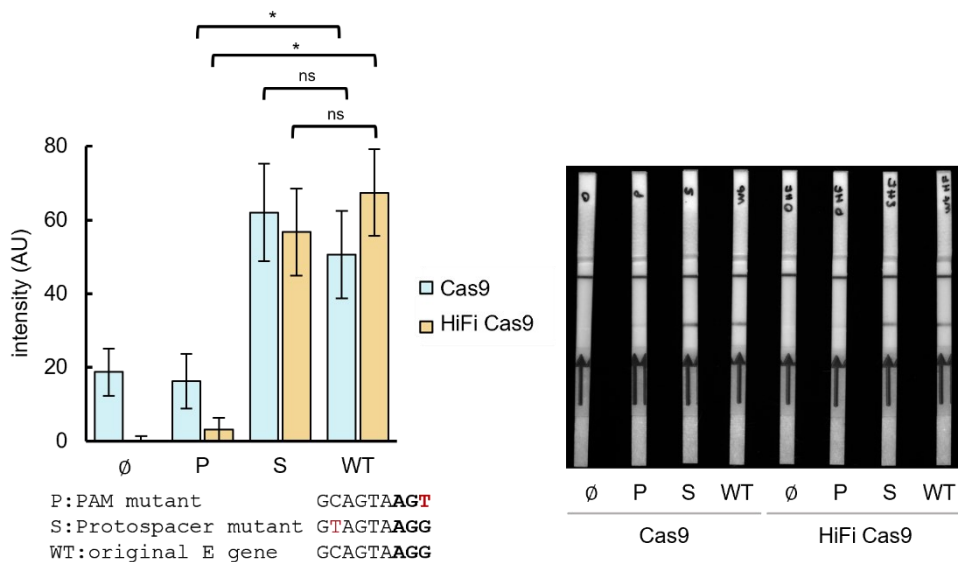


Figure 5. Lateral flow assay-based characterization of E gene substitution mutations detection with the native Cas9 and HiFi Cas9. On the left, quantification of the band intensity is shown. The amplicon sequences with substitution mutations are shown in red (PAM shown in bold). On the right, lateral flow strips photos are displayed. Error bars correspond to standard deviations ($n = 3$). *Statistical significance (Welch's t -test, two-tailed $P < 0.05$). ^{ns}Not statistically significant.

Given the availability of commercial dipsticks designed for simultaneous detection of two analytes, we also looked to demonstrate multiplexed detection of the N1 and E regions in a single reaction. These dual-test strip membranes have an additional test line coated with digoxigenin antibodies for detecting analytes labelled with FAM and digoxigenin, alongside the biotin test line present in regular lateral flow dipsticks. To achieve the simultaneous detection, we generated two differently labelled amplicons for the respective SARS-CoV-2 regions. Through RT-PCR amplification, we obtained biotin-labelled N1 amplicons and digoxigenin-labelled E amplicons. Both amplicons are FAM-labelled upon CRISPR-Cas9 targeting due to the provided sequence-specific FAM probe. When the dipstick is placed in this solution, biotin-FAM-labelled N1 amplicons are captured on the first test line containing immobilized biotin-ligand molecules, while digoxigenin-FAM-labelled E amplicons are captured at the second test line, generating a red-blue band over time. The control band is fixed on a third line. To assess the

multiplexing capability of CRISPR-Cas9, we conducted a series of combinatory reactions with different labelled amplicons. The results were consistent and showed no cross-reactivity (**Figure 7**).

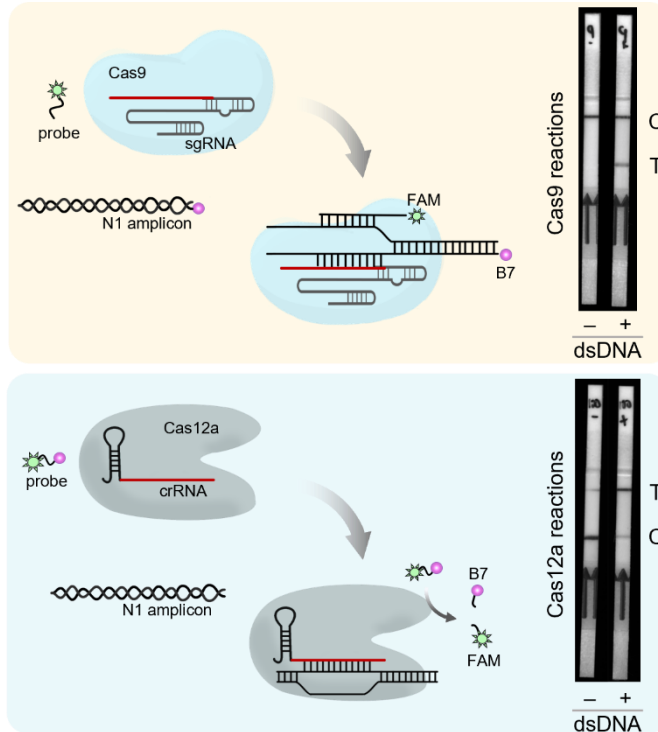


Figure 6. Comparison between the performance of a CRISPR-Cas reaction targeting N1 amplicon with either Cas9 (top) or Cas12a (bottom). Note that the control (C) and test (T) lines on the lateral flow strip are named according to the specific detection strategy being used.

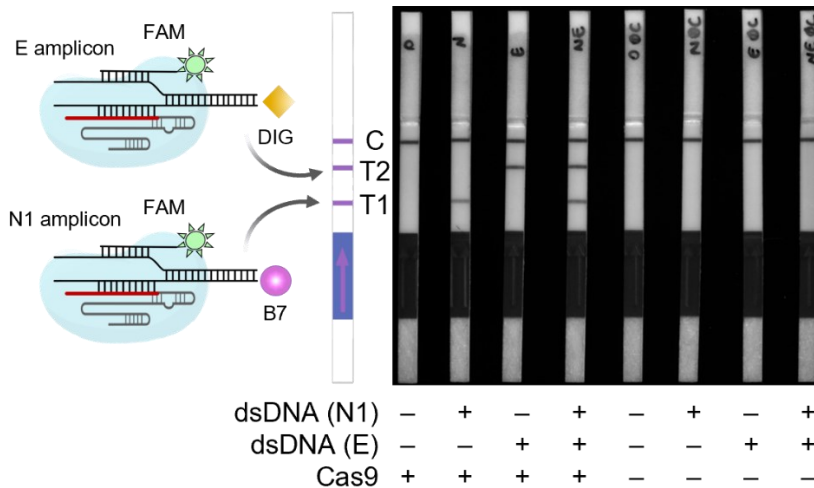
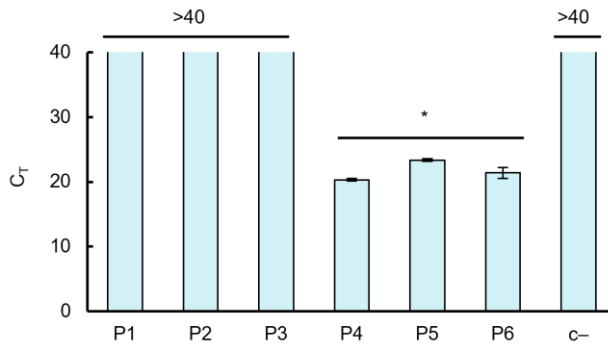


Figure 7. Multiplexed SARS-CoV-2 detection using CRISPR-Cas9-based LFA. The N1 amplicon is labelled with biotin (B7) and captured on the first test line (T1) of the dipstick. The E amplicon is labelled with digoxigenin (DIG) and captured on the second test line of the dipstick (T2). (C) control line.

2.3 Validation of the platform with SARS-CoV-2 clinical samples

Motivated by the performance of the CRISPR-Cas9 detection assay in the LFA, we proceeded to use the technology for detecting SARS-CoV-2 in clinical patient samples. Nasopharyngeal swabs were collected from individuals diagnosed as either positive or negative for the virus by RT-qPCR at the Clinic University Hospital of Valencia (Spain). We then revalidated the infections through RT-qPCR in our laboratory (**Figure 8**).



Patient	Sample type	Targeted region	Diagnostic at the hospital	C _T at our lab
P1	nasopharyngeal	N1	Negative	>40
P2	nasopharyngeal	N1	Negative	>40
P3	nasopharyngeal	N1	Negative	>40
P4	nasopharyngeal	N1	Positive	20.29
P5	nasopharyngeal	N1	Positive	23.34
P6	nasopharyngeal	N1	Positive	21.39
c-	water	N1	(-)	>40

Figure 8. RT-qPCR characterization of patient samples used in this study. The cycle threshold (C_T) values obtained in the RT-qPCR amplification for the N gene are shown alongside with the characteristics of the different patient samples used in this work. Error bars correspond to standard deviations ($n = 3$). *Statistical significance (Welch’s *t*-test, two-tailed $P < 0.05$).

Following N1 and E genes RT-RPA amplification of the patient samples using the biotin-labelled primers, and without RNA extraction, we conducted CRISPR-Cas9-based detection followed by LFA. The resulting strips displayed clear differential readouts, effectively indicating the presence of the virus (**Figure 9**).

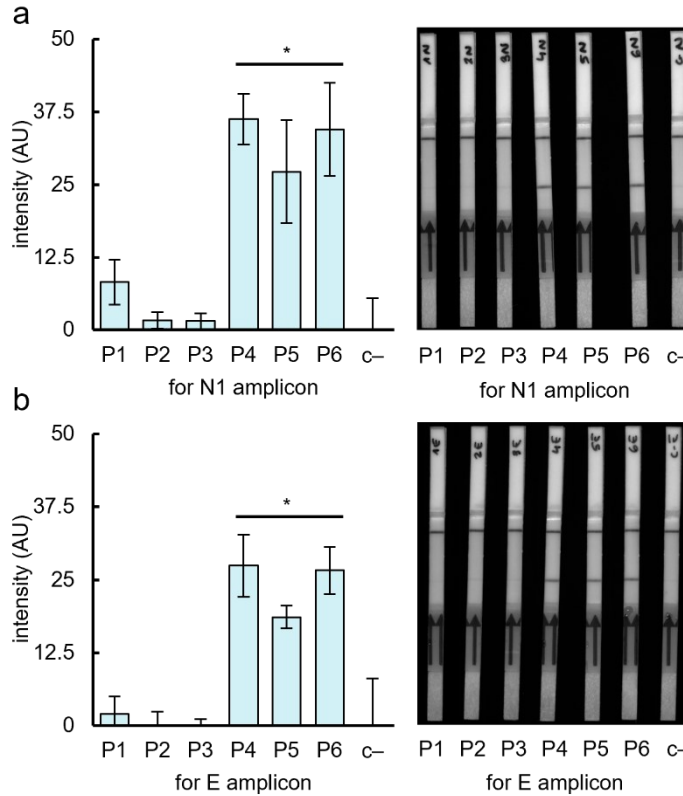


Figure 9. Detection of SARS-CoV-2 N1 and E genes in patient samples using CRISPR-Cas9-based LFA (6 patients, 3 reactions per patient); amplifications performed by RT-RPA. On the left, quantification of the band intensity is shown. On the right, lateral flow strips photos are displayed. Error bars correspond to standard deviations ($n = 3$). *Statistical significance (Welch's t -test, two-tailed $P < 0.05$).

Building on these results, we aimed to perform multiplexed detection of the viral fragments to enhance diagnostic accuracy. We conducted multiplexed RT-RPA using both N1 biotin-labelled and E digoxigenin-labelled primers, followed by the CRISPR-Cas9 detection reaction. The LFA strips revealed the two distinct test lines in samples from patients diagnosed with SARS-CoV-2 (**Figure 10**).

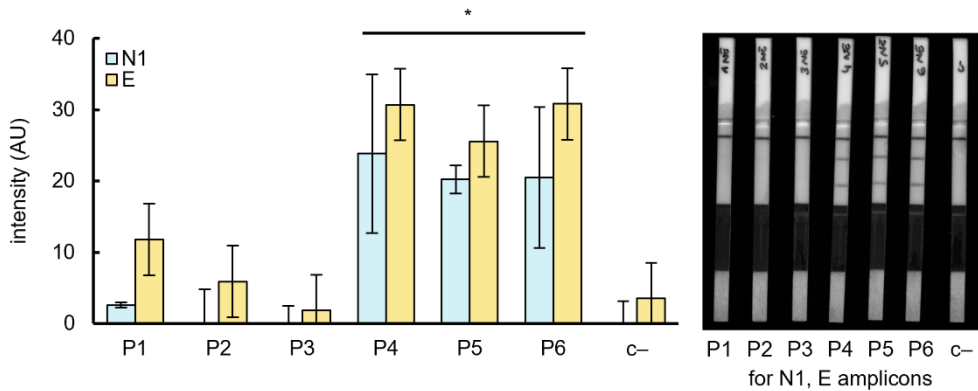


Figure 10. Multiplexed detection of SARS-CoV-2 in patient samples (6 patients, 3 reactions per patient); amplifications performed by multiplexed RT-RPA. On the left, quantification of the band intensity is shown. On the right, lateral flow strips photos are displayed. Error bars correspond to standard deviations ($n = 3$). *Statistical significance (Welch’s t -test, two-tailed $P < 0.05$).

Starting from the individual sample collection, the time until the result is ready using lateral flow technology is approximately one hour. These findings highlight the potential of the Cas9 platform coupled with LFA for fast and efficient clinical diagnostics.

2.4 Validation of the platform with plant infected samples

To extend the applicability of our technology, we decided to test its performance in detecting infections in plants. We evaluated its efficacy against different plant viruses and a viroid in single infections in *Nicotiana benthamiana* plants. Since RNA viruses constitute the majority of plant viruses and cause diseases that result in losses amounting to several billion dollars annually (Rubio *et al.*, 2020), we selected RNA viruses for our experimental assessments. For this study, we focused on *Tobacco mosaic virus* (TMV, M), *Tobacco etch virus* (TEV, E), and *Potato virus X* (PVX, X), three (+)-strand RNA viruses along with *Potato spindle tuber viroid* (PSTVd, P). TMV belongs to the family of *Virgaviridae* (genus *Tobamovirus*) infecting a wide range of plants, causing mosaic patterns and discoloration on the

leaves (Scholthof, 2004). TMV genome consists of a single-stranded ~6.4 kb RNA encoding at least four proteins (Ishibashi and Ishikawa, 2016). TEV is a member of the *Potyviridae* family (genus *Potyvirus*) inducing disease in many *Solanaceae* plant species, such as vein clearing, mottling, and etching. The TEV genome is a ~9.5 kb nucleotides-long single-stranded RNA encoding for a polyprotein yielding ten mature products (Cesaratto *et al.*, 2016). PVX is in the family *Alphaflexiviridae* (genus *Potexvirus*) causing stunting in potato plants. PVX genome is ~6.4 kb RNA expressing five viral proteins (Batten *et al.*, 2003). PSTVd belongs to the family *Pospiviroidae* (genus *Pospiviroid*) affecting potatoes and tomatoes with symptoms varying from color changes in the foliage, smaller leaves and spindle-like elongation. It consists of a ~360-nucleotide single-stranded, circular RNA molecule (Boonham *et al.*, 2004). Since viroids are not known to code any protein products, detection methods must be directly based on their genome detection.

We designed biotin-labelled primers to amplify a suitable double-stranded DNA fragment from the coat protein of three plant viruses and a viroid, trying to avoid cross-interaction with the host genome. Crude extracts from infected plants were obtained from plant tissues by using an alkaline lysis solution. By placing a small piece of plant tissue into the solution, this method allows generating plant extracts in only 5 minutes without a complex infrastructure. In comparison to the standard approach for RNA purification which requires specific equipment and is time-consuming (90 minutes), the alkaline lysis solution requires less time and instrumental devices, making it a better approach for in-field use. RT-RPA amplification produces biotin-labelled amplicons, which are subsequently FAM-labelled during the CRISPR-Cas9 reaction and then resolved in the LFA (**Figure 11**).

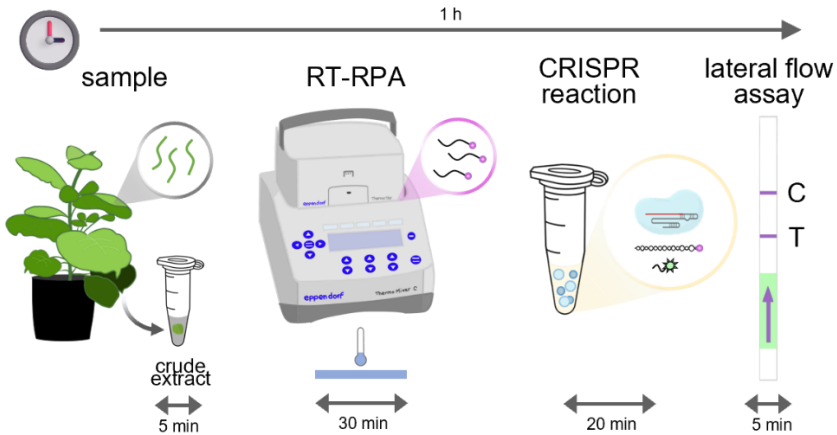


Figure 11. Schematics of the intended reaction with times. First a crude extract is obtained from infected plants by using an alkaline lysis solution. The collected samples are amplified by RT-RPA using biotin-labelled primers, resulting in biotin-labelled amplicons, which are then processed by the CRISPR-Cas9 reaction to then be resolved in the lateral flow assay.

We evaluated the ability of the system to properly detect different viral infections from plant. Infections were confirmed by RT-qPCR (**Figure 12**). Following crude extracts RT-RPA amplification, which labels the generated amplicons with biotin, we conducted a series of combinatorial reactions involving CRISPR-Cas9 components and subsequent lateral flow assays. The test line became visible within 3 minutes, showing a positive result only when all reaction components were present, while isolated elements produced no detectable color change. The resulting lateral flow strips demonstrated clear differential readouts, clearly differentiating between infected and mock plants, thereby effectively indicating the presence of the pathogen (**Figure 13**).

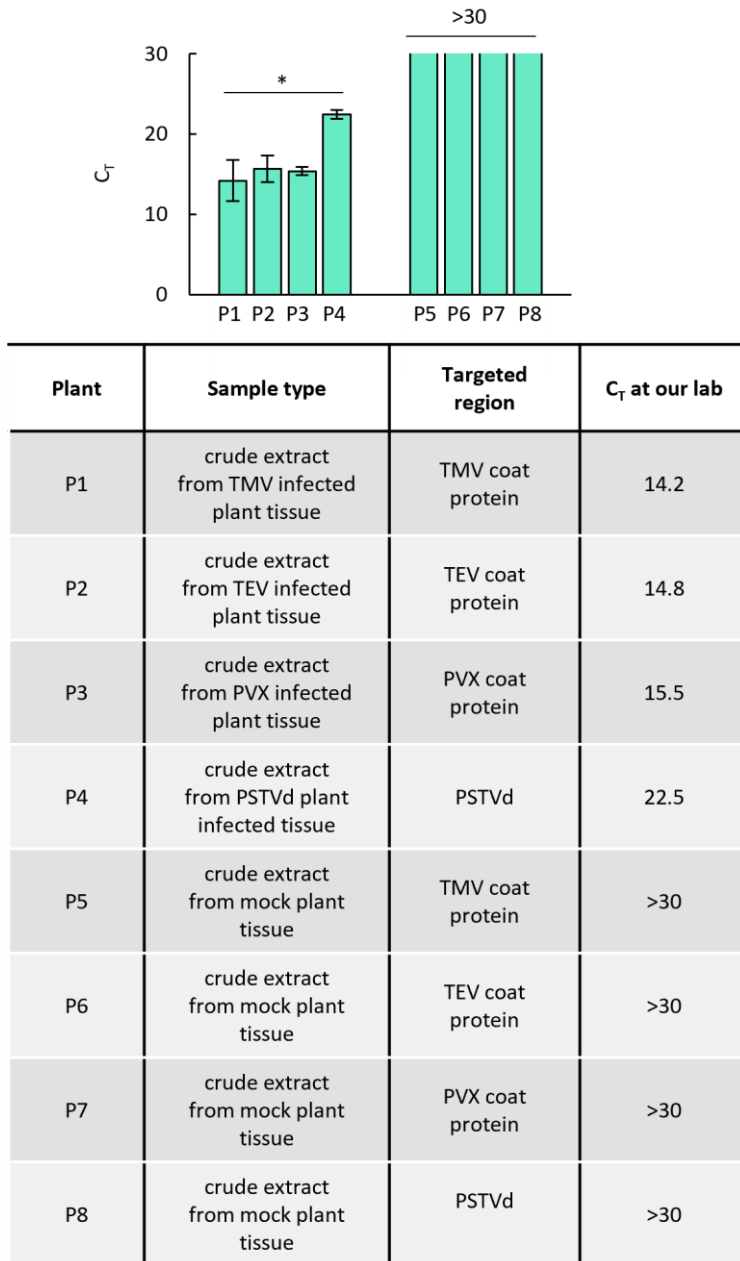


Figure 12. Detection of plant viruses by RT-qPCR. The cycle threshold (C_T) values obtained in the RT-qPCR amplification for the different virus genes are shown. Error bars correspond to standard deviations ($n = 3$). *Statistical significance (Welch's t -test, two-tailed $P < 0.05$).

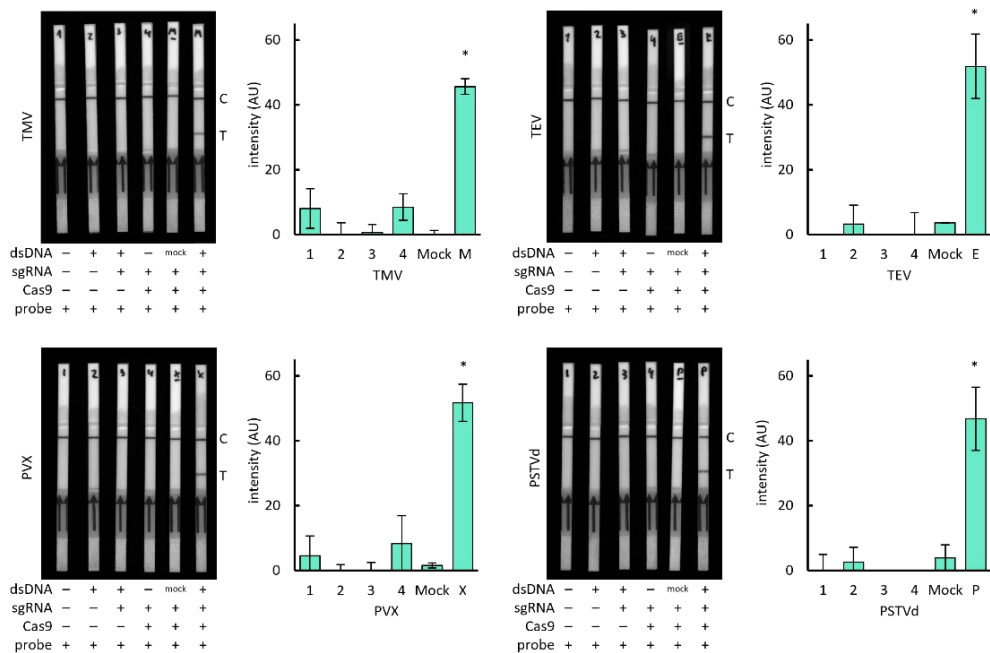


Figure 13. Different plant pathogen detection through a CRISPR-Cas9-based LFA reaction. Lateral flow strips photos are displayed on the left, quantification of the band intensity is displayed on the right. (C) control line, (T) test line. Error bars correspond to standard deviations ($n = 3$). *Statistical significance (Welch's t -test, two-tailed $P < 0.05$).

In addition, we sought to compare the performance of our Cas9-based assay with a Cas12-based approach. For the Cas12a reactions, we utilized a probe consisting of a fluorescein and biotin-labelled ssDNA molecule. The Cas12a reactions yielded inconsistent results, including false positives in negative control tests. In contrast, the Cas9-based assays demonstrated no false positives, indicating greater specificity and reliability (**Figure 14**).

Based on these promising results, we intend to continue our work on the diagnostics of infections caused by various plant pathogens using CRISPR-Cas9. Our future efforts will include the development and optimization of multiplexed detection assays resolved using LFA.

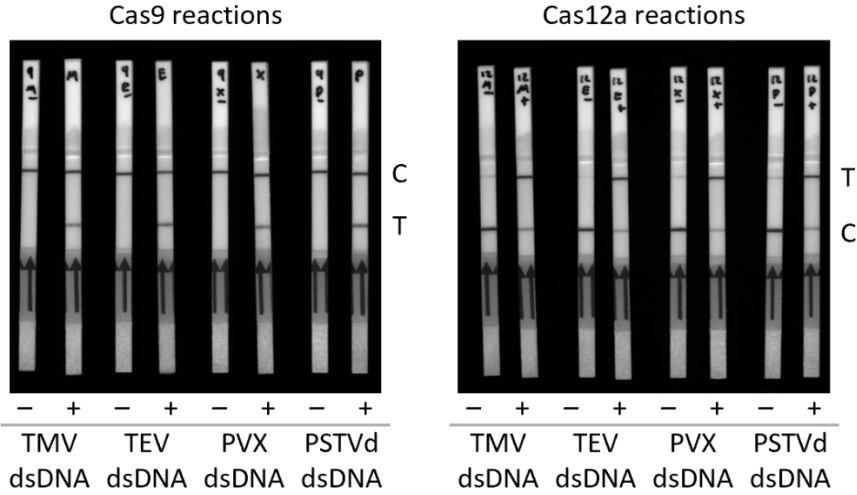


Figure 14. Comparison between the performance of a CRISPR-Cas reaction targeting plant pathogens amplicons with either Cas9 (left) or Cas12a (right). Note that the control (C) and test (T) lines on the lateral flow strip are named according to the specific detection strategy being used.

3. DISCUSSION

We have successfully integrated a CRISPR-Cas9-based detection method with lateral flow technology. We showed this mechanism is useful for the detection of different pathogen infections in a fast, simple, and effective way, even enabling multiplexed detections of different regions of the virus in the same strip. When we first developed the novel CRISPR-Cas9-based strand displacement reaction for the detection of nucleic acids of interest (Márquez-Costa *et al.*, 2023), the readout of the positive result was given by a measurable signal of fluorescence, hence highlighting the need for a fluorimeter. To prevent cross-interactions that could result in the unwanted opening of the molecular beacon and a subsequent high fluorescence signal, we had to either purify the amplified products or devise other strategies. In the fluorescence-based characterization of the detection, it was essential to ensure the molecular beacon only opened in the presence of the specific target,

thereby maintaining the accuracy and reliability of the detection system but further complicating a one-pot methodology (Ghouneimy *et al.*, 2022). We have overcome these limitations by coupling the Cas9-based detection mechanism with LFA. The direct product from the amplification process can be introduced into the CRISPR reaction, and the colorimetric readout allows for interpretation of the results with the naked eye, simplifying the diagnostic process. The ease of use and minimal equipment required for the LFA make it a practical and accessible choice for at-home testing and point-of-care applications.

The robustness and reliability of CRISPR-Cas-based detection methods ensure high sensitivity and specificity, but result interpretation remains a challenge for certain approaches. For the LFA in the CRISPR-Cas12/Cas13 detection strategies based on collateral activity, the control and test line are exchanged (Broughton *et al.*, 2020; Ding *et al.*, 2021; Marques *et al.*, 2022). This results in a completely different interpretation of the resulting signals, which can lead to confusions. An intact reporter probe in Cas12/Cas13 methods is retained at the first-control line (C), resulting in a visible C-line and no visible second-test line (T), indicating a negative test result. When the reporter is cleaved, the gold conjugate is then retained at the T-line. Thus, positive results are indicated by an increasing intensity of the T-line and a decreasing intensity of the C-line, but many precautions must be taken to achieve a satisfactory result. By interfacing the reaction with Cas9, whose detection method relies on strand displacement rather than on collateral catalysis, we can make use of the commercially available lateral flow technology in a fast intuitive way so as to minimize false positives and maximize consistency. We can obtain results within 1 hour from sample collection, making our detection method significantly faster than the traditional qPCR diagnostic technique.

The successful implementation of our novel CRISPR-Cas9 detection method with the LFA demonstrates the robustness of the technology, highlighting the potential to work in multiple detection contexts and not in just one setting. We envision our Cas9-based detection methodology to be able to adapt to the next-generation diagnostics and nanotechnology devices (Sadeghi *et al.*, 2021; Sena-Torrallba *et al.*, 2022). As detection technologies continue to

advance, our system will be well-positioned to integrate with innovative platforms such as paper-based diagnostics and microfluidic devices (Huang *et al.*, 2021; Ramachandran *et al.*, 2020; Yin *et al.*, 2021). Furthermore, we showed its potential in detecting both human and plant pathogens, showing the application of this technique can be applied to identify a wide range of other infecting agents of concern. Moreover, CRISPR-Cas systems could be engineered to recognize specific genetic markers associated with diseases, providing a powerful tool for early disease detection and management. The integration of CRISPR-Cas with LFA represents a significant advancement in the field of molecular diagnostics, displaying potential for use in POC applications, and enabling a rapid and reliable detection of a variety of nucleic acids.

4. MATERIALS AND METHODS

4.1 Test Samples

Test sample was prepared from a synthetic SARS-CoV-2 Genome (Vircell). Primers were used to amplify the N1 and E region of the virus genome. Reverse primers were labelled in their 5' end with biotin or digoxigenin. DNA amplicons with different single base mutations in the E amplicon were chemically synthesized (IDT) and then amplified by PCR to label appropriately. Sequences are provided in **Data set Table 1**.

4.2 Clinical Samples

Nasopharyngeal swabs from both SARS-CoV-2 infected and non-infected patients, confirmed by RT-qPCR diagnostics, were obtained from the Clinic University Hospital of Valencia (Spain). Samples were inactivated through the action of proteinase K followed by a heat shock (5 min at 60 °C) before proceeding with the research study. No RNA extraction protocol was

performed. The ethical committee of the Clinic University Hospital approved this study (order #2020/221).

4.3 Plant Infection with Viruses

TMV, PVX, and TEV were mechanically inoculated and propagated in five-week-old *Nicotiana benthamiana* plants using infectious extracts with sequence variants MK087763.1, MT799816.1, and DQ986288 (G273A, A1119G), respectively. Frozen aliquots of infected tissue (50 mg) were ground and homogenized in 20 volumes of inoculation buffer (50 mM potassium phosphate (pH 8.0), 1% polyvinylpyrrolidone 10, 1% polyethylene glycol (PEG) 6000, and 10 mM 2-mercaptoethanol). Then, a cotton swab was employed to spread the sample containing the virus over the surface of a single leaf in the presence of 10% carborundum in inoculation buffer. In the case of PSTVd, a viroid RNA preparation (U23058) was used for its propagation. Briefly, the RNA sample was mixed with 0.1 volumes of 0.5 M K_2HPO_4 and water to a final volume of 5 μ L. This mixture was deposited on the adaxial side of the leaf surface next to 5 μ L of a 10% carborundum dispersion in 50 mM K_2HPO_4 . Using a glass rod, both droplets were mixed and gently spread across the leaf surface.

The plants were then maintained in a growth chamber at 25 °C under a 12-hour day/night photoperiod. Plant tissue infected from virus were collected after 7 days post-infection. Viroid plant infection tissue was collected after 1-month post-infection.

4.4 Plant tissue preparation

Alkaline PEG lysis solution was used for obtaining crude extracts (Hwang *et al.*, 2013). Briefly, approximately 50 mg of plant tissue was incubated with 300 μ L of lysis solution (15% PEG 4000, 20 mM NaOH) for 5 min at room temperature. Samples were vortexed and then 50 μ L of crude plant extract

was purified by using an RNA clean and concentrator column (Zymo) by centrifugation.

4.5 CRISPR Elements

Different versions of *S. pyogenes* Cas9 were purchased from IDT. The wild-type nuclease (Cas9), the Cas9 H840A nickase (Cas9n), the catalytically dead Cas9 protein (dCas9), and the high-fidelity Cas9 nuclease (HiFi Cas9) were used. Cas12a from *L. bacterium* was purchased from NEB. sgRNAs and crRNA were designed and generated from DNA templates through *in vitro* transcription using the TranscriptAid T7 high yield transcription kit (Thermo). The sgRNAs and crRNA were then purified using the RNA clean and concentrator columns (Zymo) and quantified with a NanoDrop. Sequences are provided in **Data set Table 1** and **Table 2**.

4.6 Probes

Different kinds of probes were designed and purchased from IDT. For the Cas9 reaction, probes were designed as DNA oligonucleotides hybridizing with the displaced strand generated upon CRISPR-Cas9 targeting. Cas9 probes were labelled in their 5' end with a FAM fluorophore. The probe for Cas12a reaction is a ssDNA TTATT labelled with fluorescein-biotin at the ends. Sequences are provided in **Data set Table 1** and **Table 2**.

4.7 Nucleic Acid Amplification by RT-PCR

TaqPath 1-Step RT-PCR Master Mix, CG kit (Thermo) was used for sample amplification. 1 μL of commercial SARS-CoV-2 Genome (65 copies/ μL , Vircell) was mixed with 500 nM of forward and reverse primers. 5 μL of the Master Mix were added to the mixture for a total volume of 20 μL , adjusted

with RNase-free water. Reactions were incubated in a thermocycler (Eppendorf). The protocol was a 2 min incubation at 25 °C for uracil-N glycosylation and 50 °C for 15 min for RT, followed by an inactivation step at 95 °C for 2 min and then 40 cycles of amplification at 95 °C for 15 s and 62 °C for 60 s. RT-PCR products were purified by centrifugation using a DNA clean and concentrator column (Zymo), and quantified with a NanoDrop for gradient assay. Sequences are provided in **Data set Table 1**.

4.8 Nucleic Acid Amplification by RT-RPA

Clinical patient samples and crude extracts from plant tissues were amplified by RT-RPA. The TwistAmp basic kit (TwistDX) was used. 500 U RevertAid (Thermo), 50 U RNase inhibitor (Thermo) and 480 nM of forward and reverse primers were added to 29.5 µL of rehydration buffer for a total volume of 45.4 µL (adjusted with RNase-free water). The TwistAmp Basic reaction pellet was resuspended with this volume, and 22.7 µL, in addition to 1 µL of patient nasopharyngeal sample or 5 µL of RNA purified crude plant extract, was used per reaction. 7 mM magnesium acetate was added to start the reaction. In the case of multiplexed amplifications, each primer pair was used at 380 nM. Reactions were incubated at 42 °C for 30 min in a thermomixer C (Eppendorf), shaking 10 s at 300 rpm every 2 min. Sequences are provided in **Data set Table 1** and **Table 2**.

4.9 RT-qPCR

The TaqPath 1-step RT-qPCR Master Mix, CG was used for the reactions. 2 µL of the patient sample or 1 µL of plant crude extract were mixed with 500 nM of forward and reverse primers (CDC N1 or specific designed primers for plant pathogens), 125 nM of a single-stranded DNA probe (SARS-CoV-2 RUO kit, IDT) or 250 nM of ssDNA probe for plant pathogens, and 5 µL of the master mix, with the final volume adjusted to 20 µL using RNase-free water. The reactions were performed in a fast microplate (Applied) using

QuantStudio 3 equipment (Thermo). The protocol included incubation at 25 °C for 2 minutes for uracil-N glycosylation, followed by 53 °C for 10 min for RT, 95 °C for 2 min for RT inactivation, followed by 40 cycles of 95 °C for 3 s for denaturation and 60 °C for 30 s for annealing and extension. Sequences are provided in **Data set Table 1** and **Table 2**.

4.10 CRISPR-Cas9-Based detection coupled to Lateral Flow Assay

CRISPR-Cas9 reactions were carried out in 1x TAE buffer pH 8.5 (Invitrogen), 0.05% Tween 20 (Merck), and 12.5 mM MgCl₂ (Merck) at a final volume of 20 µL. The CRISPR-Cas9 ribonucleoprotein, preassembled at room temperature for 30 minutes, was added at a concentration of 100 nM and at 200 nM for PVX and PSTVd. For test samples, 2 µL of amplified DNA (unless otherwise specified) was used per reaction. In the multiplexed detection, 1.6 µL of amplified E amplicon and 2.4 µL of amplified N1 amplicon were used. In the case of patient samples 2 µL of amplified DNA was used. For the plant infection detection, 2 µL of direct amplified product from RT-RPA was used per reaction, except for the PSTVd in which 6 µL were used. The probe(s) was/were used at 100 nM, except for the multiplexed detection with patient samples where the N1 probe was used at 100 nM and the E probe was at 50 nM. Reactions were incubated at 37 °C for 20 min in a thermomixer C (Eppendorf). Then, 80 µL GenLine Dipstick buffer (Milenia) was added for 1:5 dilution. The lateral flow strip (HybriDetect, Milenia) was dipped into the reaction tube. Results were read after 4 min of incubation in the buffer and images were captured with a gel documentation system (Uvidoc HD6, Uvitec Cambridge). Intensity band quantification was measured with Fiji software (Schindelin *et al.*, 2012).

4.11 CRISPR-Cas12a-Based detection

A mixture of Cas12a from *L. bacterium* (NEB) crRNA was incubated at room temperature for 30 minutes in NEBuffer 2.1 (10 mM Tris-HCl, 50 mM NaCl,

10 mM MgCl₂, and 100 µg/mL BSA, pH 7.9; NEB) for a final concentration of 100 nM except for PVX and PSTVd in which final concentration was 200 nM. Subsequently, 2 µL of amplified test sample (in the case of the PSTVd, 6 µL of amplified RT-RPA product were used) was combined with 17 µL of the CRISPR-Cas12a ribonucleoprotein preparation and 100 nM of the ssDNA probe (TTATT, labelled with fluorescein-biotin at the ends), to make a total volume of 20 µL. This mixture was incubated at 37 °C in a thermomixer C (Eppendorf) for 20 min. The lateral flow assay was prepared similarly to the Cas9 reaction.

4.12 Data set

Table 1. List of sequences used in this work for SARS-CoV-2 detection

Name	Sequence 5' - 3'
N1 Primer Forward	GAGTATCATGACGTTTCGTGTTGTTTTAGATTTTC
N1 Primer Reverse	/Biotin/GTTCTCCATTCTGGTTACTGCCAGTTGAAT
N1 Primer Forward (CDC)	GACCCCAAATCAGCGAAAT
N1 Primer Reverse (CDC)	TCTGGTTACTGCCAGTTGAATCTG
N1 amplicon	GAGTATCATGACGTTTCGTGTTGTTTTAGATTTTCATCTAAA CGAACAAACTAAAATGTCTGATAATGGACCCCAAATCAG CGAAATGCACCCCGCATTACGTTTGGTGGACCCTCAGATT CAACTGGCAGTAACCAGAATGGAGAAC
E Primer Forward	/Biotin- Digoxigenin/ACAGGTACGTTAATAGTTAATAGCGT
E Primer Reverse	GACCAGAAGATCAGGAACTCTAGAAGAATTC
E amplicon	ACAGGTACGTTAATAGTTAATAGCGTACTTCTTTTTCTTGCT TTCGTGGTATTCTTGCTAGTTACACTAGCCATCCTTACTGCG CTTCGATTGTGTGCGTACTGCTGCAATATTGTTAACGTGAGT CTTGTAACCTTCTTTTTTACGTTTACTCTCGTGTTAAAAAT CTGAATTCTTCTAGAGTTCTGATCTTCTGGTC
sgRNA N1 (Cas9)	GGAAAAUAGCGAAAUGCACCCCGCAUUACGUUGUUUUAG AGCUAGAAAUAGCAAGUUAAAAUAAGGCUAGUCCGUUAUC AACUUGAAAAAGUGGCACCGAGUCGGUGCUUUU
sgRNA E (Cas9)	GGAGUAGUACGCACACAAUCGAAGCGCAGUAGUUUUAGAG CUAGAAAUAGCAAGUUAAAAUAAGGCUAGUCCGUUAUCA CUUGAAAAAGUGGCACCGAGUCGGUGCUUUU
crRNA N1 (Cas12a)	UAAUUUCUACUAAGUGUAGAUGUGGACCCUCAGAUUCAACU
Probe Cas9 N1	/FAM/GCGAAATGCTGTAATGCGGGGTGCATTTTCGC
Probe Cas9 E	/FAM/CGCACACAACTGCGCTTCGATTGTGTGCG
Probe Cas12a	/FAM/ TTATT /Biotin/

Table 2. List of sequences used in this work for plant pathogen detection

Name	Sequence 5' - 3'
TMV	
TMV Forward primer (qPCR)	AGACAATTCAGTGAGGTGTGG
TMV Reverse Primer (qPCR)	CCTAACAGTGCTGTGACTAGC
TMV qPCR probe	/56- FAM/AGGTTCCCTGACAGTGACTTTAAGGTGT/IBFQ/
TMV Forward Primer (RPA)	GACAATTCAGTGAGGTGTGGAAACCTTCAC
TMV Reverse Primer (RPA)	/Biotin/ TCGAATGCACCTAACAGTGCTGTGACTAGC
TMV amplicon	GACAATTCAGTGAGGTGTGGAAACCTTCACCACAAGTAAC TGTTAGGTTCCTGACAGTGACTTTAAGGTGTACAGGTAC AATGCGGTATTAGACCCGCTAGTCACAGCACTGTTAGGTG CATTCTGA
TMV Cas9 sgRNA	ggUAAGGUGUACAGGUACAAUGGUUUUAGAGCUAGAAAUA GCAAGUUAUUUUAAGGCUAGUCCGUUAUCAACUUGAAAAA GUGGCACCGAGUCGGUGCUUUU
TMV Cas9 probe	/FAM/ CTTTAAGGTGGTGTACCTGTACACCTTAAAG
TMV Cas12a crRNA	UAAUUUCUACUAAGUGUAGAUAGGUGUACAGGUACAAUGCG
TEV	
TEV Forward Primer (qPCR)	GTTATGATGGATGGTGAGGAGC
TEV Reverse Primer (qPCR)	TGTATGGTCGCTCCCTATTCC
TEV qPCR probe	/FAM/CGCAGCCAACACTGAGGCAAATTA/IBFQ/
TEV Forward Primer (RPA)	GAACCTGGGTTATGATGGATGGTGAGGAGC
TEV Reverse Primer (RPA)	/Biotin/ACCTAGGCATGTATGGTCGCTCCCTATTCC

TEV amplicon	GAAC TTGGGTTATGATGGATGGTGAGGAGCAAGTTTCATA CCCGCTGAAACCAATGGTTGAAAACGCGCAGCCAACACTG AGGCAAATTATGACACACTTCAGTGACCTGGCTGAAGCGT ATATTGAGATGAGGAATAGGGAGCGACCATACATGCCTAG GT
TEV Cas9 sgRNA	gGUAUAUUGAGAUGAGGAAUAGUUUUAGAGCUAGAAAUAG CAAGUUAUUUUAAGGCUAGUCCGUUAUCAACUUGAAAAAG UGGCACCGAGUCGGUGCUUUU
TEV Cas9 probe	/FAM/CGTATATTGCTCCTCATCTCAATATACG
TEV Cas12a crRNA	UAAUUUCUACUAAGUGUAGAUAUACCCGCUGAAACCAAUGG
PVX	
PVX Forward Primer (qPCR)	CAACAGTCCACCTGCTAACTGG
PVX Reverse Primer (qPCR)	CAGCAGTTTGGGCAGCATTTC
PVX qPCR probe	/FAM/TTCAATGGAGTCACCAACCCAGCT/IBFQ/
PVX Forward Primer (RPA)	ACAACAGTCCACCTGCTAACTGGCAAGCAC
PVX Reverse Primer (RPA)	/Biotin/AGCAGTTTGGGCAGCATTTCATTTTCAGCTTC
PVX amplicon	ACAACAGTCCACCTGCTAACTGGCAAGCACAAAGTTTCAA GCCTGAGCACAAATTCGCTGCATTTCGACTTCTTCAATGGA GTCACCAACCCAGCTGCCATCATGCCCAAAGAGGGGCTCA TCCGGCCACCGTCTGAAGCTGAAATGAATGCTGCCCAAAC TGCT
PVX Cas9 sgRNA	ggCUGCCAUCAUGCCCAAAGAGGUUUUAGAGCUAGAAAUA GCAAGUUAUUUUAAGGCUAGUCCGUUAUCAACUUGAAAAA GUGGCACCGAGUCGGUGCUUUU
PVX Cas9 probe	/FAM/CTGCCATGTTTGGGCATGATGGCAG
PVX Cas12a crRNA	UAAUUUCUACUAAGUGUAGAUAAAGCCUGAGCACAAAUUCGC
PSTVd	
PSTVd Forward Primer	CTCGCCCCGGAGCAAGTAAG

(qPCR)	
PSTVd Reverse Primer (qPCR)	TTCCTTTCTTCGGGTGTCCTC
PSTVd qPCR probe	/FAM/AGCTTCAGTTGTTTCCACCGGGTA/IBFQ/
PSTVd Forward Primer (RPA)	CTAAACACCCTCGCCCCGGAGCAAGTAAG
PSTVd Reverse Primer (RPA)	/Biotin/GTTTTTACCCTTCCTTTCTTCGGGTGTCCTC
PSTVd amplicon	CTAAACACCCTCGCCCCGGAGCAAGTAAGATAGAGAAAA GCGGTTCTCGGGAGCTTCAGTTGTTTCCACCGGGTAGTAG CCGAAGCGACAGCGCAAAGGGGGCGAGGGGTGGTCCTGCG GGCGCGAGGAAGGACACCCGAAGAAAGGAAGGGTGAAAC
PSTVd Cas9 sgRNA	GGGGCGAGGGGUGGUCCUGUUUUAGAGCUAGAAAUAGC AAGUUAAAAUAAGGCUAGUCCGUUAUCAACUUGAAAAAGU GGCACCGAGUCGGUGCUUUU
PSTVd Cas9 probe	/FAM/AGGGGGCTGACCACCCCTCGCCCCCT
PSTVd Cas12a crRNA	UAAUUUCUACUAAGUGUAGAUCACCGGGUAGUAGCCGAAGC

5. REFERENCES

- Ali Z, Sánchez E, Tehseen M, Mahas A, Marsic T, *et al.* (2021) Bio-SCAN: A CRISPR/dCas9-based lateral flow assay for rapid, specific, and sensitive detection of SARS-CoV-2. *ACS Synth Biol* 11, 406-419.
- Azhar M, Phutela R, Kumar M, Ansari AH, Rauthan R, *et al.* (2021) Rapid and accurate nucleobase detection using FnCas9 and its application in COVID-19 diagnosis. *Biosens Bioelectron* 183, 113207.
- Bahadır EB, Sezgintürk MK (2016) Lateral flow assays: Principles, designs, and labels. *TrAC, Trends Anal Chem* 82, 286-306.
- Batten JS, Yoshinari S, Hemenway C (2003) *Potato virus X*: a model system for virus replication, movement and gene expression. *Mol Plant Pathol* 4, 125-131.
- Boonham N, Pérez LG, Mendez MS, Peralta EL, Blockley A, *et al.* (2004) Development of a real-time RT-PCR assay for the detection of *Potato spindle tuber viroid*. *J Virol Methods* 116, 139-146.
- Boyd SD (2013) Diagnostic applications of high-throughput DNA sequencing. *Annu Rev Pathol* 8, 381-410.
- Broughton JP, Deng X, Yu G, Fasching CL, Servellita V, *et al.* (2020) CRISPR-Cas12- based detection of SARS-CoV-2. *Nat Biotechnol* 38, 870–874.
- Cesaratto F, Burrone OR, Petris G (2016) *Tobacco Etch Virus* protease: A shortcut across biotechnologies. *J Biotechnol* 231, 239-249.
- Chen JS, Ma E, Harrington LB, Da Costa M, Tian X, *et al.* (2018) CRISPR-Cas12a target binding unleashes indiscriminate single-stranded DNase activity. *Science* 360, 436-439.
- Deng Y, Jiang H, Li X, Lv X (2021) Recent advances in sensitivity enhancement for lateral flow assay. *Microchim Acta* 188, 1-15.

- Ding R, Long J, Yuan M, Zheng X, Shen Y, *et al.* (2021) CRISPR/Cas12-based ultra-sensitive and specific point-of-care detection of HBV. *Int J Mol Sci* 22, 4842.
- Fox JD (2007) Nucleic acid amplification tests for detection of respiratory viruses. *J Clin Virol* 40, S15-S23.
- Ghouneimy A, Mahas A, Marsic T, Aman R, Mahfouz M (2022) CRISPR-based diagnostics: Challenges and potential solutions toward point-of-care applications. *ACS Synth Biol* 12, 1-16.
- Gilboa T, Garden PM, Cohen L (2020) Single-molecule analysis of nucleic acid biomarkers – A review. *Anal Chim Acta* 1115, 61-85.
- Gootenberg JS, Abudayyeh OO, Kellner MJ, Joung J, Collins JJ, Zhang F (2018) Multiplexed and portable nucleic acid detection platform with Cas13, Cas12a, and Csm6. *Science* 360, 439–444.
- Gootenberg JS, Abudayyeh OO, Lee JW, Essletzbichler P, Dy AJ, *et al.* (2017) Nucleic acid detection with CRISPR-Cas13a/C2/c2. *Science* 356, 438-442.
- Huang D, Ni D, Fang M, Shi Z, Xu Z (2021) Microfluidic ruler-readout and CRISPR Cas12a-responded hydrogel-integrated paper-based analytical devices (μ ReaCH-PAD) for visible quantitative point-of-care testing of invasive fungi. *Anal Chem* 93, 16965-16973.
- Hwang H, Bae SC, Lee S, Lee YH, Chang A (2013) A rapid and simple genotyping method for various plants by direct-PCR. *Plant Breed Biotechnol* 1, 290-297.
- Ishibashi K, Ishikawa M (2016) Replication of *tobamovirus* RNA. *Annu Rev Phytopathol* 54, 55-78.
- Kaminski MM, Abudayyeh OO, Gootenberg JS, Zhang F, Collins JJ (2021) CRISPR-based diagnostics. *Nat Biomed Eng* 5, 643-656.
- Kumar A, Singh R, Kaur J, Pandey S, Sharma V, *et al.* (2021) Wuhan to world: the COVID-19 pandemic. *Front Cell Infect Microbiol* 11, 596201.

- Larremore DB, Wilder B, Lester E, Shehata S, Burke JM, *et al.* (2021) Test sensitivity is secondary to frequency and turnaround time for COVID-19 screening. *Sci Adv* 7, eabd5393.
- Liu Y, Zhan L, Qin Z, Sackrison J, Bischof JC (2021) Ultrasensitive and highly specific lateral flow assays for point-of-care diagnosis. *ACS nano* 15, 3593-3611.
- Mabey D, Peeling RW, Ustianowski A, Perkins MD (2004) Diagnostics for the developing world. *Nat Rev Microbiol* 2, 231-240.
- Marques MC, Sanchez-Vicente J, Ruiz R, Montagud-Martinez R, Márquez-Costa R, *et al.* (2022) Diagnostics of infections produced by the plant viruses TMV, TEV, and PVX with CRISPR-Cas12 and CRISPR-Cas13. *ACS Synth Biol* 11: 2384-2393.
- Márquez-Costa R, Montagud-Martinez R, Marques MC, Albert E, Navarro D, *et al.* (2023) Multiplexable and biocomputational virus detection by CRISPR-Cas9-mediated strand displacement. *Anal Chem* 95, 9564-9574.
- Marsic T, Ali Z, Tehseen M, Mahas A, Hamdan S, Mahfouz M (2021) Vigilant: an engineered VirD2-Cas9 complex for lateral flow assay-based detection of SARS-CoV2. *Nano Lett* 21, 3596-3603.
- Piepenburg O, Williams CH, Stemple DL, Armes NA (2006) DNA detection using recombination proteins. *PLOS Biol* 4, e204.
- Posthuma-Trumpie GA, Korf J, van Amerongen A (2009) Lateral flow (immuno) assay: its strengths, weaknesses, opportunities and threats. A literature survey. *Anal Bioanal Chem* 393, 569-582.
- Ramachandran A, Huyke DA, Sharma E, Sahoo MK, Huang C, *et al.* (2020) Electric field-driven microfluidics for rapid CRISPR-based diagnostics and its application to detection of SARS-CoV-2. *PNAS* 117, 29518-29525.
- Rubio L, Galipienso L, Ferriol I (2020) Detection of plant viruses and disease management: Relevance of genetic diversity and evolution. *Front Plant Sci* 11, 1092.

- Sadeghi P, Sohrabi H, Hejazi M, Jahanban-Esfahlan A, Baradaran B, *et al.* (2021) Lateral flow assays (LFA) as an alternative medical diagnosis method for detection of virus species: The intertwine of nanotechnology with sensing strategies. *TrAC Trends Anal Chem* 145, 116460.
- Schindelin J, Arganda-Carreras I, Frise E, Kaynig V, Longair M, *et al.* (2012) Fiji: an open-source platform for biological-image analysis. *Nat Methods* 9, 676-682.
- Scholthof KB (2004) *Tobacco mosaic virus*: a model system for plant biology. *Annu Rev Phytopathol* 42, 13-34.
- Sena-Torralba A, Álvarez-Diduk R, Parolo C, Piper A, Merkoçi A (2022) Toward next generation lateral flow assays: Integration of nanomaterials. *Chem Rev* 122, 14881-14910.
- Wang X, Xiong E, Tian T, Cheng M, Lin W, *et al.* (2020) Clustered regularly interspaced short palindromic repeats/Cas9-mediated lateral flow nucleic acid assay. *ACS nano* 14, 2497-2508.
- Xiong E, Jiang L, Tian T, Hu M, Yue H, *et al.* (2021) Simultaneous dual-gene diagnosis of SARS-CoV-2 based on CRISPR/Cas9-mediated lateral flow assay. *Angew Chem Int Ed Engl* 60, 5307-5315.
- Yang S, Rothman RE (2004) PCR-based diagnostics for infectious diseases: uses, limitations, and future applications in acute-care settings. *Lancet Infect Dis* 4, 337-348.
- Yin K, Ding X, Li Z, Sfeir MM, Ballesteros E, Liu C (2021) Autonomous lab-on-paper for multiplexed, CRISPR-based diagnostics of SARS-CoV-2. *Lab Chip* 21, 2730-2737.
- Zhao Y, Chen F, Li Q, Wang L, Fan C (2015) Isothermal amplification of nucleic acids. *Chem Rev* 115, 12491-12545.

CHAPTER 5

Integration of multiple signals into a CRISPR-Cas9-based detection mechanism

Part of this work has been published in a peer-reviewed journal.

See the full citation:

Márquez-Costa R, Montagud-Martinez R, Marques MC, Albert E, Navarro D, Daros JA, Ruiz R, Rodrigo G (2023) Multiplexable and biocomputational virus detection by CRISPR-Cas9-mediated strand displacement. *Analytical Chemistry* 95: 9564-9574

<https://doi.org/10.1021/acs.analchem.3c01041>

Part of this work has been done in collaboration with Yohei Yokobayashi and Samuel Hauf, from Nucleic Acid Chemistry and Engineering Unit, Okinawa Institute of Science and Technology Graduate University, Onna, Okinawa, 904-0495, Japan as part of the doctoral research stay.

My contribution to this work:

I designed most of the nucleic acid sequences and performed the experiments under the supervision of G. Rodrigo and Y. Yokobayashi. I analyzed the data, prepared the figures, and contributed to the writing of the manuscript.

1. INTRODUCTION

Clustered regularly interspaced short palindromic repeats (CRISPR) systems have revolutionized the field of biotechnology. The CRISPR-Cas9 system can virtually target any DNA sequence by using a programmable single guide RNA (sgRNA) that complements the target sequence through base pairing (Jinek *et al.*, 2020). Thanks to its simplicity and programmability, the versatile CRISPR system has been applied across a broad range of fields, whether for genome editing, gene expression regulation, chromosome imaging, or any of its other myriad uses (Pickar-Oliver and Gersbach, 2019). In parallel to investigating the broad potential of the CRISPR tool, particular efforts have been made into its functionality as a signal integrator (Gander *et al.*, 2017; Kempton *et al.*, 2020; Kim *et al.*, 2019; 2020; Shivram *et al.*, 2021). This includes developing the capability to both process and sense different signals. Advancements have been made using CRISPR-Cas systems as nucleic acid detection platforms (Kaminski *et al.*, 2021). However, the current scope of CRISPR-Cas diagnostics is largely limited to sensing a single input and generating a corresponding output. To fully realize the potential of CRISPR technology, there is a need to engineer CRISPR systems that can function as complex processing tools, responsive to a variety of signals, and capable of generating different outputs. Assays should be expanded to provide detailed information about the identified molecule, integrating and interpreting multiple biological signals simultaneously, with the objective of extending the application range beyond simple detection.

Firstly, the processing of different signals by CRISPR-Cas systems could be exploited within the framework of biocomputing. Biocomputing harnesses the inherent capabilities of biological components, such as DNA, RNA, proteins, and cellular processes to process and interpret information to perform computational task (Benenson, 2012; Li *et al.*, 2017). DNA-based digital logic circuits can be implemented for constructing synthetic chemical circuits. These circuits can incorporate a set of Boolean logic functions, including AND, OR, and NOT operations (Seelig *et al.*, 2006). CRISPR-Cas9 has been used to engineer toehold-free DNA circuits for logic computation based on strand displacement reactions (Montagud-Martinez *et al.*, 2021). We

showed that this same mechanism can also be used for nucleic acid sensing. This CRISPR-based information processing suggests then feasible applications in biocomputing in terms of biosensing.

Secondly, there is a focus on sensing different signals to regulate CRISPR-Cas activity. Currently, the majority of advances in this field have been focused around modifying the activity of the Cas9 protein to achieve the desired regulatory control (Dow *et al.*, 2015; Nihongaki *et al.*, 2015; Zetsche *et al.*, 2015). With such an approach, all target sequences are regulated in the same manner, meaning the regulation lacks multiplexing and precision. A promising alternative strategy is to engineer the sgRNA itself. By directly controlling the sgRNA, which is specific to each target sequence, it becomes possible to independently regulate each target, offering more precise control. One such method involves sequestering the spacer domain with a complementary RNA sequence, which can be removed when a specific inducer is present, activating the guide (Ferry *et al.*, 2017; Jain *et al.*, 2016; Lee *et al.*, 2016; Tang *et al.*, 2017). Another strategy involves the use of ligands to either stabilize or destabilize specific regions of the RNA guide. Ligand-responsive sgRNAs were engineered by using RNA aptamers to both activate and deactivate CRISPR-Cas9 function in response to a small molecule (Kundert *et al.*, 2019). Another strategy is based on extending the 3' end of the sgRNAs to include an extending blocking motif and an aptamer as the triggering motif; an approach which involves no significant modification of the sgRNA skeleton (Lin *et al.*, 2019).

Certainly, being able to integrate and process different signals in CRISPR activity would offer advantages in the field of CRISPR diagnostics, as enhanced sensitivity and coverage. Such developments would allow for more advanced applications, including the detection of diverse pathogens in a single test and more extensive diagnostic capabilities. Recently, we repurposed CRISPR-Cas9 as a novel nucleic acid detection platform and demonstrated that it could be applied to detect severe acute respiratory syndrome coronavirus 2 (SARS-CoV-2). Our detection platform utilizes a mechanism based on strand displacement rather than collateral catalysis (Márquez-Costa *et al.*, 2023). This absence of nonspecific collateral activity opens up the possibility for processing various signals, extending beyond the

detection paradigm. Therefore, we aim to couple the detection of SARS-CoV-2 to DNA-based computation by the engineering of two molecular programs that run after generated amplicons. In addition, we envision the coupling of signal dependent sgRNA with the CRISPR-Cas9 detection method previously described. Based on the extended blocking and triggering motif at the sgRNA 3' end, and on the recently reported DNA spike aptamer (Li *et al.*, 2021) we aimed to engineering an improved Cas9 detection method that could sense both protein and nucleic acid. In combination, this work looks to develop an advanced diagnostic platform capable of integrating, analyzing, and processing a combination of numerous signals.

2. RESULTS

2.1 Biocomputational Virus Detection with CRISPR-Cas9

The lack of collateral cleavage activity of the nuclease in our detection platform represents an advantage to couple it with DNA computing (Seelig *et al.*, 2006), thereby going beyond the simple detection paradigm. To illustrate this approach, we designed two molecular programs implementing Boolean logic gates to process combinatorial DNA amplicons from SARS-CoV-2 (we focused on the N1 and E amplicons). The displaced strand upon CRISPR-Cas9 targeting was used to interact with a complex of hybridizing ssDNA molecules. The mechanism of toehold-mediated strand displacement was used, that is, an enzyme-free reaction to exchange DNA strands. To achieve this, one of the ssDNA molecules forming that complex was designed to have an overhanging region (*i.e.*, a toehold) to seed the interaction with the displaced strand of the N1 amplicon, and similarly, another ssDNA molecule was designed to have a toehold to interact with the displaced strand of the E amplicon. These overhanging regions were at least 6 nt long. In this way, the complex of hybridizing ssDNAs was responsive to two input signals. The complex was designed to have a sufficiently high melting temperature to be stable in the absence of inputs; in this case, 35 bp were formed. First, we designed an OR gate (**Figure 1.a**), aimed at producing a fluorescence signal

when there is at least one amplicon in the reaction. The assembly of three ssDNA molecules with partial complementarity between them led to a stable nonregular structure capable of specifically interacting with the displaced strands generated by the sgRNA-Cas9 ribonucleoproteins upon targeting. These ssDNA molecules were appropriately labelled with the fluorophore Cy5 or the dark quencher IB_{RQ} to achieve the intended logic behavior. The engineered system performed well with DNA amplicons as inputs, showing a dynamic range of an almost 3-fold change in red fluorescence (**Figure 1.b**). In the absence of the sgRNA-Cas9 ribonucleoproteins, the system was irresponsive. Moreover, we assayed the system with amplified products from patient samples, finding similar results (**Figure 1.c**). As expected, the computation only took place when using positive patient samples.

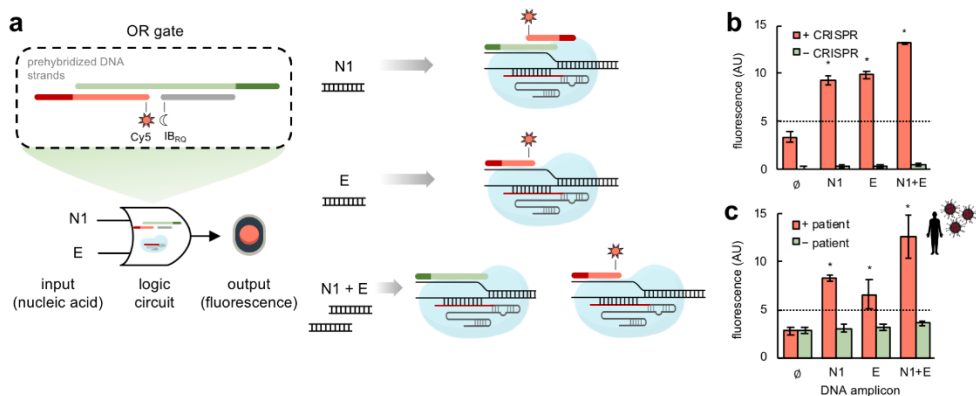


Figure 1. Biocomputational SARS-CoV-2 detection through CRISPR-Cas9-based strand displacement reactions (OR gate). a) Schematics of the OR logic circuit. Three prehybridized oligonucleotides form the OR gate, which can interact with the CRISPR complexes formed upon detection of the virus-derived DNA amplicons (N1 and E). In this case, the red strand was labelled with Cy5 in its 5' end and the gray strand with IB_{RQ} in its 3' end. The dark green and red regions represent the toeholds seeding the interactions with the corresponding CRISPR complexes (the green strand interacts with the displaced strand of the N1 amplicon, while the red strand does with the displaced strand of the E amplicon). On the right, schematics of the biocomputation reactions in response to one or two DNA amplicons. b) Fluorescence-based characterization of the OR gate performance with DNA amplicons. c) Biocomputation using patient samples (2 patients, 3 reactions per patient). The detection threshold (given by the dotted line) was set to 5 in b) and c). Amplifications performed by RT-PCR in c). Error bars correspond to standard deviations ($n = 3$). *Statistical significance (Welch's t -test, two-tailed $P < 0.05$; determined with respect to the first condition).

Second, we designed an AND gate (**Figure 2.a**), aimed at producing a fluorescence signal only when the two amplicons are present in the reaction. The very same nucleotide sequences of those ssDNA molecules used to implement the OR gate were used, but the labelling with the fluorophore Cy5 and the dark quencher IB_{RQ} changed. In this case, two quenchers and one internal fluorophore were used to achieve the intended logic behavior.

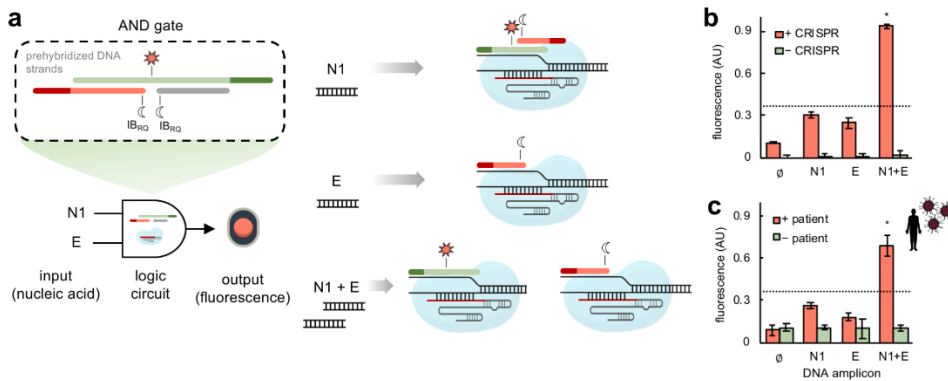


Figure 2. Biocomputational SARS-CoV-2 detection through CRISPR-Cas9-based strand displacement reactions (AND gate). a) Schematics of the AND logic circuit. Three prehybridized oligonucleotides conform the AND gate, which can interact with the CRISPR complexes formed upon detection of the virus-derived DNA amplicons (N1 and E). In this case, the green strand was labelled with Cy5 internally, the red strand with IB_{RQ} in its 5' end, and the gray strand with IB_{RQ} in its 3' end. The dark green and red regions represent the toeholds seeding the interactions with the corresponding CRISPR complexes (the green strand interacts with the displaced strand of the N1 amplicon, while the red strand does with the displaced strand of the E amplicon). On the right, schematics of the biocomputation reactions in response to one or two DNA amplicons. b) Fluorescence-based characterization of the AND gate performance with DNA amplicons. c) Biocomputation using patient samples (2 patients, 3 reactions per patient). The detection threshold (given by the dotted line) was set 0.35 in b) and c). Amplifications performed by RT-PCR in c). Error bars correspond to standard deviations ($n = 3$). *Statistical significance (Welch's t -test, two-tailed $P < 0.05$; determined with respect to the first three conditions).

The response of the engineered system with DNA amplicons as inputs showed a dynamic range of 3-fold change in red fluorescence (**Figure 2.b**). We noted, however, that the system slightly responded to just one input. As before, in the absence of the sgRNA-Cas9 ribonucleoproteins, the system was

irresponsive. Moreover, the assay of the system with amplified products from patient samples revealed similar results (**Figure 2.c**), although in this case the maximal fluorescence level was reduced.

Here, we designed AND and OR gates, but nothing prevents designing further logic systems. Overall, these results highlight the utility of the CRISPR-Cas9 system to connect a specific and sensitive virus detection with the ability to compute using DNA as a substrate, which could lead to more complex *in vitro* diagnostic programs.

2.2 Development and Optimization of a Spike Protein Aptamer-Regulated CRISPR-Cas9 System

2.2.1 Rational design of regulatory aptamers for conditional regulation of sgRNAs

We aimed to generate a regulatory aptamer sequence that would enable a conditional activation of the CRISPR-Cas9 system via interaction with a protein. Since we have already tested the potential of Cas9 nuclease to detect different nucleic acid sequences from SARS-CoV-2 (Márquez-Costa *et al.*, 2023), we decided to focus on aptamers that respond to the presence of the SARS-CoV-2 spike protein. We selected an aptamer against the spike protein described in the literature. Li *et al.* (2021) reported several DNA aptamers that recognize with high binding affinities the SARS-CoV-2 spike protein. Since they used a pool of pre-structured DNA sequences, the structure of the selected aptamers was suitable for our regulatory aim. Further, the aptamer sequences were tested to still be able to bind the spike after it was treated at 65 °C for 60 minutes, meaning they would remain functional after the typical pre-treatment of SARS-CoV-2 patient samples. We chose to use the top sequence, which they refer to as MSA1-T2, exhibiting a K_d value of 2.8 nM, for our experiments. We focused on using both the whole MSA1-T2 sequence, as well as only the core of the aptamer (**Figure 3**).

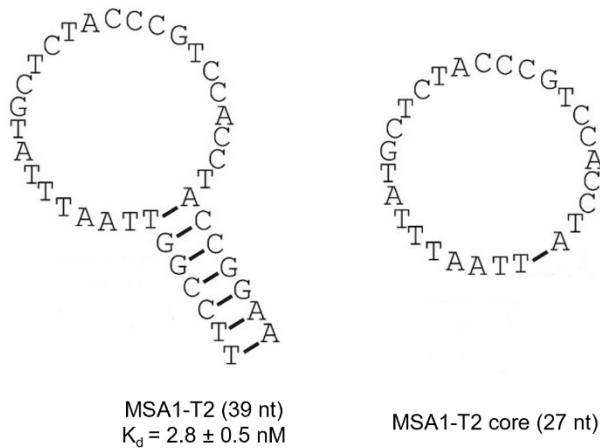


Figure 3. The predicted secondary structure and sequence of MSA1-T2 spike aptamers truncation mutants and binding affinity when applicable (Li *et al.*, 2021).

Regarding the strategy for coupling the aptamer to the sgRNA, we followed an approach consisting of generating a regulatory aptamer sequence by coupling the aptamer sequence stem with a blocking region targeting the constant region of the sgRNA. It also relies on the presence of a triggering motif containing the aptamer sequence and a competing hybridizing stem (Lin *et al.*, 2019) (**Figure 4**).

In the absence of the spike protein, a stable complementary structure is formed by the hybridization between the blocking motif and the sgRNA, inhibiting the sgRNA recognition by Cas9. In the presence of the stimulus, the spike protein interacts with its aptamer sequence, destabilizing the blocking-sgRNA hybridization. This disruption favors the release of the blocking motif, transitioning to a releasing conformation and allowing the sgRNA to become active again, restoring the CRISPR-Cas9 activity.

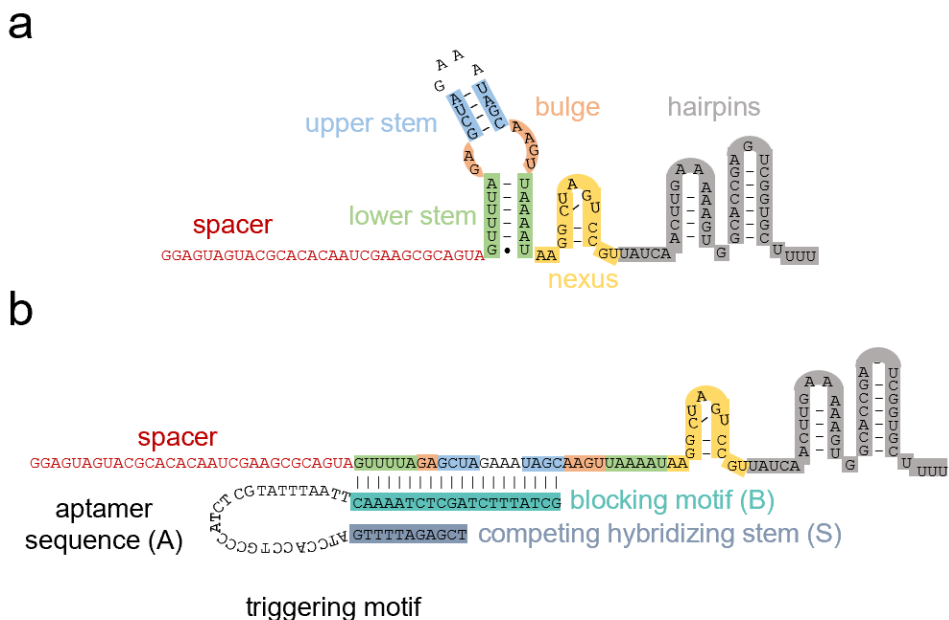


Figure 4. Sequence and structure of the sgRNA. a) Original structure of the sgRNA. b) The design principle of the regulatory aptamer sequences. A representative sequence is shown. Region highlighted in green is marked with the blocking motif (B) targeting the lower and upper stem of the sgRNA. In blue is shown the competing hybridizing stem (S) with the aptamer sequence (A).

Therefore, this system is based on two conformations: a blocking one in which the sgRNA is blocked, inhibiting the CRISPR-Cas9 reaction, and a releasing conformation where the spike protein interacts with the aptamer sequence, allowing to free the sgRNA and enabling its interaction with Cas9. As a proof of concept, the E gene amplicon from SARS-CoV-2 was chosen as a target. We labelled the amplicon with a fluorophore (FAM) and a quencher (BHQ1) allowing us to measure Cas9 activity by the fluorescent signal generated by the separation of the fluorophore from the quencher upon targeting (**Figure 5**).

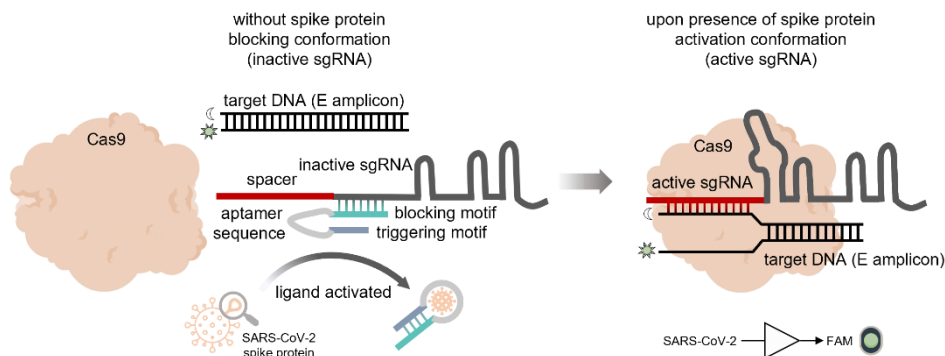


Figure 5. Schematics of intended regulation within CRISPR-Cas9 reaction. In the absence of the spike protein, the regulatory aptamer design binds to the sgRNA through a blocking motif, making the sgRNA inactive. In the inactive conformation, the sgRNA is unable to interact with Cas9. In the presence of the spike protein, the triggering motif, which includes the aptamer, interacts with it. This interaction promotes a conformational change, releasing the sgRNA from its blocked state and allowing it to adopt an active conformation, which is now able to interact with Cas9. The targeted DNA is labelled with a fluorophore (sun icon) and a quencher (moon icon). Upon targeting by the now active ribonucleoprotein, the fluorophore is spatially separated from the quencher, enabling the measure of the resulting fluorescence signal.

Different regulatory aptamer sequences were designed based on this two-confirmation strategy. In these designs, the blocking region is targeting the lower stem and upper stem of the sgRNA (Briner *et al.*, 2014) followed by a triggering motif containing the aptamer sequence. We designed different regulatory aptamers with a fixed blocking region of 20 bp, and a variable triggering motif length ranging from 5 to 11 bp containing either the core of the aptamer or the full truncated MSA1-T2 sequence. This series of regulatory aptamer sequences were referred to as An-Bn-Sn (aptamer-sgRNA blocking motif-competing hybridizing stem, where n indicates base number).

2.2.2 Optimization of assay conditions

We first confirmed the binding between the aptamer and the spike protein by MicroScale Thermophoresis (MST). MST is a technique used to analyze interactions between molecules. It is based on thermophoresis, which describes the movement of molecules in response to temperature gradients (Jerabek-Willemsen *et al.*, 2014). To check the binding, we labelled the aptamer sequence with a fluorophore, and incubated it with the spike protein. When the aptamer interacts with its partner molecule, it shows different thermophoretic properties when compared to the unbound molecules. By monitoring the changes in the fluorescence signal through the temperature gradient, MST could confirm the binding between the aptamer and the spike protein. Next, we checked the first series of regulatory aptamer sequences with variable length for the aptamer and triggering motif sequence (**Figure 6**).

We first focused on their ability to exert the blocking effect on the sgRNA, disabling Cas9 activity. We hybridized each regulatory aptamer sequence with the sgRNA, then performed the Cas9 reaction and measured the fluorescence signal (**Figure 7**). We tested different conformations of the sequences, including a control with no strong secondary structure which was more likely to bind the sgRNA (A27-B20-S5) as well as not-targeting controls (0 blocking bases). Naive sgRNA was used as a positive control. We found no solid evidence of a blocking effect, likely due to the blocking motif sequence targeting a highly structured area of the sgRNA.

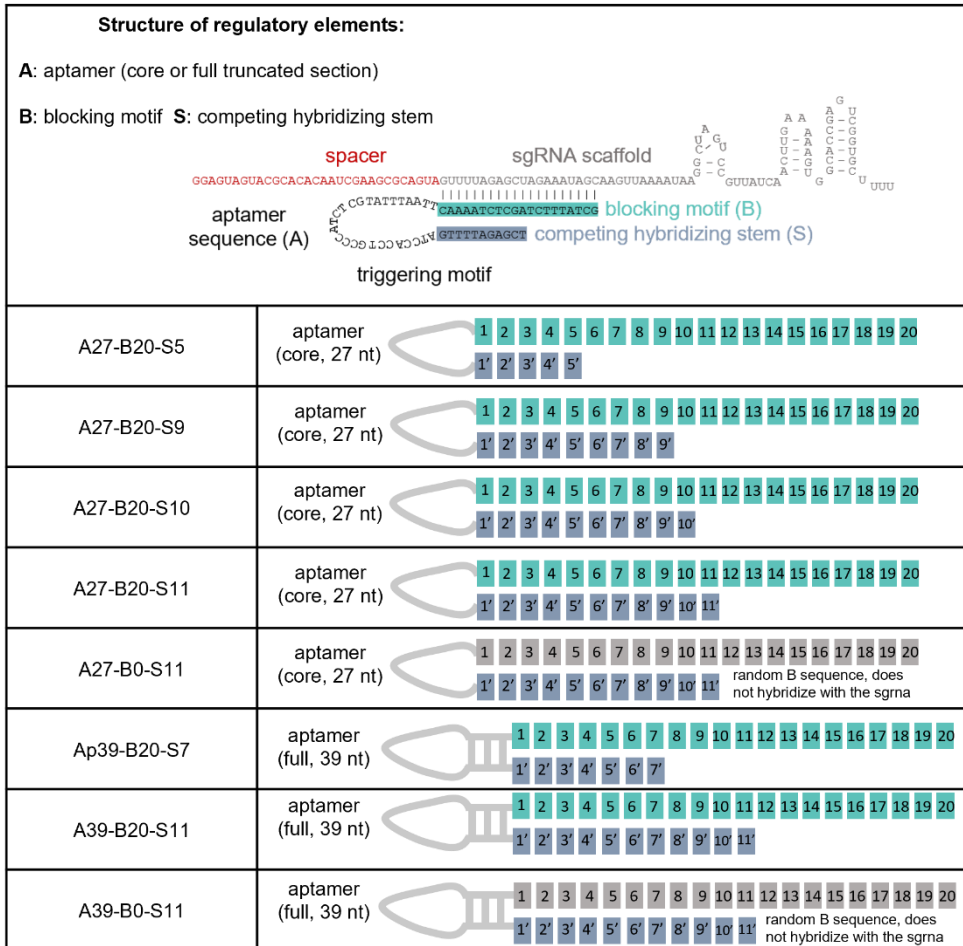


Figure 6. Structure and architecture of the different regulatory elements tested. These series of regulatory aptamer sequences are referred to as An-Bn-Sn, where A refers to the aptamer sequence used, either the core aptamer with 27 nt or the full truncated section of 39 nt. B refers to the region hybridizing with the sgRNA, and S is a competing hybridizing stem that is complementary to the first section of B. B0 controls have 0 nt complementary to the sgRNA. The number next to each letter stands for the number of nucleotides forming each region.

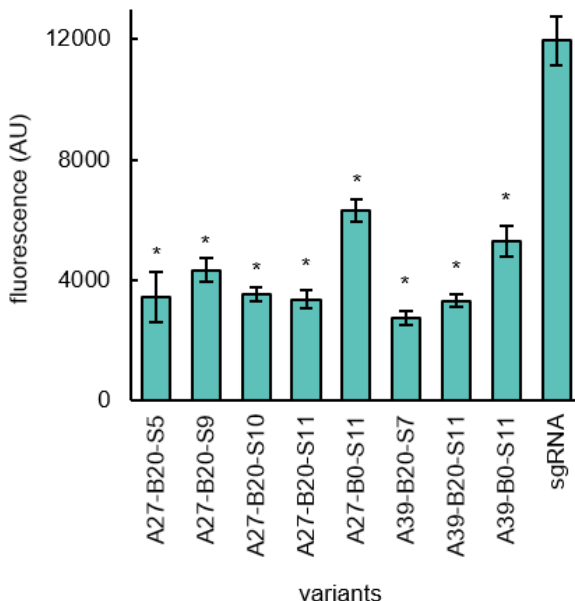
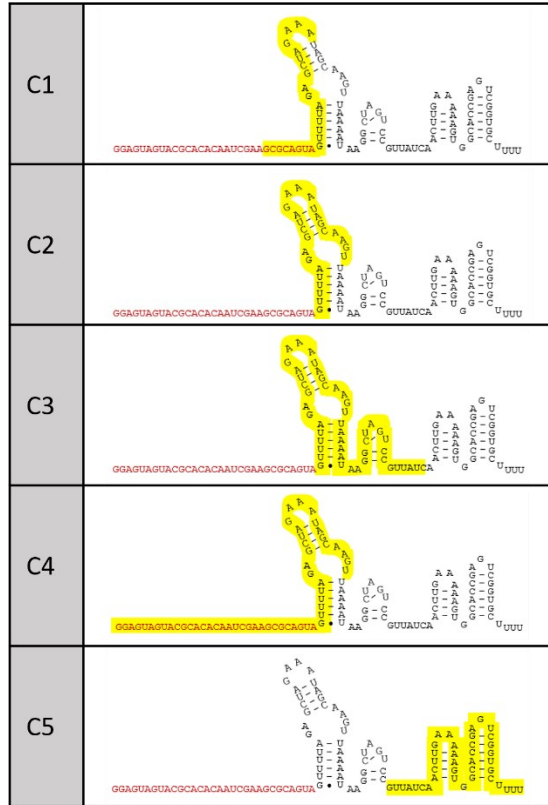


Figure 7. Fluorescence-based characterization of the blocking effect with different regulatory aptamer sequences architectures. Error bars correspond to standard deviations ($n = 3$). *Statistical significance (Welch's t -test, two-tailed $P < 0.05$).

We followed up on these results by designing and testing oligonucleotides targeting different parts of the sgRNA to investigate the optimal region for blocking. In these new updated designs, we included some nucleotides lacking secondary structure from the sgRNA that would promote and facilitate the binding of the blocking motif. Those regions include sections of the spacer, the bulge, the nexus and the 3' hairpins. A control targeting the spacer and part of the lower upper stem was also included (**Figure 8.a**). After hybridization of the oligos with the sgRNA, we measured Cas9 activity (**Figure 8.b**).

a



b

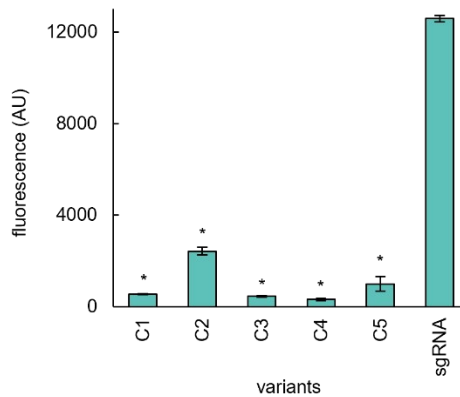


Figure 8. Assessment of targeting area of the sgRNA to exert a blocking control. a) Areas of the sgRNA structure targeted by the blocking motif are highlighted in yellow. b) Fluorescence-based characterization of different oligos targeting the different sections of the sgRNA. Error bars correspond to standard deviations ($n = 3$). *Statistical significance (Welch's t -test, two-tailed $P < 0.05$).

The results indicate that most of those targeting areas are suitable for exerting a better blocking effect. A reduction of >92% of the fluorescence was found for controls 1, 3, 4 and 5. Control 2 was not as strongly affected, still showing a reduction in fluorescence of ~80%, suggesting that even with the bulge nucleotides included, it is still not as efficient as the other designs.

Based on these results, we proceeded to design new An-Bn-Sn structure regulatory aptamer sequences, targeting the C1 area of the sgRNA (**Figure 9**).

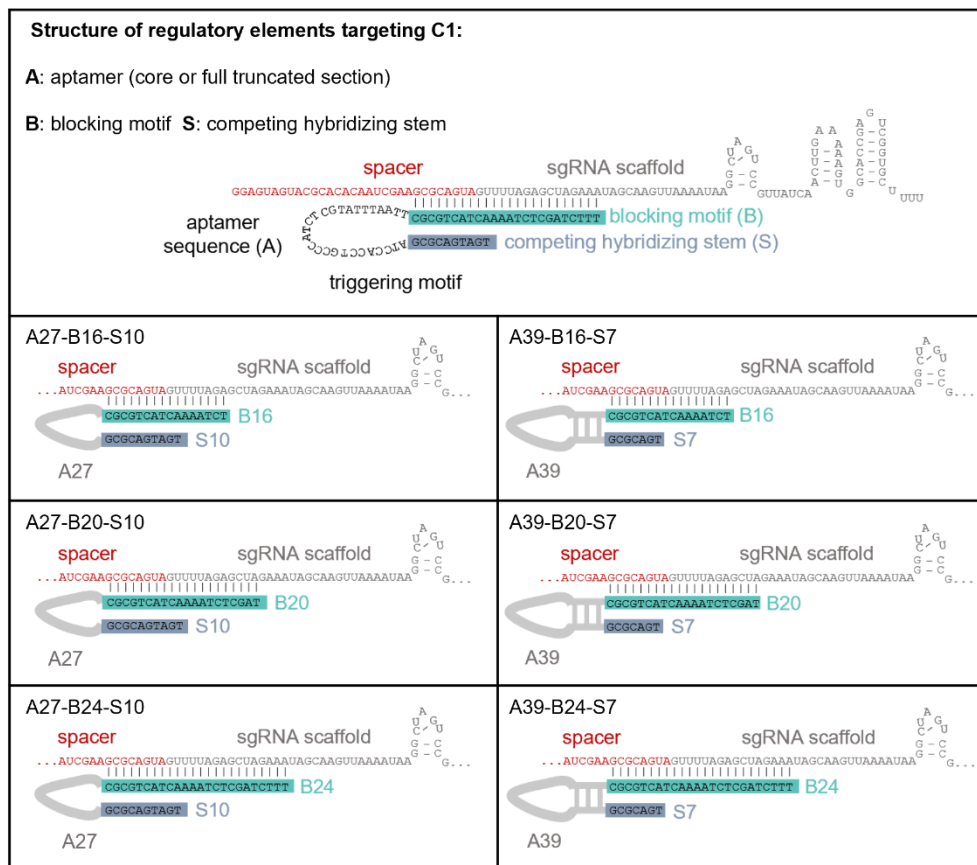


Figure 9. Structure and architecture of the different regulatory targeting the C1 region of the sgRNA. Regulatory aptamer sequences are referred to as An-Bn-Sn, where A refers to the aptamer sequence used, either the core aptamer with 27 nt or the full truncated section of 39 nt. B refers to the region hybridizing with the sgRNA, and S is a competing hybridizing stem that is complementary to the first section of B. The number next to each letter stands for the number of nucleotides forming each region.

As a proof of concept, we also designed complementary oligonucleotides to the regulatory aptamer sequences to check the feasibility of recovering Cas9 activity after the blocking exertion. With these oligos, we were able to obtain a recovery effect ranging from 49 % to 376 % increase in fluorescence (Figure 10).

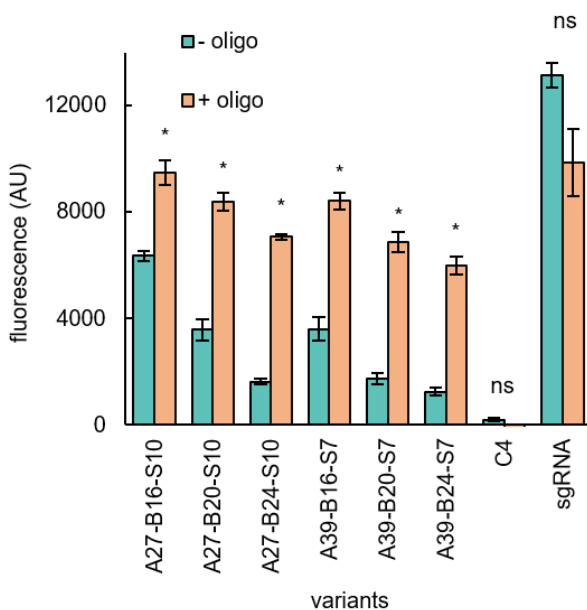


Figure 10. Fluorescence-based characterization of the blocking effect exerted by different regulatory aptamer sequences architectures targeting C1 area of the sgRNA. Recovery was tested after the addition of complementary oligonucleotides to blocked sgRNAs by the different architectures. Error bars correspond to standard deviations ($n = 3$). *Statistical significance (Welch's t -test, two-tailed $P < 0.01$). ^{ns}Not statistically significant.

2.2.3 Effect of spike protein in the system

After testing blocking and feasible recovery of the system we wanted to test how the presence of the spike protein would affect with the system. Presence of spike protein is supposed to elicit a recovery in the activity. In the blocked sgRNA conformation, the spike protein would interact with its aptamer sequence, weakening the binding between the blocking motif and the targeted

sgRNA region, favoring the releasing conformation and restoring the activity of CRISPR-Cas9. We tested the regulatory aptamer designs blocking the C1 area of the sgRNA with different spike protein concentrations. When spike protein was not present in the sample; we obtained the blocking effect exerted by the regulatory aptamer sequences, while adding spike protein allows us to check restoration of activity. We found no indication of CRISPR-Cas9 activity recovery upon presence of spike protein (**Figure 11**). These results suggest that the architecture design of the regulatory aptamer sequences may not be optimal. The interaction between the aptamer and the spike protein may also not be sufficient for achieving the desired conformational change to release the sgRNA and recover the activity of the system.

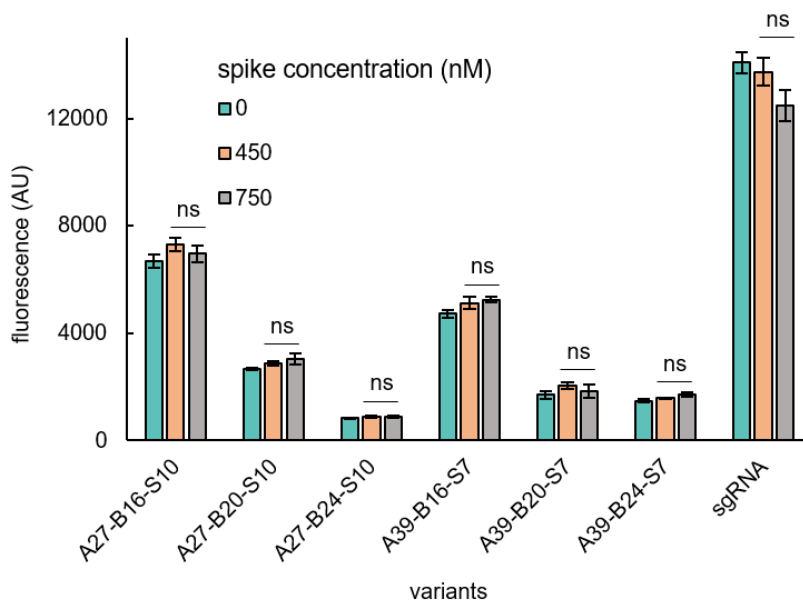


Figure 11. Fluorescence-based characterization of the spike protein presence. Error bars correspond to standard deviations ($n = 3$). ^{ns}Not statistically significant (Welch's t -test, two-tailed).

3. DISCUSSION

In conducting these experiments, we set the basis for extending CRISPR-Cas9 beyond the detection paradigm by the sensing and processing of different signals. We have demonstrated DNA computation by processing different DNA amplicons recognized by CRISPR-Cas9. We successfully engineered OR and AND gates that respond to DNA amplicons from SARS-CoV-2. In particular, they were responsive with the displaced strands generated by the detection of SARS-CoV-2 samples upon sgRNA-Cas9 ribonucleoprotein targeting. Cas13 and Cas12 have also demonstrated significant potential in nucleic acid detection applications (Aman *et al.*, 2020). Nevertheless, their fundamental property which enables detection activity also renders them unsuitable for DNA computing. These Cas proteins exhibit a collateral activity upon target recognition, which underlies their detection capabilities (Gootenberg *et al.*, 2017; Chen *et al.*, 2018), but the nonspecific nature of the collateral cleavage represents a limitation for further signal processing. Any additional nucleic acid sequence present in the sample would be subject to degradation by the collateral effect after target recognition, thereby nullifying the capability to process additional signals, making them unsuitable for DNA computing assays. With our Cas9 detection development we can overcome the limitation of other Cas nucleases, facilitating the implementation of cascade reactions, and allowing for further downstream processes.

As a proof of concept, we also aimed to incorporate an aptamer in the sgRNA to enable an additional layer of control in the CRISPR-Cas9 system. Since we tested our Cas9 detection tool with SARS-CoV-2 samples, we focused on SARS-CoV-2 spike protein aptamers. We based our strategy in a blocking-activating conformation switching strategy (Lin *et al.*, 2019) and explored different sequence architectures over that approach. Despite achieving promising results in inhibiting Cas9 activity due to the blocking of the sgRNA in the absence of the spike protein; our designs failed to elicit a recovery in the Cas9 activity when the spike protein was present in the sample. Previous works in the field use well-characterized aptamer for small molecules (Kundert *et al.*, 2019; Liu *et al.*, 2016; Tang *et al.*, 2017), and strategies are

focused on the conformational change induced in the aptamer upon interaction with its trigger. Making use of other spike aptamer sequences released in the literature (Amini *et al.*, 2022; Mironov *et al.*, 2022; Schmitz *et al.*, 2021; Song *et al.*, 2020; Valero *et al.*, 2021) may be a way forward on this front. Also, working with a protein rather than a small molecule may raise the possibility for the aptamer interaction to occur at a more superficial level. In combination with the continuous equilibrium of binding and dissociating events, there may be a scenario in which the aptamer-spike interaction is not enough to trigger the conformational change needed in the regulatory aptamer sequence that would allow for the recovery of Cas9 activity. Surface Plasmon Resonance (SPR) appears as a powerful analytical technique for tracking molecular interactions that can help elucidate the dynamics of the protein-aptamer interaction (Chang, 2021). SPR can provide valuable information into the strength and specificity of the interaction, as well as any conformational changes that may occur upon binding (Wang and Zhou, 2008). Such information could be crucial for guiding the optimization of the regulatory control of sgRNA upon aptamer interaction. Being able to expand our Cas9 diagnostic platform to be able to sense both protein and nucleic acid would be particularly advantageous in many research and diagnostic contexts. This includes disease diagnostics where both protein biomarkers and nucleic acid signatures play crucial roles (Sarhadi and Armengol, 2022).

Altogether, we explored two new capabilities for our CRISPR-Cas9 detection mechanism: biocomputing and aptamer-regulated system activity. This work sets the basis for the introduction of different signals, expanding the scope beyond simple detection. These approaches to signal integration hold promise to expand the application range of CRISPR-Cas systems and to uncover novel opportunities for innovation.

4. MATERIALS AND METHODS

4.1 Nucleic acid sequences

DNA logic circuits implementing OR and AND gates were engineered. Each gate was formed by three different ssDNA molecules that were chemically synthesized (IDT) with appropriate fluorophore (Cy5) or dark quencher (IB_{RQ}) labels. The ssDNA sequences were the same for the OR and AND gates, with the only change being the fluorophore/quencher labelling. The strand displacement ability was checked with NUPACK (Zadeh *et al.*, 2011). The hybridizing ssDNA molecules forming the gates were designed to have toeholds to seed the interactions with the displaced strands of the targeted DNA amplicons (N1 and E) and to form a stable complex at 37 °C.

A DNA amplicon for the E SARS CoV2 region was chemically synthesized (IDT) and labelled with a fluorophore (FAM) and a Quencher (BHQ1). Regulatory aptamers were chemically synthesized (IDT), whose secondary structure was checked with NUPACK and hybridizing ability was checked with ViennaRNA cofold service (Gruber *et al.*, 2008). Sequences provided in the **Data set Table 1** and **Table 2**.

4.2 CRISPR Elements

S. pyogenes wild-type Cas9 nuclease from IDT was used. sgRNAs were generated from DNA templates by *in vitro* transcription with the TranscriptAid T7 high yield transcription kit (Thermo) or ScriptMax Thermo T7 RNA Polymerase Kit (Toyobo) according to the manufacturer's instructions. sgRNAs were then purified using the RNA clean and concentrator column (Zymo) and quantified in a NanoDrop. Sequences provided in the **Data set Table 1** and **Table 2**.

4.3 Spike Protein

Spike protein was purchased from SinoBiological (SARS-CoV-2 (2019-nCoV) Spike S1-His Recombinant Protein Cat: 40591-V08B1). Microscale Thermophoresis binding assay was performed to check the binding between the aptamer and the spike protein. Spike aptamer sequence modified with 5' FAM was synthesized (IDT). 5 nM of aptamer sequence was combined with 1.63 μM spike protein in 1X Selection Buffer (50 mM HEPES, 6 mM KCl, 2.5 mM CaCl_2 , 2.5 mM MgCl_2 , 0.01% v/v Tween-20, pH 7.4). The assay was performed in Monolith 2020 TNG (MM-025) (Nanotemper).

4.4 Nucleic Acid Amplification by PCR

DNA amplicons from SARS-CoV-2 were obtained as test samples by PCR from a mix of two plasmids containing the SARS-CoV-2 N and E genes (IDT) each at 10^3 copies/ μL with the CDC N1 and Charité E-Sarbeco primers. Conditions for PCR were 250 nM of forward and reverse primers, 200 μM dNTPs (NZYTech), 0.02 U/ μL Phusion high-fidelity DNA polymerase (Thermo), 1 \times Phusion buffer, and 2 μL of sample, to reach a total volume of 20 μL , adjusted with RNase-free water. The protocol involved denaturation at 98 °C for 30 seconds, followed by 35 cycles of amplification: 98 °C for 10 seconds, 62 °C for 10 seconds, and 72 °C for 5 seconds. Patient samples were obtained from nasopharyngeal swabs corresponding to infected and noninfected patients with SARS-CoV-2 (RT-qPCR diagnostics) from the Clinic University Hospital of Valencia (Spain). Samples were inactivated through the action of proteinase K followed by a heat shock inactivation (5 min at 60 °C) before proceeding prior to further processing. RNA extraction was not performed. The study received approval from the Ethics Committee of the Clinic University Hospital (order #2020/221). For patient sample amplification, the TaqPath 1-step RT-qPCR master mix, CG, was employed. Each reaction consisted of 4 μL of sample mixed with 250 nM of forward and reverse primers. The protocol was RT step at 50 °C for 15 minutes, followed by denaturation at 95 °C for 2 minutes. This was followed by 35 cycles of

amplification of incubation at 95 °C for 15 seconds and at 62 °C for 60 seconds. The reactions were incubated in a thermocycler (Eppendorf), and subsequently, PCR products were purified via centrifugation using a DNA clean and concentrator column (Zymo).

4.5 Biocomputing Coupled to CRISPR-Cas9-Based Detection

DNA logic circuits implementing OR and AND gates were chemically synthesized as described above. Prior to their use in the CRISPR reactions, the three strands implementing a gate were heated at 95 °C for 2 min and then cooled slowly to 25 °C. The logic circuits were assayed for functionality with appropriate oligonucleotides as inputs (**Figure 12**). Sequences are provided in the **Data set Table 1**. CRISPR reactions were performed in 1× TAE buffer pH 8.5 (Invitrogen), 0.05% Tween 20 (Merck), and 12.5 mM MgCl₂ (Merck), with a final volume of 20 μL. The CRISPR-Cas9 ribonucleoprotein, previously assembled at room temperature for 30 min, was added at 100 nM, except the ribonucleoprotein targeting the N1 amplicon in the OR gate, which was added at 200 nM. Input DNA amplicons (N1 and E) were mixed in a combinatorial way, either 40 nM of each one if obtained from test samples or 2 μL of each amplified product if obtained from patient samples. The prehybridized gate was added at 200 nM. Reactions were incubated at 37 °C for 1 h in a thermomixer (Eppendorf). Reaction volumes were loaded in a black 384-well microplate with clear bottom (Falcon), which was then placed in a fluorometer (Varioskan Lux, Thermo) to measure red fluorescence (excitation was at 645/12 nm and emission at 670/12 nm) (measurement time of 100 ms, automatic range, and top optics).

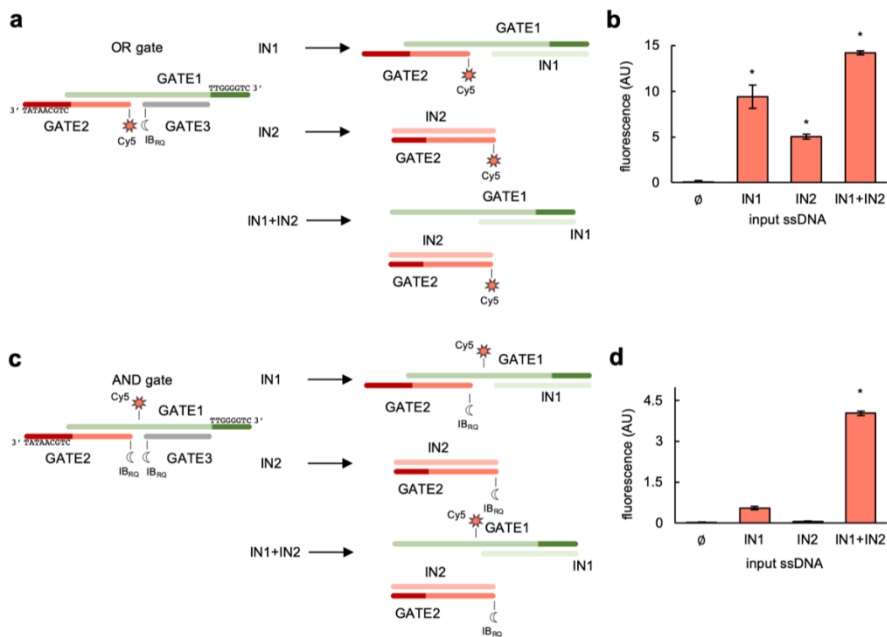


Figure 12. Characterization of the logic circuits with input ssDNA. a) Schematics of the OR gate in a pure DNA strand displacement scenario (the oligonucleotides IN1 and IN2 were the inputs). GATE1 was not labelled, GATE2 was labelled with the fluorophore Cy5 (sun icon) in the 5' end, and GATE3 was labelled with the dark quencher Iowa Black RQ (moon icon) in the 3' end. The sequences of the toeholds (seed regions) are shown. b) Fluorescence-based results for the OR gate. c) Schematics of the AND gate in a pure DNA strand displacement scenario. GATE1 was labelled with Cy5 internally, GATE2 was labelled with Iowa Black RQ in the 5' end, and GATE3 was labelled with Iowa Black RQ in the 3' end. d) Fluorescence-based results for the AND gate. Error bars correspond to standard deviations ($n = 3$). *Statistical significance (Welch's t -test, two-tailed $P < 0.05$).

4.6 Conditional CRISPR-Cas9-Based Detection

First, a hybridization between the sgRNA and the regulatory aptamer sequences was set to ensure the blocking effect. Sequences are provided in the **Data set Table 2**. sgRNAs were combined with a 10% excess of the regulatory aptamer sequence with 50 mM KCl, which was heated at 95 °C for 2 min and then cooled slowly to 25 °C. When applicable, sgRNA-Aptamer hybridization incubation with spike protein at different concentrations (0, 450

or 750 nM) was performed in 1X Selection Buffer (50 mM HEPES, 6 mM KCl, 2.5 mM CaCl₂, 2.5 mM MgCl₂, 0.01% v/v Tween-20, pH 7.4). Reactions were incubated at room temperature for 30 min.

Following this, CRISPR reactions were performed in 1× TAE buffer pH 8.5 (40mM Tris-acetate -Nacalai Tesque- 1mM EDTA -Nippon Gene-), 0.05% Tween 20 (Nacalai Tesque), and 12.5 mM MgCl₂ (Nippon Gene) at a final volume of 20 μL. sgRNA-Aptamer and Cas nuclease were added at 100 nM, target amplicon was added at 40 nM. In case of working with complementary oligos - sequences are provided in the **Data set Table 2-**, 200 nM of oligo was added to 100 nM sgRNA-Aptamer in 1× TAE buffer pH 8.5 (40mM Tris-acetate -Nacalai Tesque- 1mM EDTA -Nippon Gene-), 0.05% Tween 20 (Nacalai Tesque) and 12.5 mM MgCl₂ (Nippon Gene). Incubation took place at 37 °C for 30 min. Then 100 nM Cas9 and 40 nM amplicon were added.

CRISPR reactions were incubated at 37 °C for 20 min in a thermocycler (Bio-Rad). Reaction volumes were transferred to a 384-well microplate (Greiner Bio-One, black, non-binding, flat-bottom). Green fluorescence (FAM) was measured using the Infinite M1000 PRO microplate reader (Tecan), with excitation at 495/12 nm and emission at 520/12 nm.

4.7 Data Set

Table 1. List of sequences used for the biocomputational experiments.

Name	Sequence 5' - 3'
N1 Primer Forward	GACCCCAAATCAGCGAAAT
N1 Primer Reverse	TCTGGTACTGCCAGTTGAATCTG
N1 amplicon	GACCCCAAATCAGCGAAATGCACCCGCATTACGTTTGG TGGACCCTCAGATTCAACTGGCAGTAACCAGA
E Primer Forward	ACAGGTACGTTAATAGTTAATAGCGT
E Primer Reverse	ATATTGCAGCAGTACGCACACA
E amplicon	ACAGGTACGTTAATAGTTAATAGCGTACTTCTTTTTCTTG CTTTCGTGGTATTCTTGCTAGTTACACTAGCCATCCTTAC TGCCTTCGATTGTGTGCGTACTGCTGCAATAT
sgRNA N1	GGAAAUUAGCGAAAUGCACCCCGCAUUACGUUGUUUUAG AGCUAGAAAUAGCAAGUUAAAUAAGGCUAGUCCGUUAUC AACUUGAAAAGUGGCACCGAGUCGGUGCUUUU
sgRNA E	GGAGUAGUACGCACACAAUCGAAGCGCAGUAGUUUUAGAG CUAGAAAUAGCAAGUUAAAUAAGGCUAGUCCGUUAUCA CUUGAAAAGUGGCACCGAGUCGGUGCUUUU
IN1	GACCCCAAATCAGCGAAATGCACCC
IN2	ATATTGCAGCAGTACGCACACAATCG
OR gate	
GATE1	CAGTACGCACACAATCGAGGGTGCATTTTCGCTGATTTTGG GGTC
GATE2	/CY5/CGATTGTGTGCGTACTGCTGCAATAT
GATE3	AATCAGCGAAATGCACCC/IB _{RQ} /
AND gate	
GATE1	CAGTACGCACACAATCG/CY5/AGGGTGCATTTTCGCTGAT TTTGGGGTC
GATE2	/IB _{RQ} /CGATTGTGTGCGTACTGCTGCAATAT
GATE3	AATCAGCGAAATGCACCC/IB _{RQ} /

Table 2. List of sequences used for the aptamer regulation experiments.

Name	Sequence 5' - 3'
E_CoV2_For	CTTGCTAGTTACACTAGCCATCCTTACTGCGCTTCGATTG TGTGCGTACTGCTGCAATAT /BHQ1/
E_CoV2_Rev	/FAM/ ATATTGCAGCAGTACGCACACAATCGAAGCGCAGTAAGGA TGGCTAGTGTAAGTACTAGCAAG
sgRNA E	GGAGUAGUACGCACACAAUCGAAGCGCAGUAGUUUUAGAG CUAGAAAUAGCAAGUUAAAAUAAGGCUAGUCCGUUAUCA CUUGAAAAAGUGGCACCGAGUCGGUGCUUUU
A27-B20-S5	GCTATTTCTAGCTCTAAAACCTTAATTTATGCTCTACCCGT CCACCTAGTTTT
A27-B20-S9	GCTATTTCTAGCTCTAAAACCTTAATTTATGCTCTACCCGT CCACCTAGTTTTAGAG
A27-B20-S10	GCTATTTCTAGCTCTAAAACCTTAATTTATGCTCTACCCGT CCACCTAGTTTTAGAGC
A27-B20-S11	GCTATTTCTAGCTCTAAAACCTTAATTTATGCTCTACCCGT CCACCTAGTTTTAGAGCT
A27-B0-S11	CTCGAGCGCTAGCTAGCCTGTTAATTTATGCTCTACCCGT CCACCTACAGGCTAGCTA
Ap39-B20-S7	GCTATTTCTAGCTCTAAAACCTTCCGGTTAATTTATGCTCT ACCCGTCCACCTACCGGAAGTTTTAG
A39-B20-S11	GCTATTTCTAGCTCTAAAACCTTCCGGTTAATTTATGCTCT ACCCGTCCACCTACCGGAAGTTTTAGAGCT
A39-B0-S11	CTCGAGCGCTAGCTAGCCTGTTCCGGTTAATTTATGCTCT ACCCGTCCACCTACCGGAACAGGCTAGCTA
C1	TTTCTAGCTCTAAAACCTACTGCGCTTAATTTATGCTCTAC CCGTCCACCTA
C2	ACTTGCTATTTCTAGCTCTAAAACCTTAATTTATGCTCTAC CCGTCCACCTA
C3	GATAACGGACTAGCCTTATTTTAACTTGCTATTTCTAGCT CTAAAACCTTAATTTATGCTCTACCCGTCCACCTA
C4	ACTTGCTATTTCTAGCTCTAAAACCTACTGCGCTTCGATTG TGTGCGTACTACTCCTTAATTTATGCTCTACCCGTCCACC TA

C5	AAAAGCACCGACTCGGTGCCACTTTTTCAAGTTGATAACT TAATTTATGCTCTACCCGTCCACCTA
A27-B16-S10	TCTAAAACACTACTGCGCTTAATTTATGCTCTACCCGTCCAC CTAGCGCAGTAGT
A27-B20-S10	TAGCTCTAAAACACTACTGCGCTTAATTTATGCTCTACCCGT CCACCTAGCGCAGTAGT
A27-B24-S10	TTTCTAGCTCTAAAACACTACTGCGCTTAATTTATGCTCTAC CCGTCCACCTAGCGCAGTAGT
A27-B24-S10- complementary	ACTACTGCGCTAGGTGGACGGGTAGAGCATAAATTAAGCG CAGTAGTTTTAGAGCTAGAAA
A39-B16-S7	TCTAAAACACTACTGCGCTTCCGGTTAATTTATGCTCTACCC GTCCACCTACCGGAAGCGCAGT
A39-B20-S7	TAGCTCTAAAACACTACTGCGCTTCCGGTTAATTTATGCTCT ACCCGTCCACCTACCGGAAGCGCAGT
A39-B24-S7	TTTCTAGCTCTAAAACACTACTGCGCTTCCGGTTAATTTATG CTCTACCCGTCCACCTACCGGAAGCGCAGT
A39-B24-S7- complementary	ACTGCGCTTCCGGTAGGTGGACGGGTAGAGCATAAATTAA CCGGAAGCGCAGTAGTTTTAGAGCTAGAAA

5. REFERENCES

- Aman R, Mahas A, Mahfouz M (2020) Nucleic acid detection using CRISPR/Cas biosensing technologies. *ACS Synth Biol* 9, 1226-1233.
- Amini R, Zhang Z, Li J, Gu J, Brennan JD, Li Y (2022) Aptamers for SARS-CoV-2: Isolation, Characterization, and Diagnostic and Therapeutic Developments. *Analysis & Sensing* 2, e202200012.
- Benenson Y (2012) Biomolecular computing systems: principles, progress and potential. *Nat Rev Genet* 13, 455-468.
- Briner AE, Donohoue PD, Goma AA, Selle K, Slorach EM, *et al.* (2014) Guide RNA functional modules direct Cas9 activity and orthogonality. *Mol Cell* 56, 333-339.
- Chang CC (2021) Recent advancements in aptamer-based surface plasmon resonance biosensing strategies. *Biosensors* 11, 233.
- Chen JS, Ma E, Harrington LB, Da Costa M, Tian X, *et al.* (2018) CRISPR-Cas12a target binding unleashes indiscriminate single-stranded DNase activity. *Science* 360, 436-439.
- Dow LE, Fisher J, O'rourke KP, Muley A, Kasthuber ER, *et al.* (2015) Inducible *in vivo* genome editing with CRISPR-Cas9. *Nat Biotechnol*, 33, 390-394.
- Ferry QRV, Lyutova R, Fulga TA (2017) Rational design of inducible CRISPR guide RNAs for de novo assembly of transcriptional programs. *Nat Commun* 8, 14633.
- Gander MW, Vrana JD, Voje WE, Carothers JM, Klavins E (2017) Digital logic circuits in yeast with CRISPR-dCas9 NOR gates. *Nat Commun* 8, 15459.
- Gootenberg JS, Abudayyeh OO, Lee JW, Essletzbichler P, Dy AJ, *et al.* (2017) Nucleic acid detection with CRISPR-Cas13a/C2/c2. *Science* 356, 438-442.

- Gruber AR, Lorenz R, Bernhart SH, Neuböck R, Hofacker IL (2008) The vienna RNA websuite. *Nucleic Acids Res* 36, W70-W74.
- Jain PK, Ramanan V, Schepers AG, Dalvie NS, Panda A, *et al.* (2016) Development of light-activated CRISPR using guide RNAs with photocleavable protectors. *Angew Chem Int Ed* 55, 12440-12444.
- Jerabek-Willemsen M, André T, Wanner R, Roth HM, Duhr S, *et al.* (2014). MicroScale Thermophoresis: Interaction analysis and beyond. *J Mol Struct* 1077, 101-113.
- Jinek M, Chylinski K, Fonfara I, Hauer M, Doudna JA, Charpentier E (2012) A programmable dual-RNA-guided DNA endonuclease in adaptive bacterial immunity. *Science* 337, 816-821.
- Kaminski MM, Abudayyeh OO, Gootenberg JS, Zhang F, Collins JJ (2021) CRISPR-based diagnostics. *Nat Biomed Eng* 5, 643-656.
- Kempton HR, Goudy LE, Love KS, Qi LS (2020) Multiple input sensing and signal integration using a split Cas12a system. *Mol Cell* 78, 184-191.
- Kim H, Bojar D, Fussenegger M (2019) A CRISPR/Cas9-based central processing unit to program complex logic computation in human cells. *PNAS* 116, 7214-7219.
- Kundert K, Lucas JE, Watters KE, Fellmann C, Ng AH, *et al.* (2019) Controlling CRISPR-Cas9 with ligand-activated and ligand-deactivated sgRNAs. *Nat Commun* 10, 2127.
- Lee YJ, Hoynes-O'Connor A, Leong MC, Moon TS (2016) Programmable control of bacterial gene expression with the combined CRISPR and antisense RNA system. *Nucleic Acids Res* 44, 2462-2473.
- Li J, Green AA, Yan H, Fan C (2017) Engineering nucleic acid structures for programmable molecular circuitry and intracellular biocomputation. *Nat Chem* 9, 1056-1067.
- Li J, Zhang Z, Gu J, Stacey HD, Ang JC, *et al.* (2021) Diverse high-affinity DNA aptamers for wild-type and B. 1.1. 7 SARS-CoV-2 spike proteins from a pre-structured DNA library. *Nucleic Acids Res* 49, 7267-7279.

- Lin B, An Y, Meng L, Zhang H, Song J, *et al.* (2019) Control of CRISPR-Cas9 with small molecule-activated allosteric aptamer regulating sgRNAs. *Chem Commun* 55, 12223-12226.
- Liu Y, Zhan Y, Chen Z, He A, Li J, *et al.* (2016) Directing cellular information flow via CRISPR signal conductors. *Nat Methods* 13, 938-944.
- Márquez-Costa R, Montagud-Martinez R, Marques MC, Albert E, Navarro D, *et al.* (2023) Multiplexable and biocomputational virus detection by CRISPR-Cas9-mediated strand displacement. *Anal Chem* 95, 9564-9574.
- Mironov V, Shchugoreva IA, Artyushenko PV, Morozov D, Borbone N, *et al.* (2022) Structure-and interaction-based design of anti-SARS-CoV-2 aptamers. *Chem - Eur J* 28, e202104481.
- Montagud-Martinez R, Heras-Hernandez M, Goiriz L, Daros JA, Rodrigo G (2021) CRISPR-mediated strand displacement logic circuits with toehold-free DNA. *ACS Synth Biol* 10, 950-956.
- Nihongaki Y, Kawano F, Nakajima T, Sato M (2015) Photoactivatable CRISPR-Cas9 for optogenetic genome editing. *Nat Biotechnol* 33, 755-760.
- Pickar-Oliver A, Gersbach CA (2019) The next generation of CRISPR-Cas technologies and applications. *Nat Rev Mol Cell Biol* 20, 490-507.
- Sarhadi VK, Armengol G (2022) Molecular biomarkers in cancer. *Biomolecules* 12, 1021.
- Schmitz A, Weber A, Bayin M, Breuers S, Fieberg V, *et al.* (2021) A SARS-CoV-2 spike binding DNA Aptamer that inhibits Pseudovirus infection by an RBD-independent mechanism. *Angew Chem Int Ed* 60, 10279-10285.
- Seelig G, Soloveichik D, Zhang DY, Winfree E (2006) Enzyme-free nucleic acid logic circuits. *Science* 314, 1585-1588.
- Shivram H, Cress BF, Knott GJ, Doudna JA (2021) Controlling and enhancing CRISPR systems. *Nat Chem Biol* 17, 10-19.

- Song Y, Song J, Wei X, Huang M, Sun M, *et al.* (2020) Discovery of aptamers targeting the receptor-binding domain of the SARS-CoV-2 spike glycoprotein. *Anal Chem* 92, 9895-9900.
- Tang W, Hu JH, Liu DR (2017) Aptazyme-embedded guide RNAs enable ligand-responsive genome editing and transcriptional activation. *Nat Commun* 8, 15939.
- Valero J, Civit L, Dupont DM, Selnhhin D, Reinert LS, *et al.* (2021) A serum-stable RNA aptamer specific for SARS-CoV-2 neutralizes viral entry. *PNAS* 118, e2112942118.
- Wang J, Zhou HS (2008) Aptamer-based Au nanoparticles-enhanced surface plasmon resonance detection of small molecules. *Anal Chem* 80, 7174-7178.
- Zadeh JN, Steenberg CD, Bois JS, Wolfe BR, Pierce MB, *et al.* (2011) NUPACK: Analysis and design of nucleic acid systems. *J Comput Chem* 32, 170-173.
- Zetsche B, Volz SE, Zhang F (2015) A split-Cas9 architecture for inducible genome editing and transcription modulation. *Nat Biotechnol* 33, 139-142.

CHAPTER 6

GENERAL DISCUSSION

Since their discovery, CRISPR-Cas systems have proven to be remarkably versatile tools, offering a wide range of biotechnological solutions. Beyond their initial applications in genetic editing, CRISPR has transformed our capacity to manipulate, detect, and analyze nucleic acid sequences. CRISPR-Cas based tools continue to be developed for research, medicine, and diagnostics. In particular, CRISPR advancement in the development of novel diagnostic tools holds promise for revolutionizing disease detection and management. Already, CRISPR-based diagnostic products have been authorized by the US Food and Drug Administration (FDA) for use in centralized labs (Abudayyeh and Gootenberg, 2021). The Cas proteins exhibiting the collateral activity upon target recognition, Cas12 and Cas13, are the most often deployed in CRISPR-based diagnostics (Yin *et al.*, 2021).

In this thesis, we aimed to expand the CRISPR-based diagnostic toolkit. This included developing a novel diagnostic method based on *Streptococcus pyogenes* Cas9 nuclease (SpyCas9) and strand displacement. While our primary focus was on SpyCas9, the method is versatile and can function with other Cas9 effectors. Our system was termed COLUMBO (CRISPR-Cas9 R-loop usage for the molecular beacon opening). For detection, we employ a Cas9 nuclease coupled with its sgRNA to target a desired double-stranded DNA amplicon. Upon DNA targeting, a single-stranded motif interacts with an appropriately designed molecular beacon to report the detection signal via fluorescence. Our findings demonstrate that this novel CRISPR-Cas9 detection method is effective in sensing SARS-CoV-2 viral sequences in patients who were previously diagnosed as positive in the hospital, providing a significant distinction between positive and negative patients. In addition, our system demonstrates high detection resolution, and is able to detect virus variants and reveal specific mutations up to single nucleotide changes.

The implemented detection method is based on strand displacement rather than collateral catalysis as in other well-known CRISPR-detection tools. In systems utilizing Cas12 or Cas13 nucleases, collateral cleavage acts as a multiple conversion reaction triggered by *cis*-recognition. These enzymes are activated by target nucleic acids and indiscriminately cleave nearby non-target nucleic acids. This cleavage process results in a detectable signal when coupled with fluorescent reporters. Since each activated Cas enzyme can cleave multiple reporter molecules, the resultant signal amplification can lead to a large dynamic range (Kellner *et al.*, 2019). Nevertheless, since that catalytic activity is a non-specific process, there is no possibility to distinguish two different strands in the same reaction, or to process further *in vitro* reactions, because all nucleic acid species would be degraded. In our case, this lack of collateral activity in Cas9 allowed us to perform multiplexed detection within the same reaction, either for detection of different sequences from the same virus or different sequences from different viruses. Also, the absence of general collateral cleavage represents an opportunity to interface a CRISPR-based nucleic acid detection with further DNA computing developments, allowing to perform more complex nucleic acid circuits.

Novel CRISPR-based detection methods look to combine the high sensitivity and specificity of the direct nucleic acid detection with affordable, accessible, inexpensive and without complex instrumentation requirements diagnostic tests. We aim to develop tools capable of working in low-resource settings, providing point-of-care (POC) solutions (Mina *et al.*, 2020). In the clinic, qPCR is the gold-standard procedure for diagnostics, yet research on alternative methods is required to bypass the complex qPCR procedure. Also, the use of CRISPR-Cas adds an additional layer for sequence specificity. In qPCR, specificity is given by the primers, and often, it proves challenging to discern between closely related sequences, resulting in a more complex scenario when it comes to multiplexed detection. Our method requires a preamplification, and our data show that COLUMBO is compatible with both PCR and RPA. RPA would be the amplification method for POC applications, yet other isothermal amplification methods can also be explored, such as Loop-mediated isothermal amplification (LAMP), NASBA or EXPAR (Tomita *et al.*, 2008; Zhao *et al.*, 2015).

In the early stages of COLUMBO development, the signal readout needed to be measured in a fluorimeter. To bypass the need for such equipment in fluorescence-based assays, some approaches have been developed on portable fluorescence microscopy coupled to mobile phones (de Puig *et al.*, 2021; Fozouni *et al.*, 2021; Ning *et al.*, 2021). Additional strategies enabling colorimetric visualization by using gold nanoparticles or biotinylated elements have been described as well (Hu *et al.*, 2020; Marsic *et al.*, 2021; Yuan *et al.*, 2020). In our work, we have used biotin-labelled amplicons to enable colorimetric visualization by using commercially available lateral flow strips. In this configuration, results can be read approximately one hour after sample collection, rendering it a more viable option for POC home testing scenarios. Further, by using double test lateral flow strips and labelling amplicons with either biotin or digoxigenin, we demonstrated the multiplexing capacity of Cas9 detection methods in a colorimetric set-up.

A one-pot reaction combining the amplification, detection, and readout in a single tube, without any complex or expensive infrastructure would be ideal. Most common CRISPR detection protocols require several handling steps as well as pre-sample processing with a nucleic acid extraction protocol (Kaminski *et al.*, 2021). Several attempts have been made to combine amplification and Cas12/Cas13 detection in a single tube by refining reaction conditions and employing isothermal amplification and a thermostable Cas effector (Aman *et al.*, 2022; Arizti-Sanz *et al.*, 2020; Joung *et al.*, 2020; Li *et al.*, 2019; Mahas *et al.*, 2022). Available quick extraction protocols have also been used directly for CRISPR applications (Chandrasekaran *et al.*, 2022; Myhrvold *et al.*, 2018). In our case, we can directly work with the nasopharyngeal swabs obtained from the patients, without the need for a nucleic acid extraction. Moving forward, our objective is to continue progressing toward a one-pot POC methodology. Ideally, we strive to develop a simple and easy to perform miniaturized setup with a naked-eye diagnostic readout, suitable for at-home testing. We aim our development to improve accessibility and convenience for diagnostic purposes.

In this regard, we anticipate expanding the scope of application for this technology. In this work, we have mainly focused on viral respiratory infections affecting humans, but there are many other diseases that could

potentially be diagnosed by detecting a given nucleic acid. This method has the potential to be adapted for the detection of a wide range of other viruses, including those causing diseases like Zika, Ebola, and hepatitis. Beyond viral infections, this technology could also be utilized to detect bacterial infections, particularly those caused by antibiotic-resistant bacteria, which are of significant concern in hospital infection scenario. The detection would not only allow for fast treatment decisions, but also for effective infection control measurements and surveillance, contributing to the prevention of widespread antibiotic resistance. These pathogens are known as ESKAPE bacteria and include *Enterococcus faecium*, *Staphylococcus aureus*, *Klebsiella pneumoniae*, *Acinetobacter baumannii*, *Pseudomonas aeruginosa*, and *Enterobacter* species (Boucher *et al.*, 2009; Pendleton *et al.*, 2013).

Besides detecting exogenous genomes as in infectious agents, detection of an endogenous nucleic acid fragment could also be tested. This would include detecting genetic biomarkers of various diseases. Cell-free DNA (*i.e.*, fragmented DNA molecules found extracellularly and easily detectable in bodily fluids like urine or blood) are an ideal target for rapid diagnostics (Stewart *et al.*, 2018). Noncoding small RNAs, such as microRNAs, are being proposed as useful biomarkers of choice for various diseases in clinical diagnostics (Wang *et al.*, 2016). Dysregulation of these microRNAs has been linked to a wide range of diseases, including cancer, dementia, and cardiovascular conditions. Generally, these markers find extensive applications in cancer, serving as early diagnostic indicators or monitors of treatment efficacy (Khailany *et al.*, 2020; Rosenfeld *et al.*, 2008). CRISPR-Cas-mediated detection strategies have been already proven helpful in the detection of different kinds of cancer biomarkers including nucleic acids, proteins, and extracellular vesicles (Bruch *et al.*, 2019; Gong *et al.*, 2021).

The versatility of our diagnostic technology extends beyond human health. In addition to detecting human pathogens and potential biomarkers, our approach has been successfully adapted for the detection of plant viruses. Plant viruses and the disease generated upon infection result in losses of several billion dollars every year, making rapid and specific diagnostic tools crucial for effective viral spread control, management of diseases, and yield crop maintenance (Rubio *et al.*, 2020). Mixed viral infections in plants can be

remarkably frequent; often resulting in synergistic interactions that can increase virulence or lead to new diseases (Moreno and López-Moya, 2020; Syller, 2012). These occurrences underscore the need for specific and rapid multiplexed detection. Our technology's capability for simultaneous detection makes it well-suited to address this challenge effectively. In addition to plant viruses, viroids are a major concern in modern agriculture. Due to the absence of protein-coding capacity in viroids, detection methods must rely exclusively on the direct identification of their genomic sequences (Pallás *et al.*, 2018). This makes our method particularly useful for viroid detection. Moreover, the technology can also be utilized to detect the presence of nucleic acids of interest as environmental contaminants. Natural environments, such as wastewaters, can serve as reservoirs for various pathogens, making them potential sources of disease outbreaks. Early detection and monitoring of these pathogens can aid in identifying disease outbreaks, understanding transmission patterns, and preventing their dissemination among the population (Randazzo *et al.*, 2020).

Nevertheless, for any target suitable to be detected with Cas9, the method requires sequence design, given a series of energetic and structural specifications, of the different nucleic acid species involved. This design is often done in a manual time-consuming trial-and-error approach. The standardization and automatization of the design of the parts that conform our mechanism will boost the development of new detection devices. Hence, to be able to engineer a large collection of CRISPR-Cas9-based tests for targets of interest, we note the potential utility of employing computational methods to automate the sequence design of the different nucleic acid species that COLUMBO requires (primers, sgRNA, and molecular beacon). Our aim is to fully automate the design process in a user-friendly manner. This means that, starting from the desired sequence of interest to be detected as input, an algorithm will initiate the design process and provide the different COLUMBO elements necessary for a successful experimental implementation. The combination of computational sequence design with a more efficient analysis and screening procedure might allow optimizing the system, enhancing the dynamic range of the fluorescence signal.

Importantly, the input target DNA molecule needs to harbor a protospacer adjacent motif (PAM) for Cas9 binding. While not a major obstacle, this PAM requirement represents a design constraint. In the specific case of SpyCas9, it recognizes the motif NGG in the target sequence. This constant sequence is quite commonly found within nucleotides sequences, offering freedom to choose almost any region of a viral genome to target. In the SARS-CoV-2 genome, used in this work as a proof of concept, there are 1981 possible Cas9 PAMs. That is, about one PAM every 15 nt. Still, we understand that PAM requirements represent an additional limitation. Especially, there may be fewer options available for SNP-based discrimination and other short sequence detections. It is important for diagnostic methods to possess single-nucleotide specificity, since single nucleotide variations can significantly impact the determination of viral subtypes with varying infectivity and severity (Yin, 2020) and the disclosure of mutations that confer resistance against antibiotics (Woodford and Ellington, 2007) or antiviral drugs (Irwin *et al.*, 2016). To solve this problem, primers for amplification can be specially designed to introduce the PAM sequence, enabling the nucleic acid detection in a PAM-independent way (Li *et al.*, 2018). Efforts are also being applied to engineer or discover further Cas9 proteins with broader PAM compatibility (Collias and Beisel, 2021). Evolution methods have been used to rapidly generate Cas9 variants with relaxed PAM recognition specificity (Hu *et al.*, 2018; Kleinstiver *et al.*, 2015). Some of these engineered Cas9 proteins reported much greater DNA specificity than WT SpyCas9, as well as minimal off-target activity.

Explorations of other nuclease variants may reveal novel properties beside the PAM variations alternatives, which could optimize its performance and benefit our detection approach goal. Strategies exist, for example, for enhancing on-target specificity. Cas9-sgRNA ribonucleoprotein features a 10-12 bp seed region proximal to the PAM sequence that governs specificity, while up to 6 mismatches in the 5'-terminal region of the protospacer are tolerated (Hsu *et al.*, 2014; Jinek *et al.*, 2012). This tolerance to mismatches in the target sequence can result in off-target effects, where an unintended sequence is targeted due to a shared sequence identity with the actual DNA target. To lower off-target events, new Cas9 nucleases with high fidelity can

be employed (Kleinstiver *et al.*, 2016; Slaymaker *et al.*, 2016). As demonstrated in this study, the use of these reduced off-target nucleases can identify subtle specific mutations, achieving detection resolutions down to a single nucleotide, which is especially advantageous for identifying potential variants of concern. Exploring the full diversity of Cas9 nucleases found in nature or redesigning new enhanced variants with properties such as lower temperature requirements, faster kinetics or smaller in size, could also contribute to developing more efficient CRISPR-based diagnostics.

Our detection method also involves sgRNA and molecular beacons, so modifications toward improving these elements should also be considered. Many modifications can be incorporated into the sgRNA for improving the resistance to nucleases, increasing its stability, enhancing its binding with target DNA, or promoting its assembling with Cas9 (Filippova *et al.*, 2019). The incorporation of chemically modified nucleotides in the sgRNA structure has led to performance improvements, such as 2' O-methyl, 2'-deoxy-2'-fluoro, or phosphorothioate (Hendel *et al.*, 2015; Rahdar *et al.*, 2015; Yin *et al.*, 2017). Also, the spacer of our sgRNAs is longer than the typical 20 nt, since we opted to use standard primers, such as CDC N1 or Charité E, but truncated sgRNAs, with shorter spacers (<20 nt in length) can reduce the off-targets effects (Fu *et al.*, 2014). The incorporation of locked nucleic acids (LNA) in either the sgRNA or the molecular beacon structure can also be beneficial. LNAs are RNA nucleotides in which the 2' oxygen in the ribose forms a covalent bond to the 4' carbon. These bridge nucleic acids display improved base stacking and thermal stability (Cromwell *et al.*, 2018; Vester and Wengel, 2004). Similarly, peptide nucleic acids (PNA) can be used in place of DNA, which exhibit enhanced hybridization properties and greater chemical and enzymatic stability compared to nucleic acids. Therefore, the use of PNA in COLUMBO could also be explored as an alternative to DNA molecular beacons (Shakeel *et al.*, 2006).

Finally, we also explored the signal integration capacity of CRISPR-Cas9 and coupled it with the detection potential. We aim to make use of the absence of collateral cleavage, a key distinction from other CRISPR-based detection methods (Yin *et al.*, 2021), to extend its usage beyond nucleic acid detection and demonstrate its compatibility with DNA computing. To illustrate this, we

devised two molecular programs (OR logic gate and AND logic gate) that run after DNA amplicons are generated from the SARS-CoV-2 RNA genome and produce a logic output according to the input signals. The OR gate emitted a fluorescence signal when at least one amplicon was present in the reaction, whereas the AND gate was responsive when the two amplicons were present in the reaction. We replicated these results using amplified products from patient samples. This opens a new line of research in which CRISPR diagnostics meets the versatile functionality of DNA to implement logic programs, enabling downstream processing with additional signals (Wang *et al.*, 2021).

In addition, we investigated the regulatory control of CRISPR-Cas9 activity through a conditional sgRNA mechanism involving blocking and activation via aptamer-protein interaction. In our case, we selected spike protein from SARS-CoV-2 as the triggering element. We successfully demonstrated the ability to block the ribonucleoprotein activity in the absence of spike protein. Our attempts to restore Cas9 activity in the spike protein presence were not conclusive and did not provide clear evidence of aptamer conformational changes upon interaction with the spike protein. Apparently, the selection of spike protein aptamers is a challenging task, likely due to the difficulty of finding nucleic acids that bind to highly glycosylated proteins such as SARS-CoV-2 spike protein (Valero *et al.*, 2021). A more extensive characterization on the aptamer-protein interaction could provide valuable insights into any conformational change that may occur. Given the wide repertoire of aptamers capable of binding relevant targets, (Zhou and Rossi, 2017), exploration of alternative nucleic acid-protein combinations may offer new avenues for a successful implementation of a dual CRISPR-Cas9 detection.

Overall, CRISPR-Cas based diagnostic has provided a promising, new tool for accurate, fast, and inexpensive pathogen detection. In this thesis we aimed to expand the CRISPR-based detection tools through the development of a novel Cas9-based detection method. We demonstrate its multiplexing capacity, allowing the simultaneous detection of multiple pathogens or variants. Additionally, we explored signal integration, coupling it with DNA biocomputing and engineering logic processing, along with the sensing of other elements than nucleic acids. We envision to continue refining our

technology to overcome its current limitations and optimize the system. Our goal is to develop a rapid and specific diagnostic tool capable of detecting a wide range of nucleic acids of interest. This work exemplifies the continually growing array of applications for which CRISPR-Cas systems can be used. We aspire to further advance this technology, paving the way for improved detection tools, suitable for POC applications and field-deployable testing.

REFERENCES

- Abudayyeh OO, Gootenberg JS (2021) CRISPR diagnostics. *Science* 372, 914-915.
- Aman R, Marsic T, Sivakrishna G, Mahas A, Ali Z, *et al.* (2022) iSCAN-V2: A one-pot RT-RPA–CRISPR/Cas12b assay for point-of-care SARS-CoV-2 detection. *Front Bioeng Biotechnol* 9, 800104.
- Arizti-Sanz J, Freije CA, Stanton AC, Petros BA, Boehm CK, *et al.* (2020) Streamlined inactivation, amplification, and Cas13-based detection of SARS-CoV-2. *Nat Commun* 11, 5921.
- Boucher HW, Talbot GH, Bradley JS, Edwards JE, Gilbert D, *et al.* (2009) Bad bugs, no drugs: no ESKAPE! An update from the Infectious Diseases Society of America. *Clin Infect Dis* 48, 1-12.
- Bruch R, Baaske J, Chatelle C, Meirich M, Madlener S, *et al.* (2019) CRISPR/Cas13a-powered electrochemical microfluidic biosensor for nucleic acid amplification-free miRNA diagnostics. *Adv Mater* 31, 1905311.
- Chandrasekaran SS, Agrawal S, Fanton A, Jangid AR, Charrez B, *et al.* (2022) Rapid detection of SARS-CoV-2 RNA in saliva via Cas13. *Nat Biomed Eng* 6, 944-956.
- Collias D, Beisel CL (2021) CRISPR technologies and the search for the PAM-free nuclease. *Nat Commun* 12, 555.
- Cromwell CR, Sung K, Park J, Krysler AR, Jovel J, *et al.* (2018) Incorporation of bridged nucleic acids into CRISPR RNAs improves Cas9 endonuclease specificity. *Nature Commun* 9, 1448.
- de Puig H, Lee RA, Najjar D, Tan X, Soenksen LR, *et al.* (2021) Minimally instrumented SHERLOCK (miSHERLOCK) for CRISPR-based point-of-care diagnosis of SARS-CoV-2 and emerging variants. *Sci Adv* 7, eabh2944.

- Filippova J, Matveeva A, Zhuravlev E, Stepanov G (2019) Guide RNA modification as a way to improve CRISPR/Cas9-based genome-editing systems. *Biochimica* 167, 49-60.
- Fozouni P, Son S, Diaz de Leon Derby M, Knott GJ, Gray CN, *et al.* (2021) Amplification-free detection of SARS-CoV-2 with CRISPR-Cas13a and mobile phone microscopy. *Cell* 184, 323-333.
- Fu Y, Sander JD, Reyon D, Cascio VM, Joung JK (2014) Improving CRISPR-Cas nuclease specificity using truncated guide RNAs. *Nat Biotechnol* 32, 279-284.
- Gong S, Zhang S, Lu F, Pan W, Li N, Tang B (2021) CRISPR/Cas-based in vitro diagnostic platforms for Cancer biomarker detection. *Anal Chem* 93, 11899-11909.
- Hendel A, Bak RO, Clark JT, Kennedy AB, Ryan DE, *et al.* (2015) Chemically modified guide RNAs enhance CRISPR-Cas genome editing in human primary cells. *Nat Biotechnol* 33, 985-989.
- Hsu PD, Lander ES, Zhang F (2014) Development and applications of CRISPR-Cas9 for genome engineering. *Cell* 157, 1262-1278.
- Hu JH, Miller SM, Geurts MH, Tang W, Chen L, *et al.* (2018) Evolved Cas9 variants with broad PAM compatibility and high DNA specificity. *Nature* 556, 57-63.
- Hu M, Yuan C, Tian T, Wang X, Sun J, *et al.* (2020) Single-step, salt-aging-free, and thiol-free freezing construction of AuNP-based bioprobes for advancing CRISPR-based diagnostics. *J Am Chem Soc* 142, 7506-7513.
- Irwin KK, Renzette N, Kowalik TF, Jensen JD (2016) Antiviral drug resistance as an adaptive process. *Virus Evol* 2, vew014.
- Jinek M, Chylinski K, Fonfara I, Hauer M, Doudna JA, Charpentier E (2012) A programmable dual-RNA-guided DNA endonuclease in adaptive bacterial immunity. *Science* 337, 816-821.

- Joung J, Ladha A, Saito M, Kim NG, Woolley AE, *et al.* (2020) Detection of SARS-CoV-2 with SHERLOCK one-pot testing. *N Engl J Med* 383, 1492-1494.
- Kaminski MM, Abudayyeh OO, Gootenberg JS, Zhang F, Collins JJ (2021) CRISPR-based diagnostics. *Nat Biomed Eng* 5, 643-656.
- Kellner MJ, Koob JG, Gootenberg JS, Abudayyeh OO, Zhang F (2019) SHERLOCK: nucleic acid detection with CRISPR nucleases. *Nat Protoc* 14, 2986-3012.
- Khailany RA, Aziz SA, Najjar SM, Safdar M, Ozaslan M (2020) Genetic biomarkers: Potential roles in cancer diagnosis. *Cell Mol Biol* 66, 1-7.
- Kleinstiver BP, Pattanayak V, Prew MS, Tsai SQ, Nguyen NT, *et al.* (2016) High-fidelity CRISPR–Cas9 nucleases with no detectable genome-wide off-target effects. *Nature* 529, 490-495.
- Kleinstiver BP, Prew MS, Tsai SQ, Topkar VV, Nguyen NT, *et al.* (2015) Engineered CRISPR-Cas9 nucleases with altered PAM specificities. *Nature* 523, 481-485.
- Li L, Li S, Wu N, Wu J, Wang G, *et al.* (2019) HOLMESv2: a CRISPR-Cas12b-assisted platform for nucleic acid detection and DNA methylation quantitation. *ACS Synth Biol* 8, 2228-2237.
- Li SY, Cheng QX, Wang JM, Li XY, Zhang ZL, *et al.* (2018) CRISPR-Cas12a-assisted nucleic acid detection. *Cell Discov* 4, 20.
- Mahas A, Marsic T, Lopez-Portillo M, Wang Q, Aman R, *et al.* (2022) Characterization of a thermostable Cas13 enzyme for one-pot detection of SARS-CoV-2. *PNAS* 119, e2118260119.
- Marsic T, Ali Z, Tehseen M, Mahas A, Hamdan S, Mahfouz M (2021) Vigilant: an engineered VirD2-Cas9 complex for lateral flow assay-based detection of SARS-CoV2. *Nano Lett* 21, 3596-3603.
- Mina MJ, Parker R, Larremore DB (2020) Rethinking Covid-19 test sensitivity—a strategy for containment. *N Engl J Med* 383, e120.

- Moreno AB, López-Moya JJ (2020) When viruses play team sports: Mixed infections in plants. *Phytopathol* 110, 29-48.
- Myhrvold C, Freije CA, Gootenberg JS, Abudayyeh OO, Metsky HC, *et al.* (2018) Field-deployable viral diagnostics using CRISPR-Cas13. *Science* 360, 444-448.
- Ning B, Yu T, Zhang S, Huang Z, Tian D, *et al.* (2021) A smartphone-read ultrasensitive and quantitative saliva test for COVID-19. *Sci Adv* 7, eabe3703.
- Pallás V, Sánchez-Navarro JA, James D (2018) Recent advances on the multiplex molecular detection of plant viruses and viroids. *Front Microbiol* 9, 400508.
- Pendleton JN, Gorman SP, Gilmore BF (2013) Clinical relevance of the ESKAPE pathogens. *Expert Rev Anti Infect Ther* 11, 297-308.
- Rahdar M, McMahon MA, Prakash TP, Swayze EE, Bennett CF, Cleveland DW (2015) Synthetic CRISPR RNA-Cas9-guided genome editing in human cells. *PNAS* 112, E7110-E7117.
- Randazzo W, Cuevas-Ferrando E, Sanjuán R, Domingo-Calap P, Sánchez G (2020) Metropolitan wastewater analysis for COVID-19 epidemiological surveillance. *J Hyg Environ* 230, 113621.
- Rosenfeld N, Aharonov R, Meiri E, Rosenwald S, Spector Y, *et al.* (2008) MicroRNAs accurately identify cancer tissue origin. *Nature Biotechnol* 26, 462-469.
- Rubio L, Galipienso L, Ferriol I (2020) Detection of plant viruses and disease management: Relevance of genetic diversity and evolution. *Front Plant Sci* 11, 1092.
- Shakeel S, Karim S, Ali A (2006) Peptide nucleic acid (PNA)—a review. *J Chem Technol Biotechnol* 81, 892-899.
- Slaymaker IM, Gao L, Zetsche B, Scott DA, Yan WX, Zhang F (2016) Rationally engineered Cas9 nucleases with improved specificity. *Science* 351, 84-88.

- Stewart CM, Kothari PD, Mouliere F, Mair R, Somnay S, *et al.* (2018) The value of cell - free DNA for molecular pathology. *J Pathol* 244, 616-627.
- Syller J (2012) Facilitative and antagonistic interactions between plant viruses in mixed infections. *Mol Plant Pathol* 13, 204-216.
- Tomita N, Mori Y, Kanda H, Notomi T (2008) Loop-mediated isothermal amplification (LAMP) of gene sequences and simple visual detection of products. *Nat Protoc* 3, 877-882
- Valero J, Civit L, Dupont DM, Selnihhin D, Reinert LS, *et al.* (2021). A serum-stable RNA aptamer specific for SARS-CoV-2 neutralizes viral entry. *PNAS* 118, e2112942118.
- Vester B, Wengel J (2004) LNA (locked nucleic acid): high-affinity targeting of complementary RNA and DNA. *Biochem* 43, 13233-13241.
- Wang J, Chen J, Sen S (2016) MicroRNA as biomarkers and diagnostics. *J Cell Physiol* 231, 25-30.
- Wang K, Xu BF, Lei CY, Nie Z (2021) Advances in the integration of nucleic acid nanotechnology into CRISPR-Cas system. *J Anal Test* 5, 130-141.
- Woodford N, Ellington MJ (2007) The emergence of antibiotic resistance by mutation. *Clin Microbiol Infect* 13, 5-18.
- Yin C (2020) Genotyping coronavirus SARS-CoV-2: methods and implications. *Genomics* 112, 3588-3596.
- Yin H, Song CQ, Suresh S, Wu Q, Walsh S, *et al.* (2017) Structure-guided chemical modification of guide RNA enables potent non-viral *in vivo* genome editing. *Nat Biotechnol* 35, 1179-1187.
- Yin L, Man S, Ye S, Liu G, Ma L (2021) CRISPR-Cas based virus detection: Recent advances and perspectives. *Biosens Bioelectron* 193, 113541.
- Yuan C, Tian T, Sun J, Hu M, Wang X, *et al.* (2020) Universal and naked-eye gene detection platform based on the clustered regularly interspaced

short palindromic repeats/Cas12a/13a system. *Anal Chem* 92 4029-4037.

Zhao Y, Chen F, Li Q, Wang L, Fan C (2015) Isothermal amplification of nucleic acids. *Chem Rev* 115, 12491-12545.

Zhou J, Rossi J (2017) Aptamers as targeted therapeutics: current potential and challenges. *Nat Rev Drug Discov* 16, 181-202.

CHAPTER 7

CONCLUSIONS

This PhD dissertation aimed to expand the CRISPR-based diagnostic toolkit by developing a novel detection mechanism based on Cas9 strand displacement reaction. This work has led to the following conclusions:

1. Cas9 can be repurposed for diagnostic purposes. Nucleic acid detection can be achieved through a Cas9-based strand displacement reaction.
2. The strand displacement mechanism is instrumental for multiplexing detection within the same reaction in the same tube with a single Cas protein.
3. Our development showed a great performance in specificity and programmability, being able to detect different targets with no cross-reactions.
4. The detection method is compatible with both PCR and RPA amplification methods, and likely will have no problems incorporating future amplification methods.
5. High sensitivity allows for the detection of single point mutations, allowing us to identify variants of concern.
6. CRISPR-Cas9 can be successfully used to detect viral infections from patients' samples without RNA extraction.
7. The detection method is compatible with lateral flow assays, suitable for point-of-care applications.

8. The lack of collateral activity can be exploited for processing further sequences, allowing for DNA computing.
9. CRISPR-Cas9-based detection mechanisms have the potential to exploit conditional sgRNAs to sense other molecules beyond nucleic acids.

FUNDING AND SUPPORT

This thesis was conducted at the BioSystems Design Rodrigo Lab within the Institute for Integrative Systems Biology (I2SysBio), a joint center of the Spanish National Research Council (CSIC) and the Universitat de València (UV). The research was carried out in pursuit of a PhD degree at the Polytechnic University of Valencia (UPV).

This work was supported by a predoctoral fellowship from the Spanish Ministry of Science and Innovation (PRE2019-088531).

SCIENTIFIC CONTRIBUTION

▪ Publications in Scientific Journals

- Montagud-Martinez R, Márquez-Costa R, Heras-Hernandez M, Dolcemascolo R, Rodrigo G (2024) On the ever-growing functional versatility of the CRISPR-Cas13 system. *Microbial Biotechnology* 17: e14418
<https://doi.org/10.1111/1751-7915.14418>
- Márquez-Costa R, Montagud-Martinez R, Marques MC, Albert E, Navarro D, Daros JA, Ruiz R, Rodrigo G (2023) Multiplexable and biocomputational virus detection by CRISPR-Cas9-mediated strand displacement. *Analytical Chemistry* 95: 9564-9574
<https://doi.org/10.1021/acs.analchem.3c01041>

[“Multiplexable CRISPR-Cas9-based virus detection method”. (Spanish Patent and Trademark Office, Reference EP22382374).]
- Montagud-Martinez R, Márquez-Costa R, Rodrigo G (2023) Programmable regulation of translation by harnessing the CRISPR-Cas13 system. *Chemical Communications* 59: 2616-2619.
<https://doi.org/10.1039/D3CC00058C>
- Marques MC, Sanchez-Vicente J, Ruiz R, Montagud-Martinez R, Márquez-Costa R, Gomez G, Carbonell A, Daros JA, Rodrigo G (2022) Diagnostics of infections produced by the plant viruses TMV, TEV, and PVX with CRISPR-Cas12 and CRISPR-Cas13. *ACS synthetic biology* 11: 2384-2393

<https://doi.org/10.1021/acssynbio.2c00090>

- Marques MC, Ruiz R, Montagud-Martinez R, Márquez-Costa R, Albert S, Domingo-Calap P, Rodrigo G (2021) CRISPR-Cas12a-based detection of SARS-CoV-2 harboring the E484K mutation. *ACS Synthetic Biology* 10: 3595-3599.
<https://doi.org/10.1021/acssynbio.1c00323>

▪ **In preparation**

- Márquez-Costa R, Montagud-Martinez R, Ruiz R, Martínez-Aviño A, Ballesteros-Garrido R, Navarro D, Campins-Falco P, Rodrigo G. Virus detection by CRISPR-Cas9-mediated strand displacement in a lateral flow assay. In preparation.
- Márquez-Costa R, Ruiz R, Montagud-Martinez R, Sanchez-Vicente J, Daros JA, Rodrigo G. Multiplexable plant pathogen detection in a CRISPR-Cas9-based lateral flow assay. In preparation.

ACKNOWLEDGEMENTS

One chapter of my life is coming to an end. Overwhelmed PhD student season is over.

I am deeply grateful to my supervisor, Dr Guillermo Rodrigo, for his guidance and support; his expertise in synthetic biology was such an inspiration for pursuing this academic career. And thanks to Carmelo for his support and help with all the university administrative tasks.

Thanks to the lab mates (aka *Gresca*) Raúl, María, Roswitha, Roser, Lucas, Alejandro, Rubén, Sara, Sophie for the fun times we shared in the *drama full lab*. Special thanks to Javi and Álvaro for always listening to my drama inside and outside the lab and being my emotional support. Hopefully, someday a new lab member will check my old notes, find out about my annual reports of *La Gaceta de Sigüenza* and may find the joy in keeping track of the lab memes and inside joke the same way I did.


To my lovely group of *danzantes toxicos*, thank you for helping me break routine and free my mind. Specially to Azahara, Cristina, Álvaro, Mónica, Alegría, Conner, Guillem and Capo. Problems are faced differently when your mind is *al son cubano*. I can't wait to catch up on all the parties and *Sangria Thursdays* I had to miss because I was working on my thesis.

Of course, I am grateful to my family, my parents, and siblings, who were always a support even when they didn't really know what I was doing and kept asking why I didn't go for a stable and well-paid job position. I wish I could believe in myself the way they always do. And to my little ball of fur, Fujur, who is as much a part of my family as anyone else, for always demanding cuddles and sitting on my papers at the desk, like a protest sign, to remind me that more time should be spent with loved ones.

This thesis allowed me to spend my research stay at the beautiful island of Okinawa. I could not be more thankful for the time I had there, which marked a groundbreaking before and after in my life. Special thanks to Yokobayashi Sensei for allowing me to be part of his group, to Samuel for being such an inspiration both inside and outside the lab bench, and to Lara for all the ice creams before the typhoons and beyond. All the people I met there made my stay in Okinawa even warmer. The memories from Seaside house parties, Grandline Fridays, and the time spent under water will always be cherished.

また沖縄に行きたいです！チバリヨー！

さいしんじょうほう： 沖縄でポストドクとしてはたらきはじめる。

Last, I had to write my thesis during the most uncertain chapter of my life. I would have been consumed by frustration and anxiety if it weren't for Jack F, who was always there with memes, cozy chats, and beautiful words when I needed them most to keep me going and become my best self. Thank you, Jack, for always being here for me. If only I knew how good things were going to be .

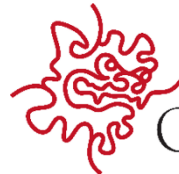


UNIVERSITAT
POLITÈCNICA
DE VALÈNCIA



CSIC

CONSEJO SUPERIOR DE INVESTIGACIONES CIENTÍFICAS



OIST

OKINAWA INSTITUTE
OF SCIENCE AND TECHNOLOGY



INSTITUTE FOR
INTEGRATIVE
SYSTEMS BIOLOGY